RADON MONITORING AND DELINEATION OF ACTIVE FAULTS IN KANGRA AND MANDI DISTRICTS OF HIMACHAL PRADESH, INDIA

A

Thesis

Submitted to

For the award of

DOCTOR OF PHILOSOPHY

IN

PHYSICS

By

Gulshan Kumar
(Reg. no. 41300119)

Supervised by:

Dr. Mukesh Kumar

Co-Supervised by:

Dr. Arvind Kumar

DEPARTMENT OF PHYSICS
LOVELY PROFESSIONAL UNIVERSITY
PUNJAB
2017

Dedicated to my family members

ACKNOWLEDGEMENTS

I honored to find opportunity to thank almighty from deep of my heart and soul for his constant innumerable blessing, strength and courage to complete my research work for Doctor of Philosophy thesis.

I owe a deep sense of gratitude to my supervisor Dr. Mukesh Kumar, Associate Professor Department of Physics, Lovely Professional University, Phagwara, Punjab and my co supervisor Dr. Arvind Kumar, Associate researcher, National Institute for earthquake Engineering, Taiwan for their keen personal interest, providing enough research guidance and encouragement without which it would be difficult to complete my Doctor of Philosophy work.

I wish to thank Dr. Jitender Kumar Assistant professor Govt. College Shillai, Sirmaur Himachal Pradesh and Dr. Sunil Dhar Associate professor Govt. College Dharamshala, Kangra for valuable help and scientific coordination to complete the work.

It is great privilege for me to express sincere thanks to Head of physics department Dr. Kailash Chander Juglaan and other faculties of Department, Lovely professional university to provide the conducive environment to explore and enhance knowledge. I owe thanks to my, Friends cum coworkers Mughavi A Tuccu, Poonam Thakur, Jyoti Gautam and Kiran for giving me moral support to complete the degree.

Finally I thank my family members my parents, wife, brother, sister for their selfless sacrifices, financial support and blessing that enables me to complete my work with great zeal.

Gulshan Kumar

DECLARATION

I hereby declare that the Thesis entitled **"Radon Monitoring and delineation of active faults in Kangra and Mandi districts of Himachal Pradesh, India"** submitted for the Doctor of Philosophy degree is entirely my original work and all ideas and references have been duly acknowledge. It does not contain any work for the award of any other degree or diploma from any other university.

Dated

Gulshan Kumar
Reg. no. 41300119

Verified by

Dr. Mukesh Kumar
Associate professor
Department of Physics
Lovely Professional University
Phagwara (Punjab)

CERTIFICATE

This to certify that Gulshan Kumar has completed Doctor of Philosophy thesis titled **"Radon Monitoring and delineation of active faults in Kangra and Mandi districts of Himachal Pradesh, India"** under my guidance and supervision to best of my knowledge, the present work is the result of his original investigation and study. No part of thesis has ever been submitted for any other degree or diploma at any university.

The thesis is fit for the submission and the partial fulfillment of the conditions for the award of Doctor of Philosophy degree.

Dated

Dr. Mukesh Kumar
Associate professor
Department of Physics
Lovely Professional University
Phagwara (Punjab)

CERTIFICATE

This to certify that Gulshan Kumar has completed Doctor of Philosophy thesis titled **"Radon Monitoring and delineation of active faults in Kangra and Mandi districts of Himachal Pradesh, India"** under my Co- Supervision to best of my knowledge, the present work is the result of his original investigation and study. No part of thesis has ever been submitted for any other degree or diploma at any university.

The thesis is fit for the submission and the partial fulfillment of the conditions for the award of Doctor of Philosophy degree.

Dated

Dr. Arvind Kumar
Associate Researcher
National Center for Research on
Earthquake Engineering (NCREE)
Taipei106,Taiwan

ABSTRACT

Because of high seismic potential of North West Himalaya, the fault delineation study in the region of Himachal Pradesh becomes very significant. The Himalayas are formed due to intercontinental collision between Indian and Eurasian Plate. As a impact of collision some thrust boundaries like MBT (Main Boundary Thrust), MCT (Main Central Thrust) and HFT (Himalayan Frontal Thrust) were formed. Many seismic events small to high magnitude (M_L= 8) have been reported so far in the region between MCT and MBT. It has been investigated by a number of researchers that many geochemical changes take place prior and after the seismic event along and across the active faults. These Phenomenon include change in the concentrations of ions, dissolved gases in water and changes in the volume of the gas leakage through the faults (especially the anomalies in the measured concentrations of radon, carbondioixide and helium).

Keeping in view the aforesaid effects the soil gas surveys have been carried out in North West Himalayan region (Active region of Kangra and Mandi of Himachal Pradesh). Since higher radon concentrations were reported by various researchers in this area therefore indoor radon survey and radon concentration in water samples have also been studied to check its impact on the health of people of concerned region.

The thesis consists of seven chapters and each chapter gives the detailed investigation and outcomes. The contents of the chapters are outlined as:

Chapter 1: This chapter is the introductory part of the thesis which includes the detail of the natural radioactivity, radon origin, its isotopes their characteristic and half life. Since high anomalies in the concentration of radon have been reported along the faults so its health effects on the population due to its increased concentrations in indoor environments and water reservoirs has also been discussed. This portion also includes the connection of gas migrations and faults with emphasis on radon migrations. The work of various researchers is also discussed in the literature review section of the chapter. Geology of study area and proposed objectives of the study are also briefed here.

Chapter 2: This chapter introduces the various measurement techniques used by the researchers to monitor the radon, classification between passive and active methods. Integrating, continuous and grab techniques to measure the radon. Use of LR-115 type II detectors in the soil gas survey, indoor monitoring and technique to measure the radon

exhalations rates is discussed in detail. The active techniques such as RAD7 and its use to measure the radon concentration in water are also explained in the chapter.

Chapter 3: This chapter reported the radon-thoron anomalies in active Dharamshala region of Kangra in Himachal Pradesh. The anomalies in radon and thoron monitoring is the premonitory sign prior to an earthquake. The plate activity in the Dharamshala region is expected to enhance the radon concentration at some places in the study region. Study is important because the region is under zone IV and V. To check this concept radon and thoron are measured using LR-115 Type II Cellose Nitrate films. The average values of radon concentration is found to be 5075Bq/m^3 with maximum of 13570Bq/m^3 and minimum of 813Bq/$m^3$and for the Thoron average value is 1154Bq/m^3 with maximum of 5903Bq/m^3 and minimum of 223Bq/m^3. The high values of the radon concentration in the region are because of the presence of neotectonic thrust in the region, likes MBT (Main Boundary Thrust), MCT (Main Central Thrust) and MFT (Main Frontal Thrust).

Chapter 4: Study has been conducted to analyse the radon and thoron flux in the soils of Mandi district, Himachal Pradesh. The detectors have been rooted at seventy one lithological locations in the north-eastern part of the district. The average values of radon concentration has been observed as 4541Bq/m^3 with maximum of 19970Bq/m^3 and minimum of 867Bq/m^3 and the thoron variation ranges from 37 to 6970Bq/m^3 with an average value of 1778Bq/m^3. The radon liberation at different positions has been correlated to the presence of the active fault to reveal the contributory aspects for abnormal release of radon in the soils. The spatial distribution of radon and thoron gas along the lines passing through the fault zones have unveiled the variances connected to the local tectonic structures. Radon exhalation rates, radium contents and porosity of soil samples have been calculated and a correlation factor of 0.64 has been detected for the observed concentrations of thoron and the porosity of the soil.

Chapter 5: The radon concentration is found to be more in Himachal Pradesh as compared to the other places of the India. According to ICRP (International commission on Radiological Protection) the indoor radon level should be 40Bq/m^3. But in Himachal Pradesh this value in found to be much more than the average expected values as suggested by the ICRP. This because the Himachal Pradesh is under highly seismically

consideration, where the radon values large due to under earth activities. This work is the study of radon in some houses which are falling in the region between the MCT(Main central thrust) and MBT(Main boundary thrust) from Barot of the Mandi district to the Salapar near to the district Bilaspur of Himachal Pradesh and Jogindernagar to Dharamshala in Kangra district of Himachal Pradesh. The study is performed using the LR-115 Type II detectors in bare mode, the average value of Radon measured in these houses is found to be 138Bq/m^3.

Chapter 6: In this chapter study of Indoor radon continuous monitoring for one year has been carried out in few dwellings of Mandi district Himachal Pradesh, India. To carry this investigation, indoor radon equilibrium equivalent concentration was measured using LR-115 type 2 detectors in fifteen to twenty houses (Total sixty five houses) in each region. The average value of equilibrium equivalent concentration of radon (EERC) in the study area was found to be 94Bq/m^3 with annual effective dose of 1.61mSv. It has been observed the values of indoor radon equilibrium equivalent concentration were usually high in the Mandi-Sundernagar region as compared to the other region of the study area. The mean value of indoor radon concentration in sampled dwellings was measured to be more than double of the world average indoor radon value of 40Bq/m^3 but less than the value of the action level 200Bq/m^3 except three locations and may not pose any significant threat to the public health.

Chapter 7: In this chapter a simple model devised on the basis of Roger model and previous works in this field is discussed. The feasibility of the model is tested on the basis of the measurement of radon exhalation rates at 96 sites in Dharamshala-Mandi area of Himachal Pradesh, NW Himalaya India using LR -115 Type II Solid state nuclear track detectors. The average measured values of Area Exhalation rate =1.50±0.52Bq $m^{-2}h^{-1}$ and Mass exhalation rate= 0.0661±0.022Bq $kg^{-1}h^{-1}$where as average radium contents were found to be 7.03±2.39Bq kg^{-1}. Average theoretically estimated area exhalation rate (= $4.62x10^{-4}$Bq $m^{-2}s^{-1}$) has been found almost equal to average experimentally measured area exhalation rate (=$4.16 x10^{-4}$Bq $m^{-2}s^{-1}$) with correlation coefficient of 0.96.

Chapter 8: This chapter deals with the radon estimation in the groundwater samples and radium content in the soils of Study area. Forty water samples are taken from the

different natural water resources. Radon concentration is determined by using RAD-7 detector whereas the radium contents of the soil samples taken from the vicinity of water resources were measured by using LR-115 type – II detector. These contents were further correlated with radon contamination in water samples and were used to estimate the potential health risks related with radon. The results show that the radon concentrations were within the range of 1.51 to 22.7Bq/l with an average value of 5.93Bq/l for all type of water samples taken from study area. All of the analysed water samples show ^{222}Rn concentrations lower than 100Bq/l (exposure limit in water recommended by the World Health Organization. The average value of radium content in the soil of study area was 6.326Bq/kg. The average effective dose received by the people of study area was 0.022mSv/y with maximum of 0.083mSv/y and minimum 0.0056mSv/y. The average dose 0.022mSv/y received by the people of study area from inhalation point of view are quite less as compared to ingestion values. The total effective doses as measured from sample locations were found well within the safe limit (0.1mSv/year) recommended by WHO.

PREFACE

The present study deals with the implications of radon measurements in context with its health hazards and its applications to study various transport phenomenon like hydraulic conductivity (ground water movement, geothermal fluids) and identifying the buried faults. The study was carried out in active Kangra - Mandi region of North- West Himalaya region of Himachal Pradesh, India. In the vicinity of MCT, MBT or any thrust systems of the area the radon anomalies were found to be higher than any other region. These anomalies were found to be higher near the MCT than to MBT. Secondly the radon concentrations in soil-gas were reported higher the some other area of the region these values confirms the presence of buried faults or local seismicity in the study area. Further the high values of radon-thoron in soil-gas have drawn the attention towards its health impact. When the study was made near to faulty area, the average value has come to more than world average and similarly when the annual effective dose was calculated on the basis of continuous annual monitoring the value was again more than world average. Similarly when the its value is calculated in the water its dose was reported less than the world average for inhalation from the water but for ingestion the value was reported higher than world average. The model was also developed to calculate radon exhalation rates; this modeling is correlated to 0.96 to its experimental counterpart.

Gulshan Kumar
Reg. no. 41300119

TABLE OF CONTENTS

LIST OF FIGURES

LIST OF TABLES

ABBREVIATIONS

MCT	**Main Central Thrust**
MBT	**Main Boundary Thrust**
HFT	**Himalayan frontal Thrust**
JMT	**Jawalamukhi Thrust**
KWF	**Kistwar fault**
SNF	**Sundernagar Fault**
ASC	**Advanced seismic computer**
HP	**Himachal Pradesh**
Mb	**Body wave magnitude**
RAD 7	**Radon detector**
SSNTD	**Solid State Nuclear detector**
TCD	**Thermal conductive detector**
WHO	**World Health Organization**
ICRP	**International Commission on Radiological Protection**
UNSCEAR	**United Nations Scientific committee on effects of atomic radiation sources and effects of ionizing Radiations**
USEPA	**United states environmental Protection Agency**
CFD	**Computational fluid dynamics**
GSD	**Geometric standard deviations**

OECD	**Organization for economic cooperation and development**
EERC	**Equilibrium equivalent radon concentration**

CHAPTER 1

INTRODUCATION AND REVIEW OF LITERATURE

The radioactive elements are presents in soil, gas and water. The inhalation and ingestion of radio nuclides from these elements above the permissible level poses hazards to health of individual. Therefore concern for monitoring these radio nuclides in the environs is increasing at all levels due to their harmful effects. One of the naturally occurring element uranium contains a mixture of three isotopes such as U^{238}, U^{235} and U^{234}. All these isotopes of uranium are radioactive and decay in to thorium, radium, radon etc; until a stable non-radioactive isotope of lead is produced (Figure 1). Out of other radionuclide, uranium is the heaviest radioactive toxic element which is found in all types of soils, rocks, sands and water. Under certain geological environments, uranium separates as a discrete mineral and forms a deposit. The compounds of uranium present in earth's crust are water-soluble and enter the human body mainly through ingestion of eatables and drinking water. The salts of uranium are highly toxic. These compounds combine with the phosphate groups on cell surface thereby blocking normal metabolic processes, which are essential for cell survival [Axelson, 1995; Bochicchio et al., 1998; Singh et al., 2005]. Also these compounds can injure the kidney preventing normal waste product elimination resulting in renal disfunction. The plants uptake uranium from soil and water which may increase the activity level of agro based food products thereby increasing the chances of exposure (to public) via ingestion. Under ordinary conditions of temperature and pressure radium is a solid radioactive element. It decays to radon by emitting α- particles followed by γ-radiations. Thus the concentration of radium decides that how many radon atoms are formed. The amount of radon atoms leave against the produced radon atoms i.e. emanate from the mineral grain or matter and enter the pore spaces depends on; place at which the radium atoms are situated in the grain, the texture and size of the soil-grain, the permeability of the grains, soil temperature and pressure [Fleischer, 1980; Tanner, 1980; Anderson et al., 1983; Durrani et al., 1997]. Thus radon monitoring is necessary for uranium and radium estimation in the parent source for public health risk assessments.

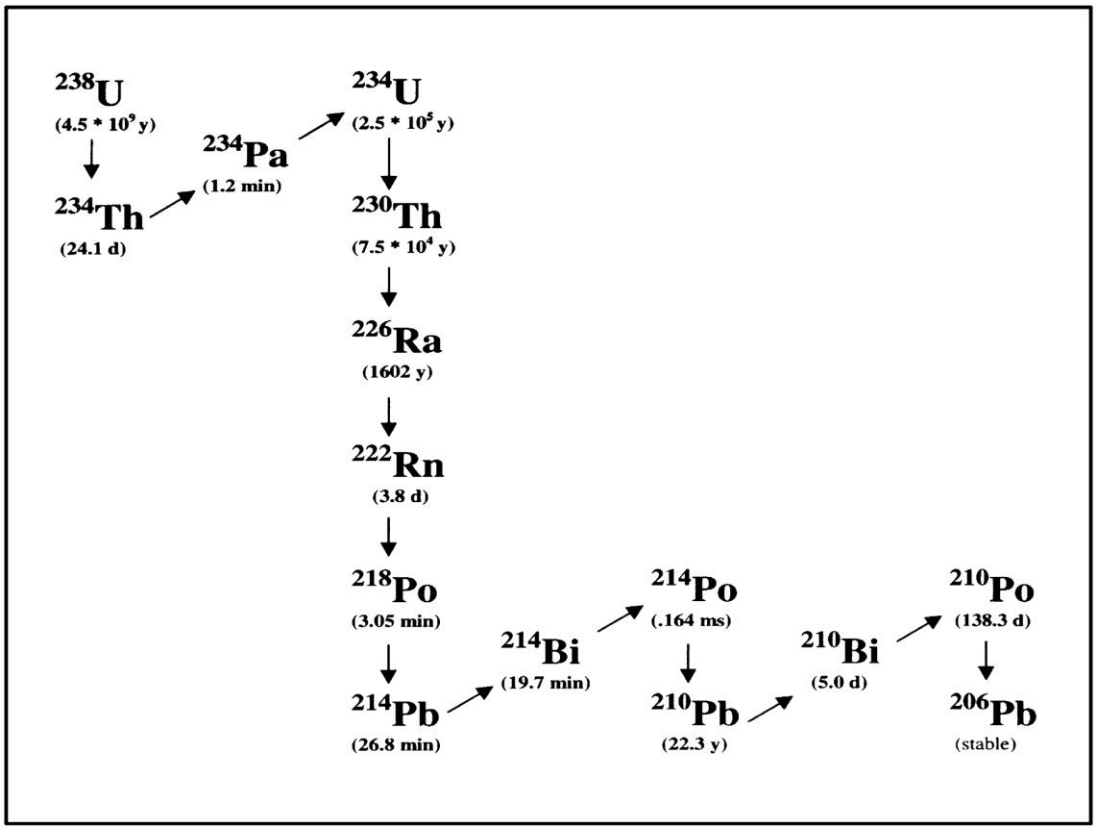

Figure 1: Decay scheme of Uranium

1.1 Radon and its health risk potentials

Radon (^{222}Rn) is a unique natural element. Although this element is in gaseous state with characteristics of noble element still it behaves as radioactive in all of its isotopic forms. At standard temperature and pressure radon has density of 9.73 kg/m^3. It glows because it emits the radiation and it is highly soluble among other noble elements in water (sparingly soluble). Being a gas, it has two significant effects first since gas is mobile and carries messages over significant distances within the earth and in the atmosphere and secondly because of its radioactive nature its inhalation can pose a problem to health. Since radon is a noble element which promises that it is not immobilized by some chemical reaction with the medium from which it permeates. As a result, free radon when moves from its parent source, generally it diminishes in concentration only by its radioactive decay. Finally, its radioactivity allows radon to be measured with remarkable sensitivity. For humans the greatest importance of the radioactivity of radon is that in high concentrations it can pose a serious health hazard like lung cancer [Axelson, 1995;

Bochicchio et al., 1998; Singh et al., 2005]. On the earth, radon and its isotopes are formed by the decay of radium whereas radium itself comes from uranium or thorium decay-usually (but not always) from trace impurities in minerals. Out of three other natural isotopes greatest importance is attributed to Rn^{222} because of its long life. The isotopes of radon are ^{222}Rn (Radon with half life of 3.82 days), ^{220}Rn (Thoron with half life of 55.6 seconds comes from the decay of thorium ^{232}Th) and ^{219}Rn (Actinon with half life of 3.96 seconds which comes from the decay of ^{227}Ac). Because of short half life of thoron only a small fraction of it can enter the interior of a house, but a small portion of it may be very harmful to health of living organisms, because its progeny ^{212}Pb (half life of 10.6 h) can accumulate in the air and may be inhaled to the lung with radiation threat. The world average of thoron concentration as suggested by United Nations scientific committee on the effect of atomic radiation is 3 Bq/m^3 but because of its shorter life time maximum researchers had avoid its contribution in radon. Although the outer air contribute very less to radon in the interior of the room, still the different types of building materials, their ages and relative humidity may contribute much to the indoor radon of the house. Radon accumulation in the houses also depends upon the life styles of the residents because it is found that its concentration is more in the air-conditioned rooms as compared to non air conditioned rooms. The radon and its progeny Po-218, Po-214 can attach to airborne particles and may be inhaled to lungs where they can release the energy by irradiating the tissue (cause of lung cancer).

Table 1: Decay-scheme of radon

Sr. no.	Parent nucleus	Life time	Daughter nucleus	Type of decay
1	$^{222}Rn_{86}$	3.82 days	$^{218}Po_{84}$	α- decay, 5.49Mev
2	$^{218}Po_{84}$	3.05 min	$^{214}Pb_{82}$	α- decay, 6.00 Mev
3	$^{214}Pb_{82}$	26.8 min	$^{214}Bi_{83}$	β- decay, 1.02Mev(max)
4	$^{214}Bi_{83}$	19.7 min	$^{214}Po_{84}$	β- decay, 3.27

				Mev(max)
5	$^{214}Po_{84}$	0.164 ms	$^{210}Pb_{82}$	α- decay, 7.64 Mev
6	$^{210}Pb_{82}$	22.3 year	$^{210}Bi_{83}$	β- decay, 0.017Mev(max)
7	$^{210}Bi_{83}$	5.013 days	$^{210}Po_{84}$	β- decay
8	$^{210}Po_{84}$	138.376 days	$^{206}Pb_{82}$ (Stable)	α- decay

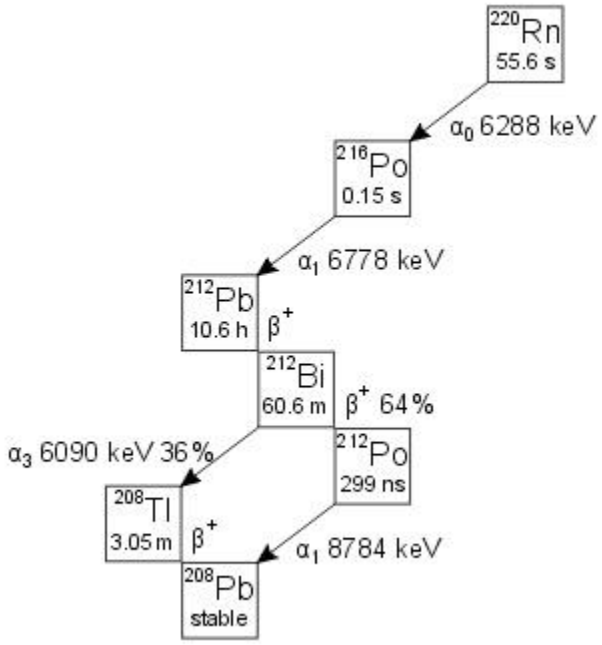

Figure 2: Decay of thoron

1.2 Radon transport mechanism

Due to gaseous nature of radon it has tendency to move to outer environment from inner of soil/rock crystalline matrix. It travel only a short distance because of its short life time. The presence of radon in any soil strata is decided by its radium contents, which further depend up on uranium contents [Dongarra and Martinelli, 1993]. The ^{226}Ra is almost

immobile in oxidizing environment and can be added to any environment using α-recoil, whose recoil length is about 0.02 to 0.05 mm [Fleisher et al., 1975]. The activities of ^{226}Ra in solution can be calculated as

$$^{226}Ra(t) = {}^{226}Ra(0)\,[1-\exp(-\lambda t)]$$

Where $^{226}Ra(t)$ and $^{226}Ra(0)$ represents activities at time t and at equilibrium [Darance, 1986]. Radium can also removed from the solution by chemical processes. Hot springs are examples of such processes (NW Himalayas especially Parvati and Beas Valley have such types of geothermal sources). Not all the radon that is produced by the radioactive parent escapes to outer surface, its emanation increases if surface area per unit mass increases. According to Tanner radon atoms which recoil through liquid or gaseous phase may be escaped from crystalline matrix. Whereas the atoms which are trapped in the rock at a distance greater than recoil length are maintained in the solid matrix and they are not available for the transport. This emission is greatly affected by other parameters such as pressure, temperature, moisture contents and faults or fracture (secondary porosity) which are caused due to tectonic activities. Therefore radon may be considered as precursor for the seismic activities.

1.2.1 Movement inside the crystal lattice

The radon concentration gradient due to its diffusion in isotropic medium is given by [Andrews et al., 1986].

$C_x = C_0\,\mathrm{Exp}(-X/L)$, C_x = Concentration of ^{222}Rn at distance X from the origin, C_0 = Initial concentration of ^{222}Rn, L = Diffusion length, $L = (D/\lambda)^{0.5}$, D = Diffusion coefficient, λ = Decay constant.

From this equation it is expected that only 5% of radon can reach up to a distance of 5 times the diffusion length, therefore the migration of radon in crystal is very less.

1.2.2 Migration to surface

When radon comes out from crystal lattice, it is accumulated in rock pores, air and in water. The radon concentration in water passing through the radon emanating rock is given by

$$C_{Rn} = (A\,\rho\,C_{Ra}) / \sigma[1-\exp(-X/V)]\exp(-X'/V')$$

[Adrews et al., 1986]

Ra = Radium activity, ρ = Rock density, σ = Porosity of rock whereas X,V and X',V' are the distance and velocity in aquifer and outside of it. A = radon released in to water / radon generated within the rock. This equation gives the estimate the radon content in aquifer.

1.2.3 Transport by molecular diffusion

In this type of transport radon atoms tends to maintain same concentration along the all parts of the rock system. The radon atoms move from higher concentration to lower concentration along a porous path (due to primary porosity). This type of radon movement is studied by Fick law:

The radon Diffusion flux ($Bqm^{-2}s^{-1}$) through big radius path in single phase is

$$\mathbf{F = -D_i \frac{dC}{dx}}$$ [Fick, 1855; Crank, 1975]

Where C = Radon concentration (Bqm^{-3}) and D_i = Diffusion coefficient (m^2s^{-1})

The solution of the equation is $C = C_0 \exp [-(\lambda/D)^{1/2} X]$ where D is diffusion coefficient, X= distance in concentration [Tanner,1964].

Table 2: Radon diffusion coefficients in different materials

Material	Radon diffusion coefficient (m^2s^{-1})	Material	Radon diffusion coefficient (m^2s^{-1})
Air	0.1	Mixed soil	4×10^{-2}
Moist air	0.5	Sand stone	3×10^{-2}
Water	1.13×10^{-5}	Argilite	8×10^{-5}
Benzene	2.36×10^{-5}	Alluvium	4×10^{-2}
Quarzite	8×10^{-5}		

1.2.4 Transport by pressure driven Mechanism

This type of mechanism is also called as mass transport or non diffusive transport or convection [Nazaroff and Nero, 1988]. The convection may also be defined as movement of soil gas by pressure gradient created because of difference in temperature at different points along the path. This type of transport mechanism plays an important role in movement of radon along faulty and fractured zones where secondary porosity is very high and pores are of large diameters. The transport of gases under convection is studied by Darcy law:

The flux of the gas through large diameter is expressed as:

$F = Cv$

Where C is the concentration (Bq/m^3) and v is the velocity (m/s), according to Darcy the velocity for one dimensional movement is given by

$V = P\eta\varepsilon x$

Where P = Pressure difference at two point separated by distance x

η = Dynamic gas viscosity

ε = Intrinsic permeability

(a) Convection of fluids due to geothermal gradient (dT/dx) is shown by equation

$Kgh^2(dT/dx) (dP/dT) \geq 4\pi^2 D\eta$

If the geothermal potential is very high than and due presence secondary porosity the convection may be very high even in less porous rocks.

(b) Movement through the carrier gases like CO_2, He, CH_4 and H_2 etc.

The concentration of ^{222}Rn at a distance of x from a surface with concentration of radon as C_0 is given by

$C_x = C_0 \exp[\{(v/2D)- (v^2/4D^2 + 1/D)^{0.5}\}]$

1.3 Faults and its connection with gas leakage

Faults are the weakened zones which comprised of highly fractured material, gouge and fluids. Faults at surface are easily visible to the geological observers however the faults beneath the earth surface can be made geologically visible only by some remote sensing equipment or some exploration methods like soil- gas measurements. The geological mapping of the faults and fault systems may be helpful to study many phenomenon like seismicity of area; primary and secondary porosity associated with rocks and hence ground water surveys or geothermal sources. Active faults are associated with gas leaks because gas leakage increases with the permeability/ porosity of soils. Gas anomalies at active faults may be of two types first is 'direct leak anomalies' where the concentration of gas measured can be related to the deep source in the earth crust and second is 'secondary anomalies' which may be linked to geochemistry of the soil with the anomalous distribution of radium [Toutain et al., 1999].

Besides its serious health hazards radon may also be helpful to study various transport mechanisms. The possibilities of radon transportation within the earth, in water and atmosphere make it a useful tracer for a remarkable variety of geophysical, geochemical, hydrological and atmospheric purpose. These applications maybe exploration for resources such as uranium and hydrocarbon deposits, to recognizing fluid transport within the earth, to attempting to predict seismic events and volcanic events through precursory signs of changes in radon concentration during these events in the atmosphere of earth. However with these fruitful transport mechanisms of radon are countered by serious health effects (sustained exposure of substantial concentrations of radon decay products to human can produce lung cancer). Radon is a tracer of convection process, fault presence and presence of uranium thorium mineral in lithology therefore profiles of soil gas radon are suitable tools to characterize active tectonic areas/structures [Quattrucchi et al., 2000].

The short half-life of radon (3.82 days) limits its diffusion in soil, so that radon measured at the ground surface cannot be released unless there exists a driving mechanism other than mere diffusion [Loannides et al., 2003]. The radon transport through rocks under the earth largely depends on lithology, compaction, porosity and

fractural/tectonic features like faults, thrusts, joints or fractures [Choubey et al., 1997 and Gunderson et al., 1998]. The important most application of radon monitoring is emerged with prediction of earthquake. Okabe, [1956] had studied the correlation between variation in radon concentration and local seismicity in Japan, with his study the real time radon monitoring had become an extensively studied area in order to give premonitory signs prior to an earthquake. The various geological changes due to stress/strain occurring within the earth's surface during an earthquake is expected to produce the anomalies in radon concentration in soil-gas. Thus an impressively good development in the study of the earth's geology pertaining to radon concentrations permits researchers to estimate on probabilities for earthquake risks. The radon concentration levels are strongly affected by geochemical and geophysical conditions and due to atmospheric factors like rainfall and barometric pressure. As temperature, rainfall, barometric pressure, all are the integrated parts of season, so radon concentration may change seasonally and this seasonal variation of radon concentration must also be studied along with its variations in rock mass under that tectonic stress which creates new pathways to gas transportation and exposes new surface to radon exhalation as a result the stress–strain developed within earth's crust before an earthquake leads to anomalies in gas transportation and increase in the level of volatiles from the deep earth to the surface due to which unusual quantities of radon come out of the pores and fractures of the rocks on surface [Thamos, 1988 and Fleischer, 1997]. Which may be concluded with the fact that during seismic activities changes in underground fluid (soil-gas) flow may account for anomalous changes in concentration of radon and its progeny [Steinitz et al., 2003]. In their study Grammakov and Clements showed that a small change in convective velocity of gas into or out of the ground causes a significant change in radon concentration at shallow soil depth that means the changes in gas flow strongly disturb the radon concentration gradient that exists between the soil and the atmosphere. A small change in the pore volume due to geological stress causes gas to flow out of the soil resulting to an increase in radon concentration level. Similarly, when pore volume increases, gas flows into the soil from the atmosphere [Grammakov, 1936 and Clement, 1974]. Thus in the region which is under stress (compression) radon concentration increases and its concentration decreases in the region of dilation. Since a little change in convective gas velocity causes

significant change in radon concentration so soil radon monitoring may be important method to detect the changes in compression or dilation associated during an earthquake event.

1.4 Tectonic features of North-West Himalayas:

North-West Himalayas region is tectonically and seismically very active. The highest intensity earthquake reported in this region are the great Kangra earthquake (1905), the Kinnaur earthquake (1975), Dharamsala earthquakes (1978, 1986), the Sundernagar earthquake (1997) and some other earthquakes of 1945, 1947 and 1950. The tectonic features of NW Himalayas are shown in Figure 3 in which the direction of shortening in quaternary period is indicated by a black arrow and azimuths of in situ stress are indicated by white arrow [Kumar et al., 2005]. It is clear from the figure 3 that the major tectonic thrusts are EW and minor faults are oblique to these thrusts and support NS under thrusting of the Indian plate is integrated fault surface area of earthquakes. Rao et al., [2003] suggest that in the NW Himalayas the seismicity dominated by reverse faulting (93%), while this value in Tibetan plateau is only 2% and is dominated by strike-slip and normal faulting (59% and 39%, respectively). The region of NW Himalaya is locus of micro, moderate and high-sized shallow focus (mainly $10 \leq h \leq 20$km) seismic activity centers [Barazangi et al., 1984].

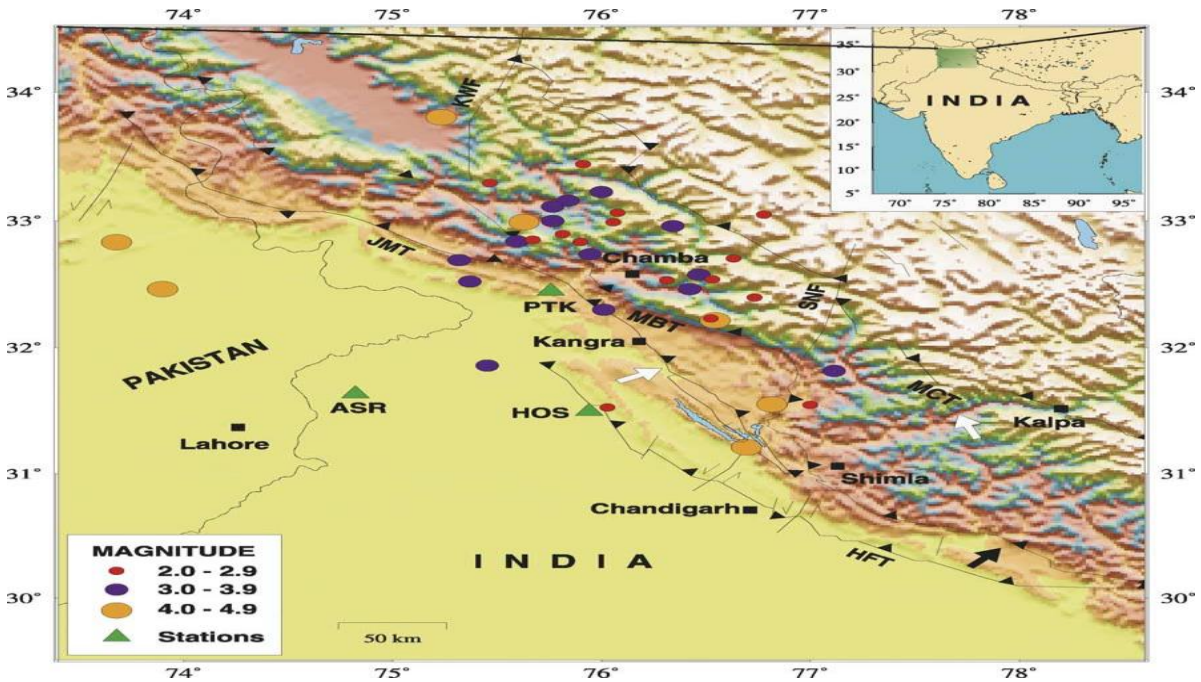

Figure 3: General Seismotectonic and topographical map of NW Himalayas and adjoining area. MCT: Main Central Thrust; MBT: Main Boundary Thrust; HFT: Himalayan frontal thrust; JMT: Jawalamukhi thrust; KWF: Kisatwar fault; SNF: Sundernagar fault; earthquake epicenters are plotted by circles, triangles represent the recording stations (PTK: Pathankot; HOS: Hoshiarpur; ASR: Amritsar) and cities are shown by squares [Kumar et al., 2005].

Regular monitoring of seismic activities and their evaluation in this tectonically active Himalayan region is of significant importance because earthquakes pose a continual threat to the safety of the people inhabiting this big and active mountain system of the earth. It may now be considered that active faults – faults which have contributed to seismic activities during recent geological time can have potential for reactivation in the future and which may contribute significantly to the seismic activity (>80% seismic activity in the region). Therefore the mapping and understanding of the nature of the active fault systems in different segments of the Himalayas is greater importance, with the fact that there is a little information about the distribution of various faults, their behavior and characteristics. In India, there is less study had been reported so far to delineate these active with the fact that enough information on the distribution of seismicity including major (M 6.5 – 7.5) and great (M8 and above) events is available.

1.5 Earthquake history of Himachal Pradesh

The Himachal Pradesh lies almost entirely in the Himalayan mountains with its part on the Punjab Himalayas. Due to its location it experiences many of low and medium intensity earthquakes every year. Earthquakes of high intensity were experienced in all parts of Himachal Pradesh, the biggest being the Kangra Earthquake of 1905. The Himalayan Frontal Thrust, the Main Boundary Thrust, the Main Central Thrust, the Krol, the Jawalamukhi thrust, the Giri, Jutogh and Nahan thrusts lie in this region. Besides that there is also presence of smaller or buried faults like the Kaurik fault which triggered the 1975 earthquake. However, it must be kept in mind that vicinity to faults does not necessarily a threat to a higher hazard as compared to locations situated far away, since damage from earthquakes depends on numerous factors such as subsurface geology as well as adherence to the building codes [ASC: Seismicity of Himachal Pradesh]. Figure 4

shows the different zones of Himachal Pradesh from small risk zone to high risk zone, the dark coloured region is more prone to earthquake than light yellowed coloured region. Chamba, Kullu, Kangra, Una, Hamirpur, Mandi, and Bilaspur Districts lie in Zone V. The remaining districts of Lahual and Spiti, Kinnaur, Shimla, Solan and Sirmaur lie in Zone IV. Since the earthquake database in India is still incomplete, especially with regards to earthquakes prior to the historical period (before 1800 A.D.), these zones reflect the denser of earthquake hazard in any these regions and hence the knowledge regarding presence of faults in these regions need to be regularly updated [ASC; Census of India 2001].

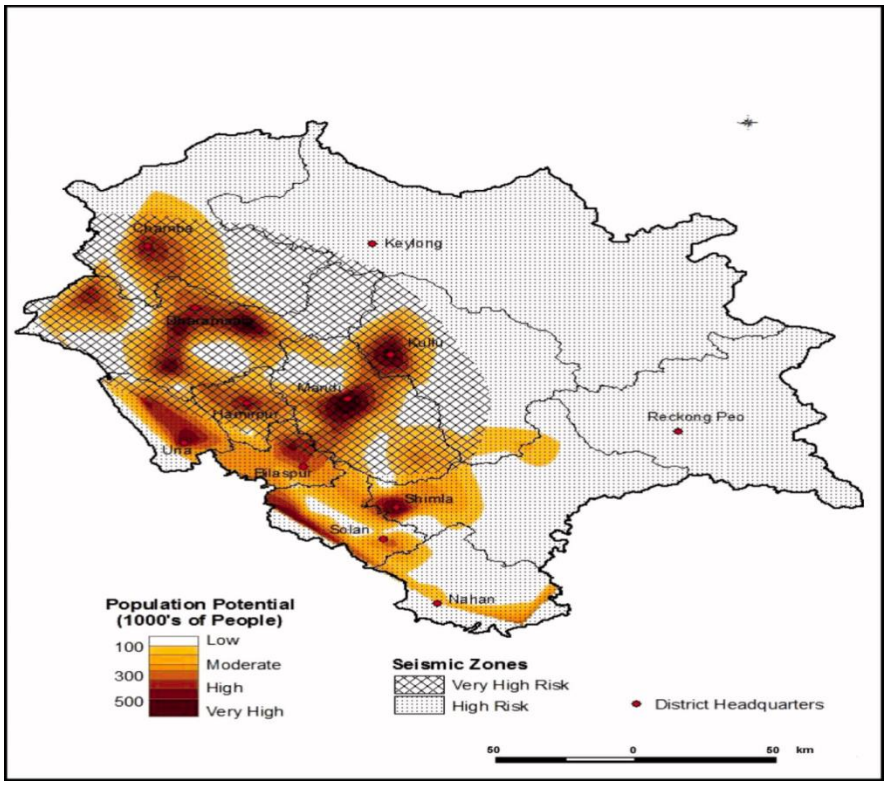

Figure 4: Himachal Pradesh Population potential and seismic risk zones

[ASC; Choubey et al., 1997]

1.5.1 Significant earthquakes in Himachal Pradesh:

The known earthquakes in this region are listed below. Whereas the Figure 3 provides general locations (epicentral) for the events which were occur in history. Some other

events which were significant for other reasons are also included [ASC; Census of India 2001].

Table 3: Some major earthquake events in Himachal Pradesh.

Acronyms Used: D=Depth, **OT**=Origin Time, **Mw**=Moment Magnitude, **Ms**=Surface Wave magnitude, **Mb**=Body Wave Magnitude, **ML**=Local Magnitude, **M**=Magnitude Type unknown

Date of occurrence of event	Station	Location	Original time(OT)	Magnitude	Remarks
4 April 1905	Kangra (Himachal Pradesh)	33.00N, 76.00E	OT=00.50UTC	Mw 7.8	About 28000 people were killed in Kangra region and adjoining Punjab region
28 February 1906	Near Kullu (Himachal Pradesh),	32.00N,77.00E	-	Mw 6.4	Damage and casualties in the Bushahar-Shimla hills states
11 May 1930	East of Sultanpur (Himachal Pradesh),	31.70N, 77.00E	11:30:36UTC	-	6.0(TS)
22 June 1945	Near Padua, Kathwad District, J&K (H.P.-J&K Border region)	32.599N, 75.90E	18:00:51UTC		6.0 (TS)
10 July 1947	Near Padua, Kathwad District, J&K	32.599N, 75.90E	10:19:20UTC		6.0 (TS)

	(H.P.-J&K Border region),				
12 August 1950	Near Padua, Kathwad District, J&K (H.P.-J&K Border region),	32.599N, 75.90E	03:59:06UTC		6.0(TS)
12 September 1951	Chamba-Udhampur Districts (H.P.--J&K Border region),	33.30N, 76.50E	20:41:48UTC,		6.0 (TS)
17 June 1955	Lahual-Spiti District (Himachal Pradesh),	32.50N, 78.60E	10:14:09UTC		6.0 (TS)
17 June 1962	Chamba-Udhampur Districts (Himachal Pradesh-J&K Border region),	33.30N, 76.20E	04:39:26.60UTC		6.0(TS),
19 January 1975	SW of Dutung, Himachal Pradesh (Indo-China Border region)	32.455N, 78.430N at 33km depth	08:02:02.50	Mw 6.2, Ms 6.8	Caused havoc in parts of the Kinnaur, Lahaul and Spiti regions of India. 60 people were killed

21 October 1991	Near Pilang (Uttarkashi District), Uttaranchal	30.78N, 78.77E	21:23:14UTC 02:53:14IST	Mw 6.8	Between 750 to 2000 people killed in the Gharwal region It was also felt very strongly in Uttar Pradesh, Chandigarh, Delhi, Haryana and Punjab. Fatalities were also reported from Himachal Pradesh. Some minor damage was reported in Chandigarh and New Delhi.
29th March 1999	Near Gopeshwar (Chamoli District), Uttaranchal,	30.492N,79.288E	19:05:11UTC	Mw 6.5 (HRV)	115 people killed in the Gharwal region. The quake was felt very strongly in Uttar Pradesh,

					Chandigarh, Delhi and Haryana. In Haryana, one person was killed in the city of Ambala and 2 at Nakodar in the neighbouring state of Punjab. Minor damage to buildings in New Delhi, most significantly in Patparganj. Minor damage also reported from Chandigarh.
11 November 2004	Bharmour, Kangra region	32.442N, 76.512E at depth of 34km	02:13:45UTC	Mw 5.1	It was felt strongly in the Kangra-Dharamsala region and event caused minor damage to buildings in the region

*UTC = It is the world Standard coordinated universal Time, the basis of this time is the civil time today, this is a 24 hours standard time which is made operative with precise atomic clocks kept synchronized with earth's rotation.

Table 4: Some minor recent seismic actvities in Himachal Pradesh (source: Metreological centre Govt.of Himachal Pradesh, India)

Date	Time	Location	Depth (from surface)	Magnitude	Region
9.2.16	15:13:47	32.8 N, 77.4E	10km	4.4	Lahaul Spiti
21.7.16	14:42:07	31.4 N, 77.6E	5km	3.5	Kullu
1.8.16	12:34:00	30.9 N, 77.1E	10km	3.0	Solan
1.8.16	13:38:00	31.4 N, 77.6E	10km	3.6	Rampur (Shimla)
28.8.16	1:14:32	31.4 N, 77.5E	10km	4.6	Kullu
27.8.16	01:35:07	31.4 N, 77.5E	10km	4.3	Kullu
27.8.16	03:38:15	31.4 N, 77.4E	10km	4.2	Kullu
27.8.16	7:07:21	31.3 N, 77.6E	10km	3.7	Rampur (Shimla)
04.2.17	12:35:01	32.6 N, 76.6E	10km	3.5	Chamba

.

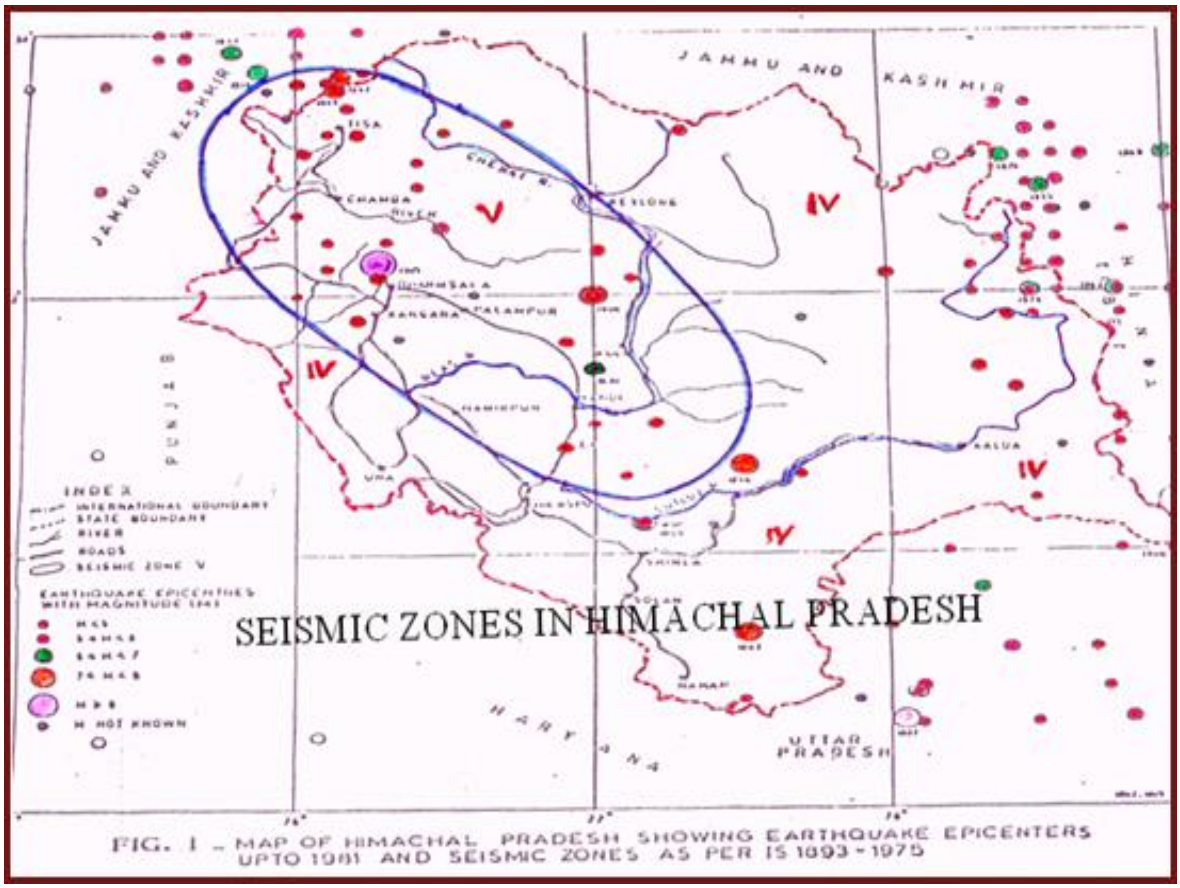

Figure 5: The seismic zones existing in the area during 1893-1975; whereas the area covered by blue coloured ring was more active during for this period.

A good effort has been made by various research organizations in instrumental monitoring of earthquakes during last three decades or so, but not much effort has been given to identify the tectonically/geochemically active faults producing many damaging earthquakes in our country, which appears more important from earthquake hazard mitigation point of view. The proposed study will summarize and conclude the health effects and the potential benefits of radon and its progeny for fault delineation studies in Mandi and Dharamshala region of Himachal Pradesh, North West Himalaya, INDIA.

1.6 Study Area:

The collision of the Indian and Eurasian converging plates results in to the high seismicity and associated geological phenomena along the Himalayan belt. This collision

lead to geological and tectonic formations including major thrust planes such as the main central thrust (MCT), the main boundary thrust (MBT) and Himalayan frontal thrust (HFT) [Gansser, 1964]. The main area of Himachal Pradesh which includes both MCT and MBT are Dharamshala region and Mandi region of Himachal Pradesh (figure 6).

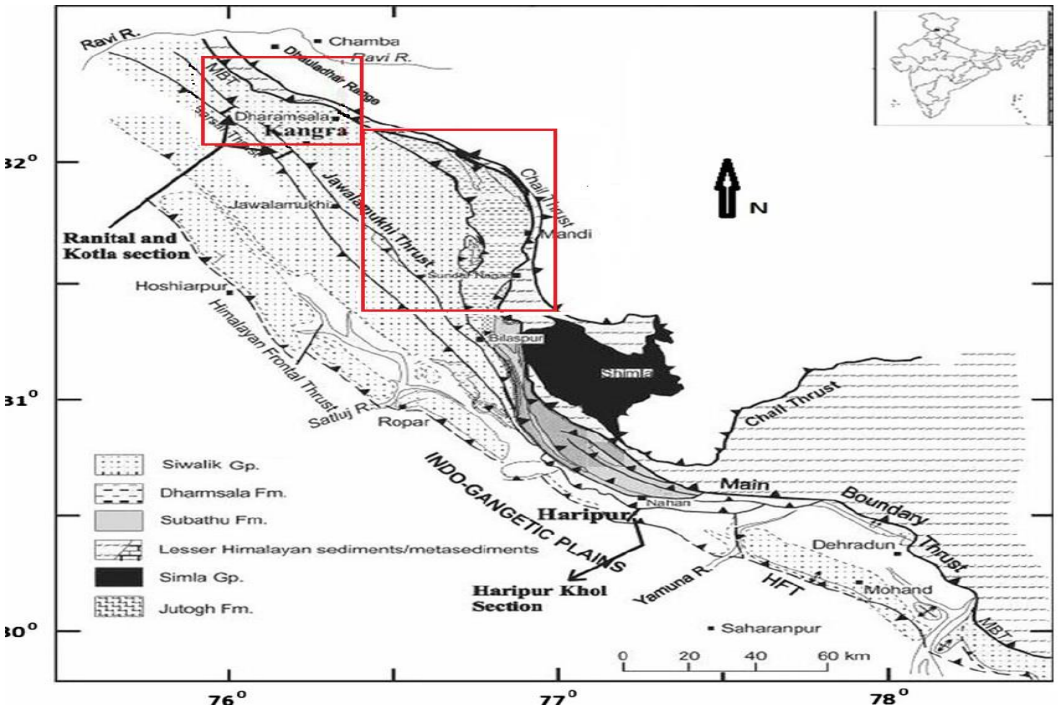

Figure 6: Geology of study Area [Gansser, 1964].

1.6.1 Active region of Kangra (Dharamshala region):

Dharamshala area (32˚13′N, 76˚19′E, D/SW) of the NW Himalaya lies on the southern slope of the Dhauladhar range. The geology of Dharamshala area which forms a part of lesser and outer Himalaya is characterized by the occurrence of the following formations. Dhauladhar granite, Chail formation Dharamshala traps, Dharamkot limestone, Sabathus, Dharamshala group and Shiwalik group. Diverse lithology with in small region makes this area tectonically and environmentally significant. Diverse lithology [Mahajan et al., 1997] within a short span of distance makes the study area tectonically and environmentally significant and shows the features of ductile shear zone due to the presence of distinct. Thrust planes. From south to north, these are MBT-2 (locally known as Drini Thrust), MBT and MCT (locally known as Chail Thrust). The individual formations and groups are separated from one another by longitudinal thrust systems

[Mahajan and Virdi, 2000] and the area is cross-cut by transverse faults/lineaments trending northeast–southwest. Kumar and Mahajan [2001] have correlated the Kangra earthquake (1905) and the Dharamsala earthquake (1986) with MBT and its subsidiary Drini thrust in the northeast to southwest direction while the Dharamsala earthquake (1978) is correlated with a transverse fault.

1.6.2 Active region of Mandi:

The Mandi is situated between (31°13′26″- 32°04′22″ north latitude and 76°36′08″-70°23′26″ east longitude). Which includes the various thrust and fault systems Especially MBT (Main boundary thrust), Chail thrust, Palampur thrust, Galma thrust, Riwalsar thrust and fault systems. These faults and thrust are formed because of collision of Indian and Eurasian converging Plates [Gansser, 1964]. This district lies partly on rocks belonging to the central Himalayan zone some part of district lies on tertiary shales and sand stone. The rocks or the central zone consist of slates, conglomerates and Krol group of Shimla area. The stand stone and shales of sub Himalayan zone belonging to the Sirmaur series (lower tertiary) and to the Shiwalik series (Upper tertiary). The Rock formation found in Mandi district lay in strike continuity of those in the Shimla Himalayas and can be classified in to the sub Himalayan series, comprised of tertiary rocks and the Himalayan series of unmetamorphosed sedimentary rocks. In the northern Mandi, there are some red slaty shales, which are known as urla red slate. These are succeeded by maroon coloured shales. This district lies partly on rocks belonging to the central Himalayan zone some part of district lies on tertiary shale and sand stone. Rocks of area represent the Palaeoproterozoic period and are strongly foliated with well-developed augen-gneiss, Sericite- chlorite, carbonaceous slates with lime stone residues, Phyllite quartzite, mylonitic gneiss and porphyroblasticbiotite gneiss with non-foliated granitoids. These types of Geological formations near MCT are cause of some geothermal regions in Himachal Pradesh. The high intensity of Thermal energy ($>100mW/\mathrm{m}^2$) with temperature gradient of more than $200℃/km$ have been observed at some places in north west Himalaya [Shanker, 1988]. The areas where aquifers are situated near to earth surface geothermal sources like, Manikaran in Kullu and Tatapani in Mandi district formed. Whereas micaceous purple clay and silt with intrusive granite

are found near MBT. The region under study has a good average rainfall (about 1331.5mm as compare to Himachal Pradesh's average of 1251mm) including more than 2000mm in the Jogindernagar belt hence a good quantity of the fresh water is seeped to the ground, when this feature is added to high porosity at certain places, unconfined aquifers situation is formed, which causes the elevated ground water levels around MCT and MBT in Mandi district [Walia et al., 2005; Chandrasekharam et al., 2008]. The Rocks in this area are the oldest types of rocks that exposed in Himachal Pradesh, they comprised and characterized dominantly by interstratified basic lava flows of the Mandi-Darla Volcanic and purple coloured arenaceous sediments with argillites [Geology and Mineral resources of Himachal Pradesh, 2012].

Mandi district is rich in mineral and is famous for its salt mines. There are three mines of rock salt in district at Migal, Drang and Guma towards Palampur from Mandi. Besides the salt mines, a number of minerals like coal, clay, copper, gold, iron ores, dolomite and slates are found in the district. Of these, only lime stone is available in the large quantity.

The area is 3950 sq km. This district is Divided into nine tehsils and seven sub-tehsil; Kharsog, Chachyot, Mandi Sadar, Sundernagar, Padhar, Lad Bharol, Thunag, Sarkaghat, Jogindernagar, Dharampur and Sub-tehsils at Kotali, Aut, Nihari, Balichowki, Sandhol, Baldwara. [District census hand book, Kullu and Mandi, 2011]. Figure 7 shows the location of different tehsils and subtehsils of Mandi District. According to the 2011 census Mandi district has a population of 999,518 roughly equal to the nation of Fiji or the US state of Montana this gives it a ranking of 446th in India (out of a total of 640 The district has a population density of 253 inhabitants per square kilometer (660 /sq mi) [District census hand book, 2011; The wonderland Himachal Pradesh]..

Main ranges of the district are:

1. Dhola Dhar: This Mountain range runs along the eastern boundary of the district from north to south and covers more than half of the Suket territory. As this range reaches the Sutlej River it runs toward the north-east and joins the Kullu hills.
2. Ghogar Dhar: This is second largest range in the district; it contains the rock salt of Gumma and Drang.

3. Sikandra Dhar: This range includes two sub ranges Kamlah range and Lindi range.

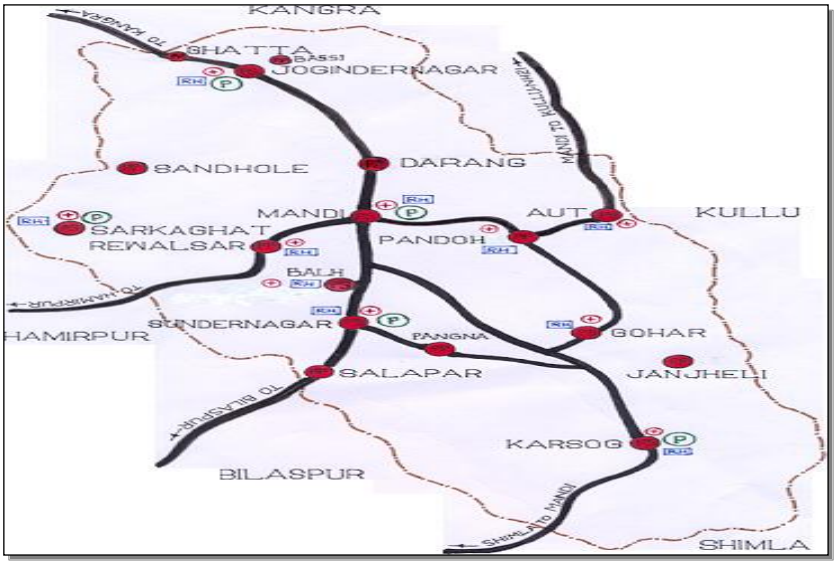

Figure 7: District Map of Mandi District, Himachal Pradesh.

1.7 Significance of the Study

The investigatory study all-round the earth since last two decades provides the evidences which indicate that anomalies in measurements of radon and other soil gases may occur in association with major geophysical events such as earthquake and volcanic events. The region under study contains the epicenter concentration-zone which includes earthquake magnitudes from below 4.0 to above 7.0.Therefore the investigation of spatial variation of soil gases, especially radon being used in present study, can certainly generate valuable information that can be quite useful in the study of tectonic activities within the earth's crust. The indoor radon measurements and radon monitoring in water in the study areas will be helpful for health risk assessments. Figure 8 shows the epicenter concentration zones in Himachal Pradesh, from map it is cleared that the major line passes through Mandi district and Dharamshala region of Himachal Pradesh.

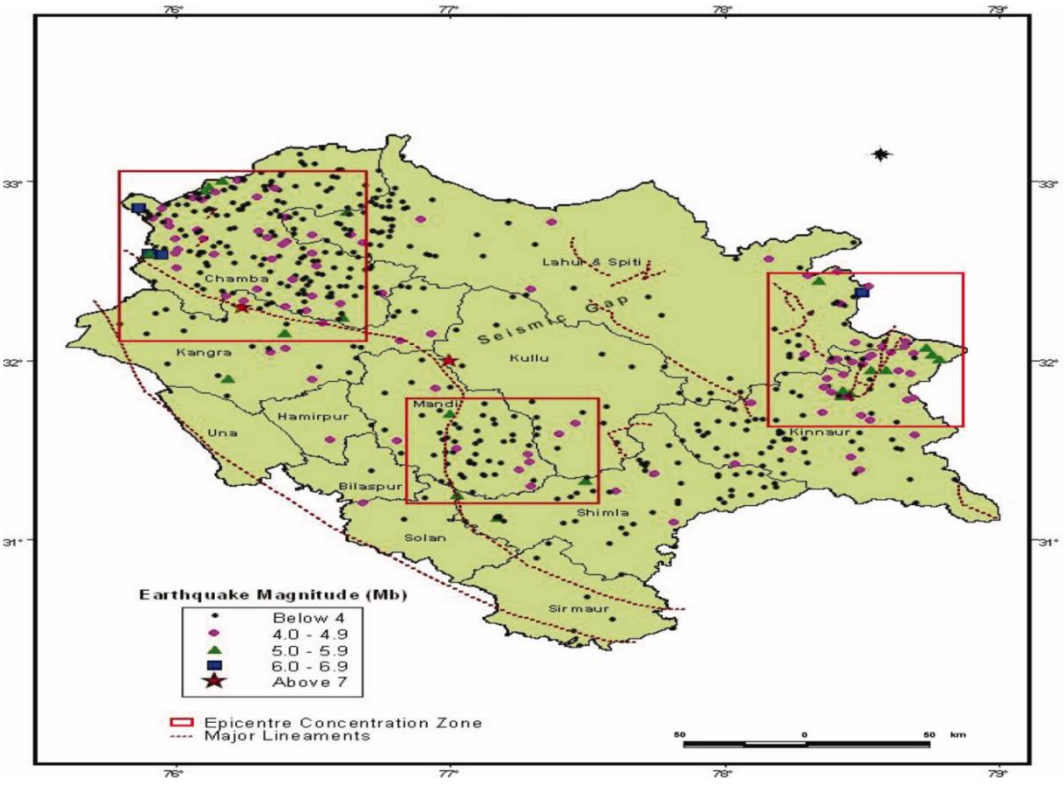

Figure 8: Himachal Pradesh earthquake epicenter distribution, 1800-2008.(ASC)

1.8 Literature Review

The research concerning the seismotectonic study using radon-thoron monitoring and health effects of these radio nuclides on human beings has received enormous attention recently. The study conducted by various researchers had shown that the anomalous behavior of radon concentration measurement in soil-gas and groundwater resources may be a reliable precursor for an impending earthquake. Since earlier prediction of earthquake may or may not be possible, Still prediction research has increased our understanding and acknowledgement of source mechanisms, complex structure of faulty zones, its recurrence frequency or interval and next expectation at a given location.

Soil –gas radon study

Study related to soil gas which has been carried out by some researchers is as follow:

Balducci et al., [1994] had continuously monitored ^{222}Rn concentrations in the soil gas from December 1990 to May 1993 at nineteen stations of Garfagnana valley (Central Italy). The Garfagnana area represents the inner margin of the Apennines (Northern Apennines are characteristics by a passive subduction plate margin) which is the locus of seismicity mainly related to the major normal faults that constitute the Serchio area. This area includes deep ground water circulation and because of seismicity of this area helium and radon concentration in water is high. The radon concentration along fault was carried out by passive methods including solid state nuclear track detectors which were made of nitro cellulose and polymers. The alpha particles which were created by decay of radon/thoron formed the tracks on the films. The tracks were chemically enlarged and counted using optical microscope and spark counter and then converted into radon concentrations. The track density patterns that were resulted from the study showed that high radon anomaly could not always be related to the activity of fault, some time weather/climatic condition also affect its concentrations. Finally they concluded from their study that during monitoring period no significant correlation was observed between measured value of radon concentration and between seismic events recorded in the area.

Ciotoli et al., [1998] used as combined approach of geochemical and structural morphological methods to analyze the clay sediments in the ofanto-valley of southern Italy. In their study they analyzed soil gas samples for CO_2, Rn and He concentrations to correlate these concentrations with faults and tectonic features of the area. Such correlations were found to be agreed with the geology of the ofanto valley in Italy.

Al-Tamimi et al., [2001] sampled the radon anomalies in five different locations in limestone area of Jordan using SSNTD's CR-39. Radon levels near traceable fault planes were measured higher by a factor of 3-10 than away from faults. The study concluded that radon gas is proved to be a good tool for fault zone detection.

Kies et al., [2002] monitored radon signal due to variable pressure and stresses applied to rocks of the earth's crust which causes local deformation of crust. The radon signal due to variable pressure and rock stresses was measured in a natural laboratory under reservoir at Vianden Power station in Luxemburg using GM counter. The power station of Viandan is situated in the Devonian of northern Grand Duchy of Luxemburg. Water

was pumped regularly from the lower river reservoir in to upper reservoir which fed the electric power turbines. Water roofed bottom of the reservoir contained the drainage systems and accessible gallaries, which were partly cut to the rocks. The work of these rocks is to collect the seepage water with the measured discharge rates. During first study, radon was measured at different places in one of these galleries. To avoid temperature induced air movements [Kies and Massen, 1999] 1m deep vertical boreholes of 10 cm diameter were drilled through the concrete floor of gallery into the bed rock. In these boreholes radon concentrations were measured by indirect methods RM-80 Geiger Muller counter. Comparison of alphaguard and sarad radon monitors in the radon room and simultaneous measurement with a flow through radium radon monitor (radium) in a borehole showed a good correlation between radon concentrations and gamma dosage from Geiger counters. Conclusions were drawn from two types of radon monitoring, first from permanent borehole where radon was continuously monitored for 2 years and second monitoring from represents the results obtained from the other recently drilled boreholes. With the variations in water levels the significant variations in radon concentrations in borehole was observed. In case of localized loads, a small effect on water level was anti correlated with the radon concentrations, modeled by a small- scale interactions with a high response time. The changing water levels of reservoirs have a much higher influence on radon levels. Long- scale interactions through a macro scales network of clusters of cracks and fractures may be responsible for these observations. In their study they concluded that radon concentration can be influenced by small scale grain interaction, when grain scale defects interact with stress energy.

Hernandez et al., [2004] had carried out soil gas (radon) surveys in Candas caldera, Tenerife, Canary Island of Spain in summar seasons in 1992 and 1995. These surveys were made using SSNTD (cellulose nitrate films) and Emanometry techniques. For 1992 the results for radon concentration were ranged from 1.0 to 1990 pci/l and in 1995 radon concentration results were ranged from 0.1 to 618 pci/l. There was difference in the radon concentrations were due the passive counting and accumulative radon in SSNTD technique and active radon counting in the Emanomerty technique. The radon gas anomalies were higher near the Teide volcano, from which researchers concluded that soil gas surveys can provide evidence of presences of faults and hidden volcanoes in the

geology of any region.

Gosh et al., [2007] had monitored the radon as precursory sign of a seismic event. The geological stress and strain under earth during an earthquake may increase the radon concentration in soil gas, the advantage of measurement of concentration in soil gas over its measurement in water is that its value is enriched in the soil gas and can be measured by simple Track etch Technique. The monitoring station was at 22 32'N and 88 24'E while experimentation were carried out at school of studies in Environmental radiation and Archeological Sciences and Nuclear and Particle Physics Research Centre, Jadavpur University Kolkata. The Radon was measured using CR-39 cellulose nitrate film (SSNTD) which were exposed to 48 hrs and then tracks made by radon on film were enlarged using chemical etching of 6N NaOH solution. The Tracks were counted by magnification of 100X. Finally the authors reported that radon anomalies which were other than the seismic events.

Walia et al., [2008] had made soil–gas study in the neotectonic fault zones in Dharamsala area, NW Himalayas, India. They measured the helium and radon gas activities using ionization chamber and an ASM 100HDS. Forty soil samples for this purpose were collected at depth of 0.7-1.0m. in sample bags. They reported the anomalous behavior of radon and helium near tectonic structures and at different lithography of soil.

Cinti et al., [2009] carried out a geochemical survey on thermal water resources in Beas and Parvati valleys of Kullu district of Himachal Pradesh and Sohana Town of Haryana to study the fluid geochemistry along faulty zones in these areas. The specific aim of the study was to observe the origin of emerging fluids, trace elements, to reconstruct the circular paths, to study rock-water interactions and to observe ground water geochemistry keeping in view the fault systems of the area. In their study they collected six thermal water samples from Beas and Parvati valley and one Thermal water sample from the Sohana village of the Haryana. The parameters like Temperature, pH, electrical conductivity, alkalinity, acidity and presence of different cations and anions were determined in the collected samples using mass spectrometry technique. The geochemical analysis of thermal waters from Beas and Parvati valley along with the Sohana spring showed that:

(a) The presence of faults and fractures in the zone causes easy upward movement of thermal fluids.

(b) The discharge temperatures are higher in the Parvati valley as compared to Beas valley and Sohana Spring.

(c) At Sohana spring the water was having high salinity which was supported by the high He concentration.

(d) Large amount of dissolved hydrogen were detected in Beas, Parvati valley and Sohana spring.

Singh et al., [2010] carried out the continuous monitoring of radon gas in Sarol and daily monitoring of the radon gas level in water at Banikhet in chamber valley NW Himalaya, India. Soil gas was measured by Barasol probe and radon activity was measured using RAD7 detector. The study was related to the correlation of radon anomalies in relation to the seismic activities. They also have studied the effect of different physical parameters on radon concentration. The radon anomalies have been correlated to the seismic events of 2.2 to 5.0.

Mahajan et al., [2010] aimed to access the relationship between variation in radon and helium with newly developed neotectonic features in Nupur and Nabha area of north west Himalayas. During their survey they found that Nabha area shows higher values of radon and helium concentrations along Himalayan Frontal thrust as compared to nearby regions. Concluded that there exist some faults along HFF. According to them the MBT is more active than HFT. The study also revealed that radon and helium gas profiles can provide the information about deformation of tectonic zones.

Vaupotic et al., [2010] had studied the radon concentration in soil gas and radon exhalation rates along Ravne fault in NW Slovenia. This fault is responsible for elevated seismic activities at the Italian- slovne border. In this Paper they presented the radon activity concentration in soil gas, radon exhalation rates, soil permeability and gamma dose rate to estimate the influence of Fault on radon transport. Radon gas was pumped to ionization chamber by alpha guard probe and alpha pump at low flow rate therefore the contribution of thoron in radon value was negligible (55s).The concentrations of Radon in soil gas were less than mean value for Slovenia, they further stress to increase the soil

profiling and use of more database to study the fault activities in Slovenia.

Sac et al., [2011] had monitored the radon concentration of active fault in western Turkey. For this type of study they had chosen four sampling stations at Cumali, Karakoc, Doganbey1 and Doganbey2 in seismic area of Tuzla fault Line. The radon concentration was measured using LR-115 Solid state nuclear track detectors and through on line monitoring was done at monitoring station at Cumali. On line monitoring station unit was made of Alpha meter, Data logger, power supply unit and GSM modem. They found that there was linear correlation between radon emission rates and seismic activities.

Li et al., [2013] had measured the soil gas concentration of Hg, Rn, H_2, He and CO_2 at 756 sites in Tangshan area where earthquake of magnitude 7.8 was observed in 1976. The area under study was composed of complex tectonic structures and high seismic hazards zones which include earthquake epicenter and active faults. Since the concentration of gases in soil-gas can be affected by the factors like moisture contents of soil, air temperature and barometric pressure so study was performed in a period of stable meteorological conditions in North china. The radon concentration was measured with the help of HDC-B radon detector which operates on emission of alpha particles during decay of various radioactive gases. The concentration of Hg was measured by a RA-915+ Zeeman effect atomic absorption spectrometer, whereas the H_2, He and CO_2 gases were analysed with tha help of Agilent 3000 gas chromatography instrument. The result shows that there are anomalous pattern of soil gases in Tangshan along active faults. They further concluded that monitoring of soil gases can be used as earthquake precursor.

Kumar et al., [2013] had studied the radon-thoron levels in the soils of the Dharamsala area of North-West Himalayas, India using solid state nuclear track detectors (LR-115 type-2). They installed twenty five radon-thoron discriminator which contained the LR-115 solid state nuclear track detector films. The recordings of the alpha particle due to radon - thoron decay has been used to measure the radon thoron concentration. The anomalous values of radon and thoron have been reported by them near faults like MBT and MCT as well as near neotectonic regions. In this study the reported value of radon concentrations were higher than that for thoron; due to short half life of thoron it is difficult to detect it on surface from its source at greater depths. Authors also suggested

that moisture contents near to proximity of earth surface may cause suppression of thoron signal. They measured the anomalies in radon and thoron concentrations at mean value plus one standard deviation value, they ignored the anomaly at higher value according to them this may cause unnecessary high deviation.

Duggal et al., [2013] performed the analysis using gamma ray spectrometer with an NaI(Tl) detector for 40 soil samples collected from the four district of the Rajasthan for measurement of the ^{226}Ra, ^{232}Th and ^{40}K activities. The measured activity concentration of ^{226}Ra and ^{40}K in soil was higher and for ^{232}Th was lower than maximum permissible level. Radium equivalent activities were also calculated from the soil samples to access the radiation hazards. The calculated mean value of radium contents was less than recommended limit as set by organization for economic cooperation. Authors concluded that the higher values of ^{40}K in soil was due to use of potassium-containing fertilizers while the radium equivalent activities and gamma equivalents doses of the elements as computed on the basis of the guidelines set by UNSCEAR were less than the recommended safe limits.

Kumar etal., [2014] had used the twin cup dosimeter to measure the radon and thoron concentrations in the indoor environment in some parts of northern Haryana, India. Along with indoor measurement their values in soil of same environment has also been made. The indoor radon-thoron concentration was found to vary from 17 Bq/m^3-51 Bq/m^3 and 9 Bq/m^3-73 Bq/m^3 while their values in soil was found to be varied from 2.80k Bq/m^3 to 6.46k Bq/m^{3s}. They reported the good correlation between soil gas concentration and indoor radon-thoron concentration.

Han etal., [2014] had studied the spatial and temporal variations of Rn and CO_2 across active faults in soil gas in the capital area of china (38.7- 41.3° N, 114.1-119.9° E). for fault activities and assessment of seismic hazards. The area under study consists of Beijing, Tianjin, Zhangjiakou and Tangshan. Because of presence of hidden faults this area is seismically very active; several major and minor events had been reported in this area so far. Rn and CO_2 samples were collected using hollow stainless steel chambers of 3 cm diameter and placed at the depth of 80 cm, this container was attached to radon detector (which was RAD7 detector) through the rubber tubes. The sensitivity and

experimental error of the detector were 14.8 Bq/m^3 and $\pm$ 5% respectively. Soil gas CO_2 was analyzed by using an Agilent 3000 gas chromatograph (GC) which was equipped with thermal conductivity detector (TCD), with experimental error of device was $\pm$ 5% . Two soil gas surveys were conducted from August- September 2011 and September to October 2012. Monthly mean values of air temperature, air humidity, wind speed and barometric pressure and precipitation was also considered (including daily average). Authors had performed sampling of soil gas along a line of 20 m separation along with 5m separation between two measuring lines. At 188 sites sampling of soil gas was carried out in Qixinzhuang (QX), Pangezhuang (PG) and Dadangguan (DG) villages in three profiles along Xiadian fault and 83 samplings were carried out across the NEYF fault (Yanqing- Fanshan sub basin fault) where 71 soil gas samples were studied across Tangshan fault. The authors concluded that since the other meteorological parameters (pressure, temperature, relative humidity and precipitation) was almost same in two surveys therefore the increased concentrations of Rn and CO_2 may be due to the seismic activities in area. Variation in gases in the year 2011 and 2012 along Tanshan fault (in one profile) are shown in Figure 9.

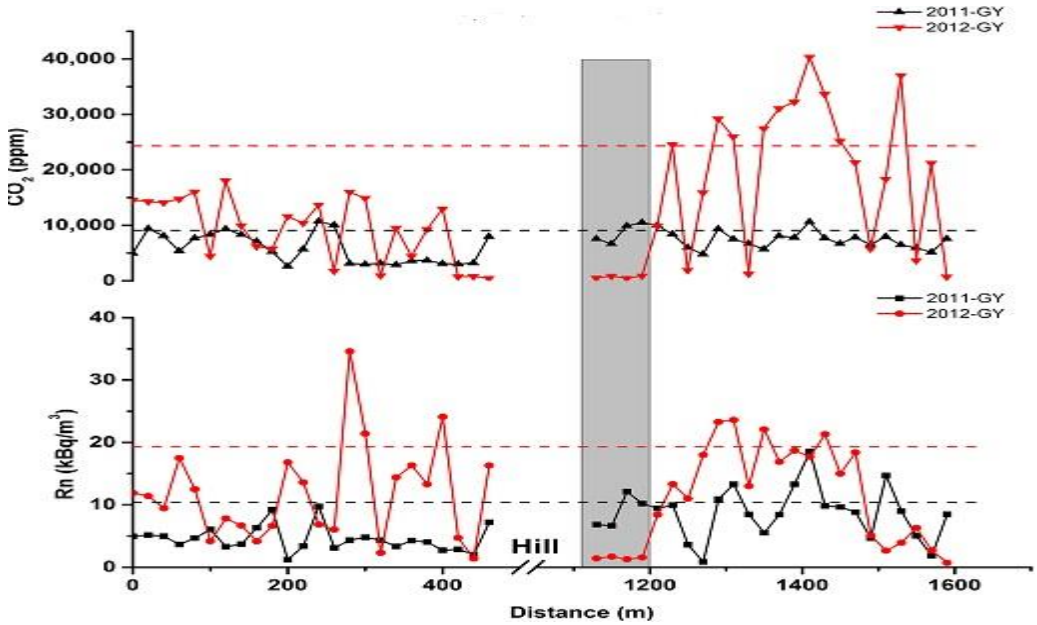

Figure 9: Rn and CO_2 concentrations along Tangshan fault in 2011 and 2012

Koike et al., [2014] studied the radon concentration in soil gas at locus of seven active

faults, the Atotsugawa (AT), Atera (AR), Nojima (NJ), Beppu- Haneyama (BH), Futagawa (FG), Hinagu (HN) and Izumi (IM) in Japan related to seismic events. Out of different isotopes of radon only ^{222}Rn was used to locate and characterize the faults because of longer life of this isotope. For this study soil samples were taken from the bottom of the bore hole after soil gas samples (the sample of Soil gas was taken from a hole with depth of 60 cm and diameter of 3 cm). The alpha- particles coming out from radio nuclei were counted using Portable scintillation counter to measure the amount of radon and its progeny. Theses samples were dried at 80℃ for 24 hrs, thereafter the samples were crushed to particle size of about 0.28mm and a specimen was extracted with mass of 150g. The radioactivity related to ^{226}Ra (with γ- ray intensity) of the soil was measured using a Ge- semiconductor counter this is because only the activity of ^{226}Ra is related to ^{222}Rn. The convective gas velocity was less in the study area that was considered the cause of shallow source inside surface. The diffusion length of radon is given by $\sqrt{(D/\lambda)}$, D (m^2/s) is the diffusion coefficient and λ (s^{-1}) is the decay constant (Lehmann et al., 2000). Using D = 5.0×10^{-6} m^2/s the diffusion length was calculated to 1.6 m. The values of ^{226}Ra and ^{222}Rn were also analyzed from the surface geology (Geological survey of Japan, 2013). A scattered diagram of the ^{226}Ra and ^{222}Rn showed a very less correlation R=0.17 this feature resulted in the interpretation that high value of radon concentration did not originate from the parent nucleus but it was due to the ascent velocity of the carrier gas. Study was concluded with the fact that enhanced radon concentration and its variation be may associated with the active fault.

Jaishi et al., [2014] had monitored the radon along the Mat- fault for the earthquake precursory studies. This fault is most active fault in Mizoram state, it cuts N-S trend of indo- Burmese arc and is traceable across entire Mizoram on the satellite and on geological mapping. The monitoring was carried out at most prominent part of Mat-fault in Serchhip district along Serchhip-Thenzawl road, during July,2011 to May,2013. The radon monitoring was done by LR-115(II) solid state nuclear track detectors, which were placed in the dosimeters developed at BARC, India (Figure 10). The multiple analysis of radon data collected from (Mat bridge and Tuichang) along Mat fault, with other meteorological parameters (relative Humidity, temperature and pressure) provided the evidences of radon anomalies with seismic events. At Mat Bridge authors correlated 57%

of radon anomalies with seismic events and at Tuichang 28.6% anomalies could be correlated. They concluded that Mat bridge area is highly seismically active and need to be regularly monitored.

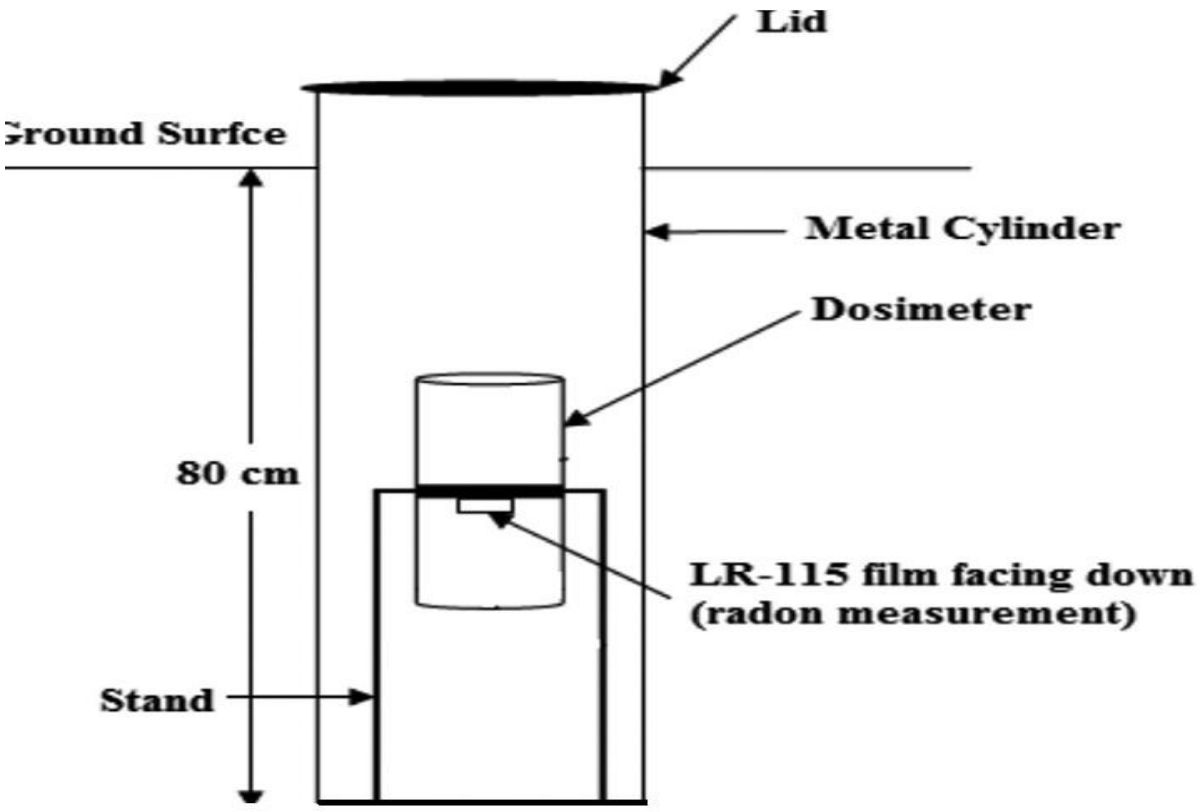

Figure10: The dosimeter used to monitor the radon concentrations along the Mat-fault.

Piersanti et al., [2015] presented the result of continuous radon monitoring for long term which was started in year 2010 and ended with 2013 in a seismically active area. Authors employed both cross- correlation and correlation to find out possible link between radon anomalies, seismic events and metrological parameters. The area where the study was performed contained the 60 km long fault system Alto Tiberina fault (ATF) in the Umbria- Marche region of Italy. The measured value of radon concentration ranged from less than 50 to more than 500 and with in the range of 100 to 300 for the most of the measurements. During the tine window of three events $M_L > 3.7$on August 26, 2013, $M_L > 3.9$ on December 18, 2013 and $M_L > 3.9$ on December 22, 2013 (Figure11) they observed no radon anomaly before and after the events. However the radon concentration

was decreasing continuously before the event and at the time of event its value was increased. The reason behind this pulse was that the rocks under fault were in continuous stress and when the stress was released the radon concentration increased. Finally they concluded that results did not given any feasibility between local Seismic activity and single radon anomaly, but there were more or less evidences of correlation between seismic moment release activities and anomalies in measurement of soil gas radon concentrations.

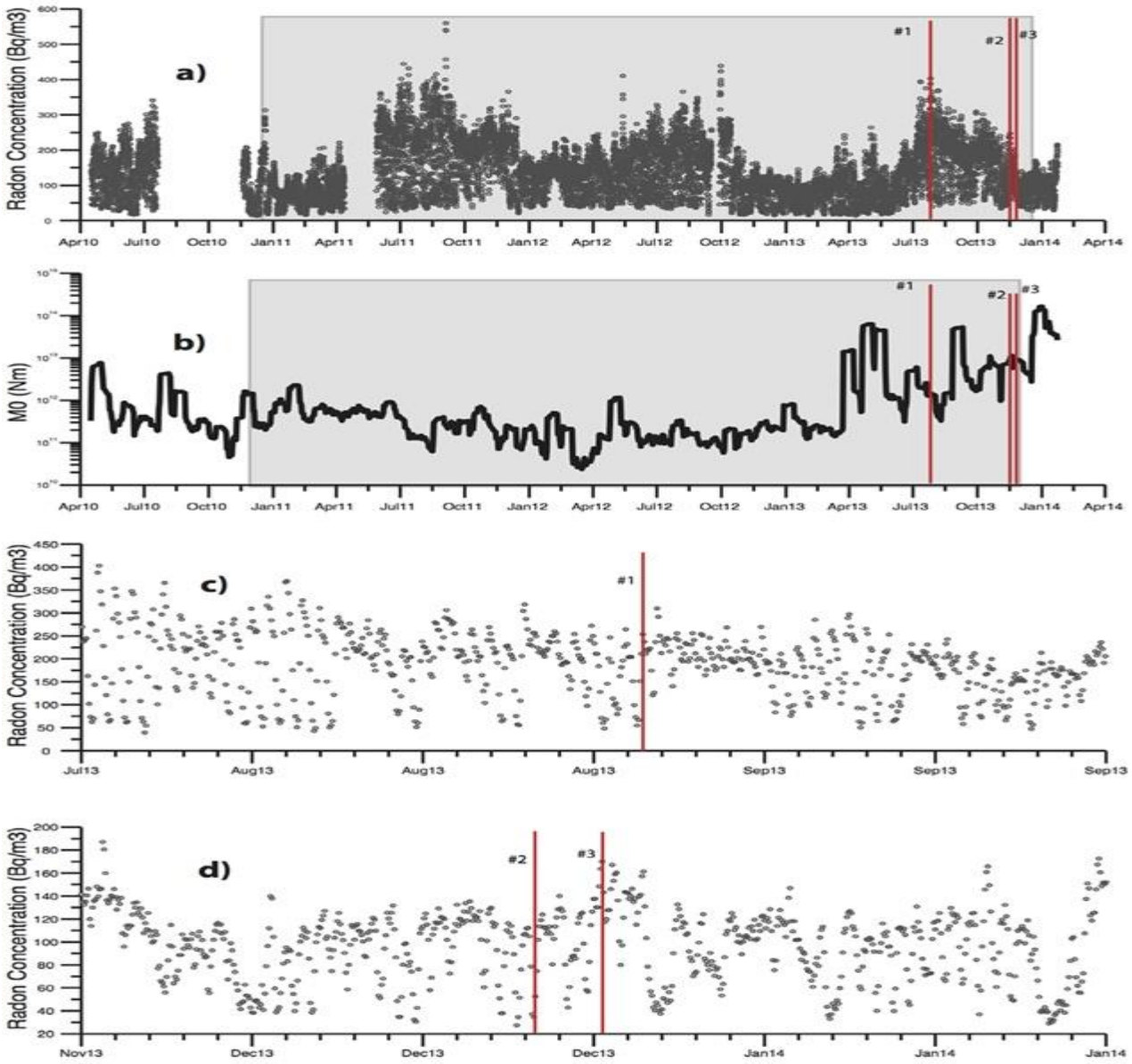

Figure 11: Radon time series between 2010 to 2013 at radon measuring station in Italy.

Ciotoli et al., [2016] were carried out soil gas observations for ^{222}Rn, ^{220}Rn, CO_2, CO_2 flux to study post gas release at earthquake centre (M_L = 6.0) of 24th August, 2016, large part of the Central Apennine between municipalities of Norica (PG) and Amatrica (RI) in Central Italy was affected due to this earthquake. The aim of such experimentation was to explore the migration mechanism of different gases from active fault. The soil gas observations were made in September with average temperature of 25℃. Total of 50 soil gas samples and 69 CO_2 flux measurements were made along two profiles. The soil gas samples were collected using 6.4mm thick walled stainless steel probe pounded in the soil at a depth of about 0.6 to 0.8m by using co-axial hammer, then these soil samples were pumped into portable devices with a pumping speed of 1L/min. Radon and thoron were measured using Durridge RAD7 detector, while other gases are analyzed using Draeger X-am7000 device. The CO_2 flux measurements were carried out using the west system accumulation chamber equipped with CO_2 Infrared sensor. The higher values of concentrations were reported for ^{222}Rn, ^{220}Rn across the buried part of fault whereas lower mean values occur across the active part (Figure 12 and Figure 13). However the nearly equal average CO_2 concentrations were observed along both profiles (figure 12).

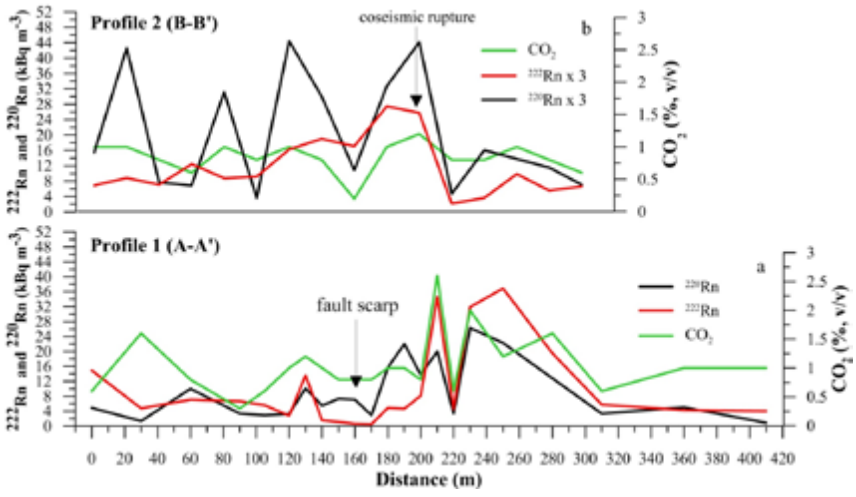

Figure 12: Radon, thoron and CO_2 concentrations along both profiles.

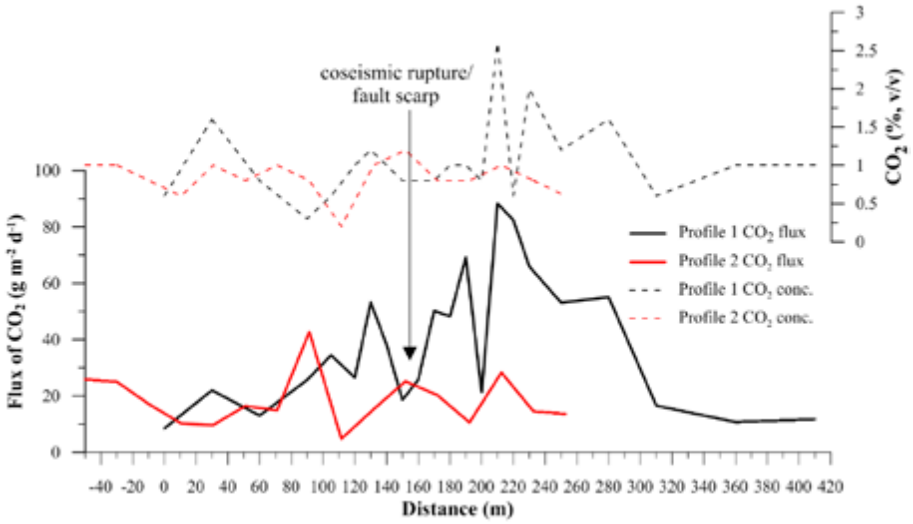

Figure 13: Comparable CO_2 flux value and CO_2 concentrations along both profiles.

Radon measurement for health hazard assessment

The numerous studies of radon concentration (for indoor radon concentrations and in waters samples from water resources) have been made in different countries for health hazards and their relation to seismic activity by various researchers all over the world. The contribution of some of them are briefed as

Singh et al., [2001] recorded the ^{222}Rn concentration activities in dwellings of uranium rich, Kullu area of Himachal Pradesh (77.06° E and 31.54° N). The geological strata of Kullu includes quartzite overlain by chlorite schists and gneisses (including some traces of Pitchblende). For indoor survey they have chosen 15 villages and about five to Nine houses in each village were considered for survey. The study was performed using LR-115 type-II detectors (SSNTD) which were suspended in room at the centre at about 2.0m above the ground level. This value was compared with recording made by four other pieces of detector film which were placed on the four walls. After exposure of three months these detectors were removed and chemically etched in 2.5 N NaOH solution for 120 minutes at 60℃ and finally these tracks were counted at a magnification of 400×. Beside this study a continuous monitoring of radon for seasonal variation was

also carried out at village Jaree from May, 93 to May, 94. The measurement is also performed by using γ-ray scintillation counter.

About 78% of houses during the survey resulted in radon concentration less than recommended action level (< 600 Bq/m^3) and only 22% of houses were having radon concentration above the recommended values of ICRP. The annual effective doses received by the people of area were well within the permissible range (3-10 mSv) per year as recommended by the ICRP. However the doses received by the residents of Balsari village were higher than the recommended limit, according to authors which may be due to the higher value of uranium contents in geology of the area. The ratio of radon concentration in winter to summer season at Jaree village was 1.54, this difference was due to poor ventilation condition of the houses which may gone worst in winter.

Singh et al., [2005] have been made the indoor radon studies in dwellings of Bathinda district of Punjab along with the radon exhalation rates. The indoor radon was measured using LR-115, type-2 detectors while radon exhalation rates and concentration of radon were carried out using can technique. They concluded that there was a positive correlation between uranium concentration and radon exhalation rates of soil.

Singh et al., [2005] carried out the indoor radon measurements in 105 dewellings of 21 villages of Mukatsar and Ferozepur district of Malwa region, Punjab using LR-115,type-2 detectors in bare mode. The seasonal variation for study showed that there were higher values of radon concentration in winter and lower in summer. The indoor radon values investigated by them were more than world average 40Bq/m^3 as suggested by UNESCEAR, [2000] .

Popit et al., [2005] Performed geochemical and geophysical monitoring in thermal water at Zatolmin and Bled (NW Slovenia) they continuously monitored radon concentrations, Electrical conductivity, Water temperature, ionic concentration, pH and Eh per hour as well as changes in these parameters per month with an aim to relate these parameters with seismic activities. Slovenia itself lies at the junction of European, Adriatic and Tiszian tectonic plates, the intensity seismic event was observed in this area in 1895(VIII-IX MSK) which damaged the city of Ljubljana. Radon concentration is

measured continuously with a Barasol MC 450 probe (Algade france). Radon enters the detection chamber through a filter, which prevents radon decay products from entering the chamber. The detection of radon is made by SSNTD unit through the alpha counting. The sensitivity of the radon detector is 50Bq/m^3 and temperature is measured to an accuracy of $\pm 0.01℃$. The conductivity and water temperature were measured per hour with EC electrical conductivity sensor with sensitivity factor of 0.01μs/cm. Eh and pH are measured monthly by portable redox combination electrodes. The ionic concentration was measured by Inductively coupled Mass spectrometer (ICP/MS). After performing this type of study they concluded that most of variation in these parameters was due to non seismic events like chnges in the rainfall levels and level of Tolminka river in the vicinity of monitoring stations. However radon concentration was always above 1σ and in few times it was reached up to 2σ over the mean value in the period between June to November, 2002. But between January and April, 2003 radon level was constant up to 1σ below the mean value. If precipitation would increase the level of the radon concentration then it must be larger in March and April,2003 due to heavy rain fall in these months. Thus it was concluded that radon behaviour cannot be simply related to meteorological factors. In a period with radon levels exceeding 1σ over the mean value six earthquakes ($M_L \leq 1$) were occurred. However the changes in other parameters like pH, Eh, electrical conductivity, ionic conductivity and water temperature in the thermal spring of the Bled showed no correlation with meteorological parameters.

Zaher et al., [2008] studied the variation in the radon concentration in ten houses of Alexandria city Egypt. The houses were taken such that there may not be any variation in construction material of these houses. They have reported the radon concentration level from 38.62 to 120.39Bq/m^3. They concluded that radiation doses have negligible effect on health's peoples of study area.

Badhan et al., [2010] calculated the radon concentration in ground water using RAD7 and assessed indoor concentration of radon in the environment of NITJ Punjab, India, using LR-115 type-2 detectors. Average value of Indoor radon concentration measured by them was 124.50Bq/m^3 and radon concentration in water was found to 5143.33Bq/m^3.The study made by them concluded that there is no correlation between

the pH value of the water and radon concentration in it.

Mehra et al., [2010] had studied the radon levels of ground water and they correlate it with indoor radon levels in dwellings. Their study was related to measurement of radon concentrations and its health hazards at the sites selected from some villages and towns of Hoshiarpur district of Punjab, India. They measured the radon levels using RAD7 detector, in this technique they collected the water samples in sealed radon-tight bottles of 250ml capacity. The measured radon concentrations from 2.03Bq/l to 6.65 Bq/l with mean value of 4.27Bq/l whereas the indoor radon varies from 10 Bq/m^3 to 28.2 Bq/m^3 with mean of 20.28Bq/m^3. The measured value of indoor radon levels in drinking water are well within the safe limit. The variations in radon concentration was appeared due to use of building materials used for construction of house and the degree of their ventilations.

Akoto et al., [2011] have been measured the Indoor radon concentration, the annual effective dose, the annual dose equivalent rate to the lung and populace risk in sandcrete houses of Dome in Ghana using time –Integrated passive radon detector using LR-115 type-II solid state nuclear track detector. They installed the detectors for 3months. The annual effective was found to be (14.13±0.22)mSv/y. they reported ventilation condition and life style of people affect changes level of radon doses to population.

Gupta et al., [2011] installed the fifty seven Solid state nuclear track detectors LR-115 type -2 at different occupant dwelling of Delhi for100 days in order to Monitor the indoor radon and its progeny concentration. They reported that radon concentration varies from 43.5 to 334.5 Bq/m^3 in their study.

Ramola, [2011] had measured the radon thoron and their progeny in some houses of Garhwal and Kumaun Himalayas of India. The experiment was carried out by solid state nuclear track detectors. SSNTD films were placed inside twin cup radon dosimeter, which used these film in bare mode, filter mode and membrane mode. The films were placed the dosimeter at a height of 2.5m from the floor for a exposure time of three months. Then the SSNTD films were chemically etched to enlarge the tracks. Finally these tracks were measured using spark counter. The radon thoron and their progeny

concentration were calculated by using the following equations:

$C_R = T_m/(d\sigma_m)$, $C_T = (T_f - d\, C_R\, \sigma_{rf}) /(d\, \sigma_{rf})$

$R_N = C_R\, F_R/3.7$, $R_T = C_T\, F_T/0.275$

$F_R = 0.104f_{RA} + 0.51f_{RB} + 0.37f_{RC}$

$F_T = 0.91f_{TB} + 0.09f_{TC}$

Where T_m = Track density of film in membrane mode, d = exposure time, σ_m = Sensitivity factor, T_f = Track density of film in filter mode, σ_{rf} = Sensitivity of ^{222}Rn in film compartment. C_R & C_T are the concentrations of radon and thoron, R_N & R_T refers to the progeny concentration of the radon and thoron whereas F_R and F_T are their equilibrium factors. f_{RA} ,f_{RB} and f_{RC} are the activity fractions.

The annual effective dose (mSv/y) is estimated by using following conversion

$D = 0.07\times [(0.17 + 9F_R)\, C_R + (0.11 + 40F_T)\, C_T]$

After such type of study author concluded that radon ,thoron and their progeny concentrations as well as effective doses in the study area were higher than the world average but below the recommended values of ICRP.

Akbari et al., [2013] had monitored the radon under different ventilation rate using continuous radon monitor(CRM). In this study they used computational fluild dynamics software package to stimulate radon entry into the building. The experiment showed that air change rate, indoor temperature and moisture significantly affect indoor radon concentration.

Abojassim, [2013] studied the radon concentration in water sample from Kufa city of Iraq, where the sampling sites were selected using GIS system using RAD7- H_2O detector . This study was performed for about period of one month. It was found that the range of radon concentration for the study area was (3.9 ± 0.432 to 2.26 ± 8.876)Bq/m^3. With effective dose between 0.54834 and 31.7756 μSv /y. These results were well below the reference levels of 1mSv/y. The researcher concluded his study with the fact that

drinking water in Kufa city is safe for consumption.

Mehra et al., [2014] performed the radon measurement related to indoor concentration and soil concentration in Hamirpur district of Himachal Pradesh using RAD7 and solid state nuclear track detector. The average value of indoor radon was 189.43Bq/m^3 while radon concentration in soil was found to be 462.56Bq/m^3. They reported a good correlation between levels soil gas radon and indoor radon (R^2 = 0.726).

Kitto [2014] from Department of Health New York has conducted the program to assist the measurement and reduction of radon concentrations in 186 schools located in Zone I for 20 years. The radon measurements were made in ground level and first floor level according to EPA recommended protocols for school buildings. The short term measurements were made using electrets type detectors, while long term measurements were made by alpha track detectors. Results of long term and short term monitoring were correlated to r^2= 0.86. The result of such study showed that majority of rooms contained radon level below 148 Bq/m^3 and less than 10% of all exceeded this level. DOH (Department of Health) has developed values of radon potential for all towns and cities in the state based on measurement and correlations to superficial Geology. DOH had also shown that indoor radon levels could occasionally be reduced sufficiently through simple adjustment of the Heat/ Ventilation system. The school representatives were also properly educated to reduce the radon concentration levels in rooms.

Chauhan et al., [2014] aimed to implement CFD based modeling for studying indoor radon gas distribution. The study had made the comparison between experimental techniques a CFD modeling based on spatial distribution of in model test room (dimensions 3.01m x 3.01m x 3.0m). The active and passive monitoring of radon concentration was found to be quite close to CFD predicted results.

Kumar et al., [2014] had worked for measurement of indoor radon concentration from measured radon concentration from measured exhalation rates of building materials calculated using different models [Nazaroff and Nero, 1988; Stoulos etal.,2003; Sahoo etal., 2011] and d/L values for walls and roofs of different dwellings. The results showed that the radon concentrations predicted by models agree with experimental value (which

were measured by calibrated pin hole based radon –thoron dosimeter).

Saidu et al., [2014] had carried out the radon measurements in the uranium regions of Poli and Lolodorf where uranium deposits were lied before their exploitation. They measured indoor radon concentration in 103 and 50 dwellings located in Poli and Lolodorf using E-PERM electret chamber detectors. The radon concentration so measured ranges from 29-2240 Bq/m^3 in Poli and 24-4390 Bq/m^3 in Lolodorf [68].

Kumar et al., [2016] carried out indoor radon equivalent concentration monitoring in three different areas Jogindernagar, Sarkaghat and Mandi- Sundernagar of Mandi district of Himachal Pradesh, India using LR-115 Type-II SSNTD's. Total 65 sample houses were selected by the researchers, thirty in Sundernagar –Mandi region, fifteen in Sarkaghat region and twenty in Jogindernagar region. They observed the indoor equivalent concentration to 94Bq/m^3 with annual effective dose of 1.61 mSv. This value was higher than world average of 40Bq/m^3. But these values were less than the action level of 200Bq/m^3-600Bq/m^3. They reported that indoor radon levels are less affected by weather conditions in comparison to ventilation in the dwellings and uranium contents in the soil of study area.

Radon Modeling

Various researchers had given their contribution to measure Radon exhalation rates and to develop theories / theoretical modeling regarding estimation of radon concentration and radon exhalation rates .

Roger et al., [1991] had developed a mathematical model to calculate radon emanation rates and its transportation which accounts for simultaneous radon emanation from a partially leached radium parent nucleus. This model deals with the diffusion of radon in gaseous and liquid phase, adsorption in solid phase, advection in the gas phase and absorption in the liquid phase. Researchers had shown that Rn diffusion through soil moisture affected by radon absorption. This absorption of radon was incorporated into Rn diffusion equation and then into RAECOM computer code, which is the recommended tool for uranium mill tailing impoundment design. In this model most aspects of Rn emanation, diffusion, advection, absorption, adsorption and their phase interactions have

been incorporated. The model is validated by two comparisons with measurement first of which included soil gas Rn concentrations and surface radon fluxes for a two region systems at the Mexican Hat uranium mill tailing pile. The second comparison is with measured surface Rn fluxes in a three region advection dominated system in the laboratory. In both calculations the theoretical results were comparable to the experimental values.

According to Rogers model at soil-gas interface the balance equation for
Rn concentration is given by:

$$\frac{dC}{dt} = D_i d^2C/dx^2 - [g/v\ p\ (1\text{-}m)]\ P \frac{dC}{dx} - \lambda\ C + [R\ p\ \lambda\ \varepsilon\ /p\ (1\text{-}m)] - [R\ m\ \lambda\ /(1\text{-}m)\ K] + T_{la} - T_{as}$$

Sun et al., [2004] collected the 7777 soil samples in grid area of approx.25x25 km^2 from china and Radon exhalation rates were measured using gamma ray spectrometer. After then they prepared a model using soil moisture and soil emanation rates, they found that the values of radon exhalation rates measured experimentally were close to their theoretically verified values. This model was developed to avoid the large numbers of field measurements. In this work the mechanism of radon emanation, transportation and exhalation in soil were reviewed and theoretical analyzed. In this model only diffusion mechanism is considered for estimated of long term average values. By considering the one dimensional steady state model foe radon transportation in soil they deduced the exhalation rate (F) as $\mathbf{F = \sqrt{(\lambda D)}\ p\varepsilon R}$ where p is soil porosity, D is radon diffusion coefficient. ε is the radon emanation coefficient and R is the Radium activity rate in the soil. Based on this model and the existing database, the annual averaged radon exhalation rate from soil estimated for Beijing was 16.7m Bq $m^{-2}s^{-1}$ where as the measured value of the radon exhalation rate was 24.9m Bq $m^{-2}s^{-1}$ the measured value of rate was 30% more than the estimated rate. They further concluded with the fact that more field measurements were needed to validate the projected model.

Valentina, [2005] had carried out the theoretical study related to the radon transport in the homogenous medium. This type of study is very essential in solving many geophysical changes. According to author if the radon concentration distribution is

known then following parameters such as the radon equilibrium concentration. Radon potential and the depth at which the equilibrium will exist can be calculated by the Flick's law using convective velocity of radon. The approach that the author had used in his study was based on the diffusion convective radon transport model. According to this model the radon concentration in the air present in the soil profile along Z-axis is given by

$C(Z) = C(\infty)[1- \exp\{-(\sqrt{\{(v^2/2D) + (\lambda/D) + (v/2D)\}z\}}]$ [Jonsson,1997]

$C(Z)$ = radon concentration (Bq/m^3), v = convective radon flux velocity (m/s) and $C(\infty)$ is given by

$C(\infty) = \varepsilon C_{Ra} \rho (1- \sigma)/ \sigma$ in this equation ε is the radon emanation coefficient, C_{Ra} = radium activity(Bq/kg) whereas ρ is soil density and σ is the porosity of the soil. To calculate the radon equilibrium concentration, the radon concentrations were measured at the height h and 2h and these concentrations were designated as C_1 and C_2 putting these values in C(Z) they calculated

$C(Z) = C_1/(2- C_2/C_1) [1- \exp\{-(1/h_1 \ln (C_1/(C_2-C_1)\}z]$, thus the value $C(\infty) = C_1/(2- C_2/C_1)$ and the radon convective velocity is given by

$V=(D/h_1) \ln (C_1/(C_2-C_1) + \lambda h_1/ \ln (C_1/(C_2-C_1)$ [Ryzhakova and yakovleva, 2002]

Zhou et al., [2006] had analysed twenty soil -samples (six- clay, six- silt and eight- sand) to study the effect of moisture contents of the soil on radon emanation rates. The experimental work was performed in controlled temperature room at 25℃. The monitoring system was consisted of radon accumulator and radon monitor. The accumulator was vacuum desiccators with a inner volume of 7 litre. The Radon monitor was a scintillation counter. After measurement of radon flux, researchers developed a model based transport theory by considering the soil as homogeneous and porous media including the factors like temperature and moisture. They combined the two representative models Roger model and Schery model. The combined model for radon flux density used in this study is as below

$$\mathbf{F = R\rho\varepsilon(T/273)^{0.75} \{\lambda Dp \exp(-6s-6s^{14p})\}^{0.5}}$$

Where R is the ^{226}Ra contents in soil (Bq/kg) , ρ is the soil bulk density(kg/m^3), T is the soil temperature (K), λ is the ^{222}Rn decay constant, D is the radon diffusion coefficient in air(1.1×10^{-5} m^2 s^{-1}), S is the fraction of pore space filled with water and p is the total porosity of soil. The radon flux density which was calculated with the help of the model suggested by Zhou et al., [2006] are well correlated with the experimental values. Annual / Seasonal radon flux densities estimated by the combined model are agreed with the measured data with $\pm$ 25% in the 10 sites. The results of model and related study indicated that suggested model is useful for estimation of radon flux densities from the earth surface.

Barooah et al., [2013] measured the radon exhalation rates, radium contents and annual effective dose due to radon inhalation in coalfield of Assam, India using LR-115 Type II solid state nuclear track detectors. The results were represented with corresponding geometric means (GM) and geometric standard deviations (GSD) with standard error. For this purpose they collected 32 samples 16 each from coal and soil side of the Dilli Jeypore Coal field mine, they reported the 0.999 correlation between radium contents and radon exhalation rates. They found these rates slightly more than the surrounding mines of area. The Dilli Jeypore coalfield is located with in a narrow belt in the foot hills, Boarding Dibrugarh and Sivasagar districts of Assam . It was also reported by them that radium contents in the soil and coal were found to be less than maximum permissible value of 370 Bq/ kg as per recommendation of OECD. Thus area is safe to construction of dwellings in accordance of concerns of radium contents .

Chauhan et al., [2014] had made computational fluid dynamics (CFD) technique to develop a theoretical model. The model was tested in test room in which radon concentration was measured using pin hole dosimeter in which LR-115 Type 2 detector was used. The results so obtained were similar to the theoretical results calculated from CFD modeling using radon exhalation rates of the building materials used for construction of house. The CFD solves the concerned fluid equations and provides solutions in terms of variables such as pressure, temperature, energy density. CFD solutions also provide the convective-velocity flow and distribution pattern of indoor pollutant. The area radon-exhalation rates from floor, wall and ceiling surface acts input

component for the CFD simulations. The distribution of radon gas inside the room was estimated using the following equation

$$\frac{dC}{dt} = s + \nabla \cdot (D\nabla C) - \nabla \cdot (UC) - \lambda C$$

Where C represents radon concentration in the room, D is turbulent radon diffusion coefficient (1.1×10^{-5} m^2 s^{-1}), U is the mean air velocity (m/s). S is the radon source term (Bq m^{-3} s^{-1}) and λ is the radon decay constant (2.1×10^{-6} s^{-1}).

1.9 Objectives of the Study

From existing Literature, it has been reviewed that the Radon monitoring can be an effective tool to delineate fault systems. As on one side it may be a precursor but on other side it has also serious health hazards. It may further be signified that solid state nuclear track detectors are one of the cheap and reliable detectors for measurement of radon concentration as passive technique, whereas for measurement of radon in water samples the active technique like RAD7 is reliable and cost effective.

From the survey of the area has been observed that fault line was passing through the Mandi district, along the border of the Kullu district. Starting from the boundary of the Kangra (from the Dharamshala where the density of all thrusts and fault systems is very high) district, this line passes through the Barot of the Jogindernagar along the Uhl river, after it from the lower of the Padoh tehsil along the border of tehsil sadar Mandi, the lower region of the tehsil Chachiyot, middle of the Sundernagar tehsil and leaves Mandi district close to Salapar near. Since presence of MCT and MBT had made this area under high stress and strain because of which various faults and fractured zones were created cross and along it. Our aim is to explore the hidden faults using soil gas technique in Mandi-Dharamshala region and develop a possible connection of soil gas radon - thoron anomalies with faults, seismic activities and health hazard. For this purpose following objectives of study were set

1. To determine the level of radon concentration in soil along fault zones in the study area.
2. To study the level of indoor radon activity in the dwellings of the study area. The seasonal variation of indoor radon activity will also be observed at selected sites.
3. To study the level of radon in the drinking water samples from the study areas (active Kangra and Mandi region of Himachal Pradesh).
4. To determine the Radon exhalation rate in soil of study area.
5. To determine the possible connection between eventual radon gas anomalies related to major active fault systems in the study areas.

CHAPTER 2

MATERIALS AND METHODS

The collected radon data when analyzed and interpreted is called as radon survey. These types of survey were used by various researchers for petrochemical traces, geothermal studies, faults and neotectonic studies, ground water survey and even for indoor radiation measurements since early twenty century. These types of surveys consume more time than direct methods but they are cost effective as well many random errors are eliminated to larger extent by these types of surveys.

2.1 Methods to perform radon surveys

Radon surveys can be performed by two methods:

1. Passive method: The detectors are placed in soil (for soil gas survey) and hanged from roofs of the room in case of indoor surveys for long time e.g. solid state nuclear track detectors LR-115 (type-II) and CR-39.
2. Active methods: In these type of methods the radon gas is pumped into a container which is connected to a counting/detecting device e.g. RAD7 and RTM 2100.

2.2 Radon monitoring Techniques

The radon is measured on the detection of α –Particles. The energy of emitting α –particles are 5.5 MeV for ^{222}Rn, 6.0 MeV for ^{218}Po and 7.7MeV for ^{214}Po. There are three types of measurements (a) Instantaneous (b) Integrating (c) continuous.

(a) Instantaneous measurement in which scintillation counter is used to measure the energy α –particle is used to detect the radon. Example is the Electronic digital counter records the radon concentrations (e.g. RAD7 and Alpha-scintillmeter GB2100).

(b) Integrating methods are used for long time radon measurements. They used the SSNTDs like LR-115 and CR-39 which provides the window only for the energy emitted by α –particle of radon only.

(c) Continuous Radon monitor are used for real time measuring of radon concentrations on the basis sampling and analysis e.g. Barasol detectors with use of semiconductor detector which uses the computer aided system with software.

2.3 Methodology used in the study

Solid state nuclear track detector Films (LR-115 type-II) which were made of cellulose nitrate used for the measurements of indoor radon level in the dwellings and soil- gas radon and thoron concentrations. It is red colored cellulose nitrate of thickness 11.5 to 12.0 μm placed on 100 μm thick polyester base. The detailed use of detector films is described below:

2.3.1 Radon concentration measurements in the Soil-gas

Experimental method for radon detection and measurement are based on counting of alpha particles those results from decay of radon and its daughter's nuclei. Both active and passive counting methods and concerning devices are available in the literature for this purpose. In our research investigations we have utilized the passive method using the SSNTD's for measurement of radon gas in the soil. These detector films are sensitive to alpha particles in the energy range of the particle emitted by radon (5 MeV to 6 MeV). SSNTD's give consistent results even in different environmental conditions as they are less affected by humidity, low temperatures, moderate heating and light [Eappen and Mayya, 2004; Kumar et al., 2013; Jaishi et al., 2014].

The LR-115 Type 2 plastic track detectors with a size of about 1.5 cm × 1.5cm were fixed at the top and bottom inside the cylindrical container of length 25cm and diameter 6cm. The sensitive portion of the detector film was freely exposed to the emergent radon so that it was capable of recording the tracks created by alpha-particles resulting from the decay of radon in the container. The detector fixed at the top of the container was capable to record alpha particles due to Radon while the other fixed at the bottom has recorded alpha particles both from radon and thoron. Container along-with the detectors was placed about 0.5 to 0.75m inside the soil, in the study region. After exposure of 15 days detectors were taken off and processed through the chemical etching to enlarge the tracks caused by alpha particles. Chemical etching was done by treating the detectors with 10% of NaOH solution at (60 ±1)ºC, for 90 min, in a constant temperature water bath. The tracks were counted by using the calibrated optical microscope and then converted in to the radon concentration in soil by using the relation [Eappen and Mayya, 2004]

0.020±0.002 tracks/cm^2 /day= 1Bq/m^3

Figure 14: Constant temperature bath and shaker (Etching bath)

Figure15: Radon-thoron discriminator (Plastic cane with side cap including LR-115 films at the top of the cane and at the bottom of the cane)

Figure 16: Placement of radon thoron discriminator during soil - gas survey (1)

Figure 17: Placement of radon thoron discriminator during soil - gas survey (2)

2.3.2 Indoor radon measurements

The LR-115 type- II detectors were cut into rectangles and fixed on glass slides. The detectors were placed in the various rooms/ dwellings of sample houses in Mandi district at a height of 2 m from the surface. The radon sensitive part of the detector was exposed to the radon; this portion recorded the alpha particles which were coming out from the decay of radon in the room.

After exposure of radon to standard duration of 90 days, the detector films were subjected to chemical processing in a 10 M analytical grade sodium hydroxide solution at (60 ±1)ºC, for 90 min, in a constant temperature water bath to enlarge the latent tracks produced by alpha particles from the decay of radon. After the etching, the detectors were placed under running cold water for 30 minutes, then washed with distilled water and finally with a 50% water-alcohol solution. After a few minutes of drying under shadow (with air), they were developed to the level of track counting. The etched tracks were counted under an optical microscope (at 400× magnification) [Eappen and Mayya, 2004; Kalsi et al., 2005].

The counted tracks were then converted in to the radon concentration by using the relation given by Eappen and Mayya, [2004].

Figure 18: Placement of detector in bare mode for indoor radon survey

2.3.3 Measurement of the radon exhalation rate

To measure the radon exhalation rates in the soil samples were collected from geological different sites of the study area, we have used the sealed cylindrical containers of radius 3.5cm and length 7.5 cm. The soil samples of 100g after drying and grinding were placed at bottom of the cylinder and then LR-115 type-II SSNTD (1.5cm X 1.5cm) were placed at the top of the cylindrical enclosures. After sealing of container, the recording for the tracks of the alpha particles was made for 90 days. After then the detectors were taken out and etched in 10M NaOH at (60 ±1) ºC for 90 min, in a constant temperature water bath. Now the enlarged latent tracks were counted using optical microscope (400 X). The counted tracks were then converted in to radon activity using the calibration factor of 0.02tracks/cm^2 /day= 1Bq/m^3 [Singh et al, 1997; Amrani and Cherouati, 1999; Eappen and Mayya, 2004]. After which the radon exhalation rates have been calculated as:

$$E = \frac{CV\lambda}{A\left[T+\frac{1}{\lambda}\left(e^{-\lambda T}-1\right)\right]}$$

Where E = Exhalation rate (Bq/m^{2}h), C= radon exposure measured by LR-115, type -2 (Bq/m^{3}h), SSNTD's. V= effective volume of the can (m^3), A= area of the can (m^2), λ = decay constant for radon (h^{-1}), T= exposure time [Singh et al., 1997; Sharma et al., 1998]

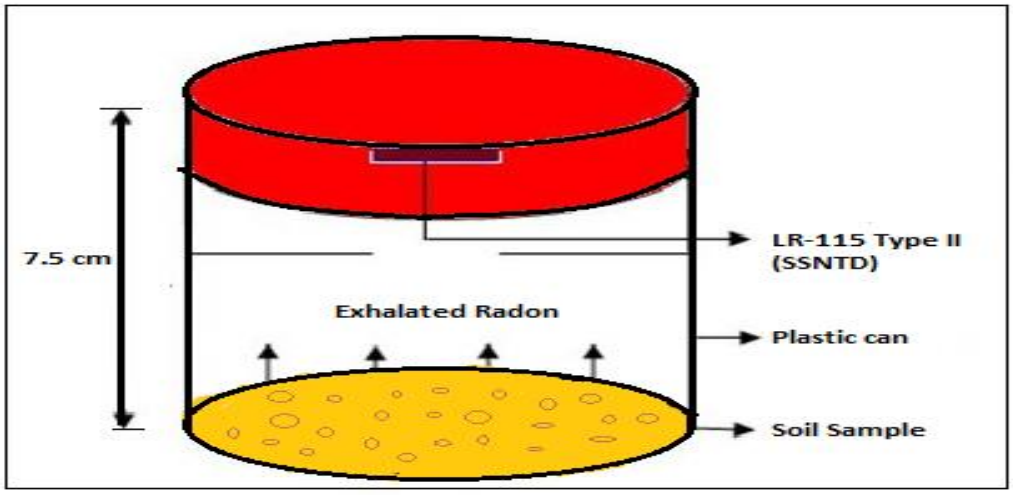

Figure19: container to measure the soil exhalation rates

2.3.4 Measurement of radon concentration in water

Ground water radon measurement in the present study was observed by using a calibrated Durridge RAD 7 (Figure 20), with special accessories for radon measurement in water. With the help of transducers the RAD7 detector converts sensitivity to alpha-radiation in to an electric signal proportional to the energy of the resulting particle, through which the alpha particles of different isotopes (^{218}Po, ^{214}Po) produced by radiation can be distinguished, application is further extended to distinguish instantaneously between old and new radon, radon from thoron, and signal from noise [Mehra et al., 2014].

Figure 20: RAD 7

(a) Preparation of the RAD7

Before taking any a measurement it is ensured that the RAD7 must be free of radon that was collected by it during last measurement and it must also be free of moisture (dry). This is achieved by purging it for some time so that humidity it shows less than 6%. Drierite desiccant is used for this process.

(b) Collection of Samples

For the measurement of radon concentration a samples of 250ml water will be collected from the study areas. The radon sampling is a difficult process in the sense that the gas easily escapes from water and so sampling is performed in such way that there should not be any aeration which might lead to radon leakage. So the water sample will be collected in such a way that there will be no bubbling.

(c) RAD-H_2O technique

The RAD-H_2O is an extension to the *RAD7* through which we can measure the radon concentration in water with a range of less than 50pCi/L to greater than 105pCi/L. Its lowest detection limit is less than 10pCi/L. By diluting our sample, we can extend the upper level of concentration to any range by diluting the sample. The equipment is battery operated with fast measurement efficiency and can be taken to any place with ease. An accurate measurement of radon in well water can be done within an hour of taking the sample. The RAD-H_2O gives results in 30 minutes with a sensitivity that matches or exceeds that of standard laboratory methods. No harmful chemicals are used in this method. In this method a closed loop aeration scheme is employed in which both the air and water volume are constant and independent of the flow rate. The air is made to circulate through the water many times to extract continuously the radon until a state of equilibrium is achieved. The RAD-H_2O system reaches this state of equilibrium within about 5 minutes, after which it stops extracting radon from the water. The setup consists of three components, the RAD7, on the right, the vial, center front, and the tube of desiccant, top left. The case provides a convenient stand for the tube of desiccant, held up between the two clasps on the lid, and also for the vial in the foam cavity. With the aeration of 5 minutes, about 95% or more of the available radon is removed from the water sample.

CHAPTER 3

SOIL GAS RADON THORON MONITORING IN ACTIVE REGION OF KANGRA

3.1 Introduction

Mapping faults and studying fault zone properties are important for seismic hazard analysis and for understanding earthquake physics. A fault is a fracture or zone of fractures that separates different blocks of crust and accumulates a seismic strain subjected to large stress concentrations. When the energy associated with the accumulated strain is suddenly released, an earthquake occurs on the fault. During most earthquakes, fault motion stays below the earth's surface, but in large earthquakes, fault motion may break through to the surface, offsetting rocks and sediments, as well as anything built on the fault, as much as ten feet or more. Knowing the location of active faults is important so that planners and developers can avoid building houses or other structures, which would be destroyed when the fault breaks the earth's surface, on the faults. The variations of radon concentrations in the soil gas has considered useful tool for earthquake monitoring and prediction in active fault zones [Liu et al. 1985; King 1986; Igarashi et al. 1995; Chyi et al. 2005; Yang et al. 2005,2011; Singh et al. 2010; Kumar et al. 2009,2012; Walia et al. 2009, 2012] as well as for tracing neotectonic faults [Ciotoli et al., 1998; Etiope and Lombardi, 1995; Fu et al., 2005; Guerra and Lombardi, 2001; Walia et al. 2005,2010]. A few studies have mentioned thoron (^{220}Rn) for the same applications due to its short half-life [La Brecque 2002; Yang *et al*. 2005]. For simultaneous monitoring of radon- thoron, various techniques (active as well as passive) have been reported in literature. However, instruments available in the market are cost prohibitive. Application of solid state nuclear track detectors (SSNTDs) for radon-thoron measurements is widely accepted [Beck and Gingrich 1976; Gingrich and Fisher 1976]. Since these detectors are affordable and have the advantage to withstand parametric changes in the atmosphere when deployed in open environments [Tommasino, 1990]. Various types of SSNTDs are used in different exposure modes for the measurement of radon. Dosimeters of specific designs have been developed using SSNTDs [Eappen and Mayya 2004; Al-Azmi 2009]. In the present study solid state nuclear track detectors (LR115 films) has been used in radon thoron discriminator for the measurement of soil gas radon-thoron at 25 locations in Dharamshala region (active region of Kangra shown in figure 21) NW Himalayas, India to check the effectiveness of this cost prohibited

technique and to know the variations of soil gas radon-thoron concentrations in the tectonically and environmentally significant area (technique is explained in chapter 2).

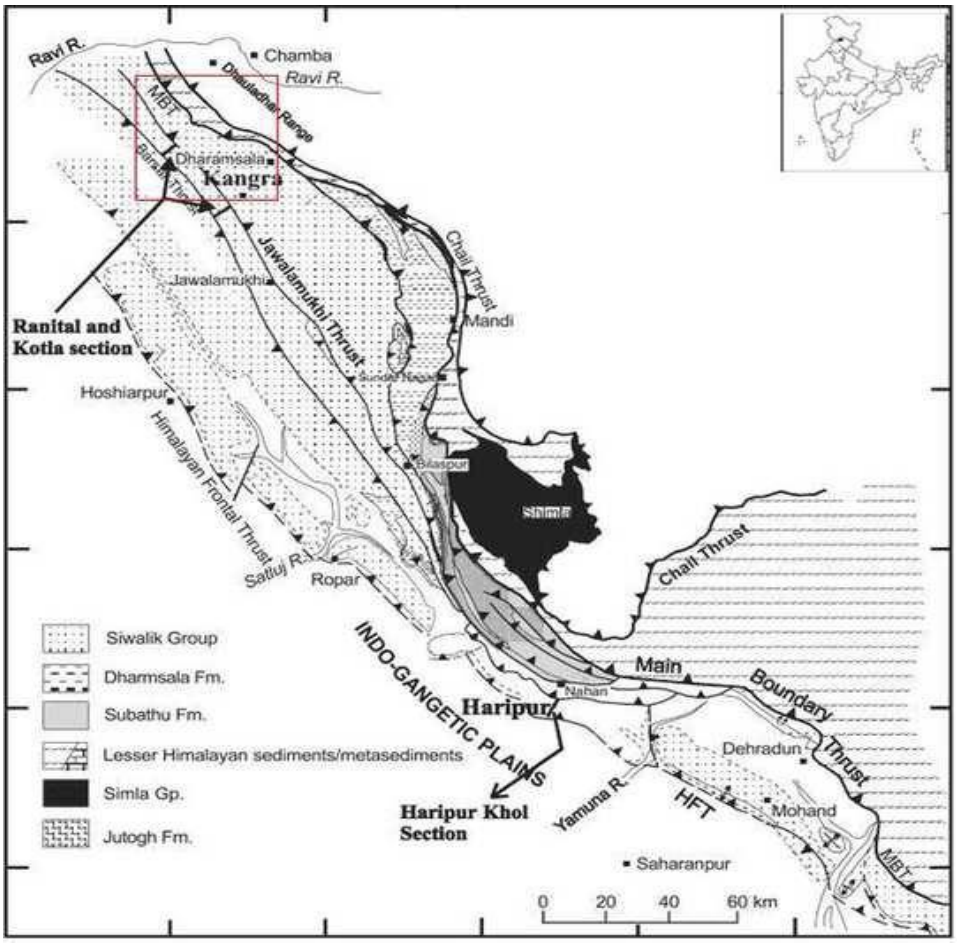

Figure 21: Geological map showing the location of study area.

3.2 Results and discussions

Soil gas measurement have been carried out at 25 locations (shown in Figure 22) in Dharamshala region using Fission Track etch technique and the results of radon and thoron gas concentration are reported in table 5.

Table 5: Radon- thoron concentration in soil at different places in Dharamshala region

S.N.	Place	Radon conc. in Bq/m^3	Thoron conc. in Bq/m^3	Latitude	Longitude	Height in metre
1	Aganjar Mahadev	6003	1307	N 32°12.62′	E 76°22.39′	1380

2	Mohli-I	5700	710	N 32°12.58′	E 76°22.27′	1348
3	Mohli-II	5553	660	N 32°12.46′	E 76°22.24′	1328
4	Chakban	8187	1704	N 32°12.42′	E 76°22.59′	1441
5	Lunta	9000	1817	N 32°12.45′	E 76°22.74′	1469
6	Darnu-I Below road	3747	464	N 32°12.78′	E 76°20.48′	1267
7	Darnu-II Below road	1743	593	N 32°12.74′	E 76°20.44′	1246
8	Khanyara-I	5080	897	N 32°12.86′	E 76°21.35′	1294
9	Khanyara-II	6887	1223	N 32°12.88′	E 76°21.53′	1334
10	Upper Khanyara	2380	643	N 32°13.15′	E 76°21.80′	1407
11	Khanyara (Near Manjhi micro Project	1873	223	N 32°13.27′	E 76°21.70′	1363
12	Darnu-I Above road	5507	527	N 32°12.86′	E 76°20.41′	1291
13	Darnu-II Above road	12827	2920	N 32°12.83′	E 76°20.45′	1283
14	Dari	5117	507	N 32°12.03′	E 76°20.20′	1150
15	Narwana Khas-I	2263	723	N 32°10.92′	E 76°24.07′	1256
16	Narwana Khas-II	2000	244	N 32°10.87′	E 76°24.05′	1248
17	Andrad (Narwana)	1593	253	N 32°10.96′	E 76°24.29′	1324
18	Narwana (home)	6597	997	N 32°10.47′	E 76°23.59′	1138
19	Near ITI	2260	290	N 32°12.07′	E 76°19.96′	1136
20	Upper Barol-I	2557	250	N 32°12.38′	E 76°19.93′	1174
21	Upper Barol-II	6387	2203	N 32°12.36′	E 76°20.12′	1168

22	Sakoh-I	13570	1320	N 32°11.69′	E 76°19.10′	1072
23	Chalian Near Jawahar Nagar	3150	963	N 32°11.44′	E 76°19.23′	1085
24	Chilghari	5757	727	N 32°12.27′	E 76°18.96′	1164
25	Sakoh Near Radio colony	6583	1243	N 32°11.72′	E 76°19.10′	1076

The recorded radon concentration varies from 1593 to 13570Bq/m3 with an average value of 5292Bq/m3 whereas recorded thoron concentration varies from 23 to 2920 Bq/m3 with an average value of 901Bq/m3. In the present study, radon has shown higher values than of thoron due to short half-life of thoron, it cannot be detected from the greater depth. Further, the effect of moisture on the film at the lower part of discriminator due to its close proximity to the surface can also be considered as one of the factors in suppressing the thoron signals. The recorded average radon value in the present study is closer to the average values of the radon reported in the Nurpur area of NW Himalayas using SSNTDs [Singh et al., 2006] whereas it is less than the average value reported in the Nurpur [Mahajan et al., 2010] and the Dharamsala area [Walia et al. 2008] of NW Himalayas using active detectors. The difference in the average radon value in the present study with Mahajan et al., [2010] and Walia et al., [2008] may be due to the different techniques used for radon monitoring. In order to identify possible threshold values of anomalous soil radon–thoron concentrations, various statistical methods have been used by different authors in the past [Guerra and Lombardi, 2001; Fu et al., 2005; Walia et al., 2005; Pereira et al., 2010]. In our context, statistical threshold values of radon–thoron gas anomalies are fixed at mean plus one standard deviation and anomalously high values were neglected, which may cause unnecessary high deviation and perturb the real anomalies. Figure 3 shows the high anomalous value of radon–thoron in the study areas. The primary vertical axis in the figure represents radon values and the secondary vertical axis represent thoron values at each sampling location whereas the line drawn (i.e., for X + 1σ) in the figure is for both radon and thoron. The value of radon concentration was

found to be anomalous at sampling points 2, 3, 12, 14, 20, 21 and 22 whereas the value of thoron concentration was found to be anomalous at sampling points 3, 8, 12, 17, 20 and 21, respectively. At sampling points 14 and 22, the recorded radon concentrations found to be anomalous whereas thoron concentrations were not. This may be due to the deeper source of gas in the study area as reported by Yang et al., [2005]. Also at sampling points 8 and 17, the recorded values of thoron were anomalous where as radon concentrations were not. It may be due to the shallower gas source in the study area [Yang et al., 2005]. This gas source can only provide a small amount of radon/thoron gas to the surface due to the micro fracture and this small amount of gas may not increase the radon concentration clearly due to its original relative high background level. In contrast, it will significantly enhance the thoron concentration. At sampling points 3, 12, 20 and 21, both radon and thoron values were found to be anomalous. The sampling point 3, where the recorded values for both radon and thoron were anomalous lying on the Drini thrust (MBT2). The sampling point 14 where the recorded values for radon was anomalous and sampling point 17 where the recorded values for thoron was anomalous, this may be attributed to the presence of MBT nearby or due to probable lineaments which are common features along different drainage systems in the study area as reported by earlier studies [Dhar et al., 2002; Walia et al., 2008]. The sampling point 12 where both radon–thoron values were anomalous lying very close to Syncline. The points 20 and 21, where the recorded values for radon–thoron were anomalous lying very close to Manuni Khud lineament. At sampling point 8 where the recorded thoron value was anomalous lying in between Churan Khad and Manjhi Khad. The low value for radon and thoron has been recorded at sampling points 15 and 16 located in fault junction. The possible reason for low values for radon and thoron is that these two points are in the ductile zone in between MBT and MCT, may be having higher porosity, but low permeability. The sampling points 1, 2, 3 and 4 are located around the MBT2. However, only two sampling points, i.e., 2 and 3 have identified anomalous values of radon/thoron. Although, the points 1 and 4 have not shown anomalous values, the value of radon at point 1 and value of thoron at point 4 are found to be higher than the average value, respectively. Overall the anomalous values of radon and thoron were found near to the faults, i.e., main boundary thrust (MBT and MBT2) as well as near Churan Khad (CK), Manuni Khad (MK) and Manji Khad (MJK).

These anomalies indicate the presence of lineaments controlling this drainage system. Dhar et al., [2002] have already observed intersection pattern of longitudinal thrust and transverse lineaments along Manji Khad (MJK) in the area of Dharamsala. Walia et al., [2008] have also studied soil-gas activity in the vicinity of neotectonic fault zones within the Dharamsala area in the region of the NW Himalayas, India, using active detectors. The authors have also reported anomalous value of radon near to the neotectonic thrust in the regions like main boundary thrust (MBT2) and also along the drainage system in the study area. The similar work is also in progress for soil gas radon– thoron monitoring using SSNTDs in other seismically active zones of NW Himalayas, India and will be reported in the future.

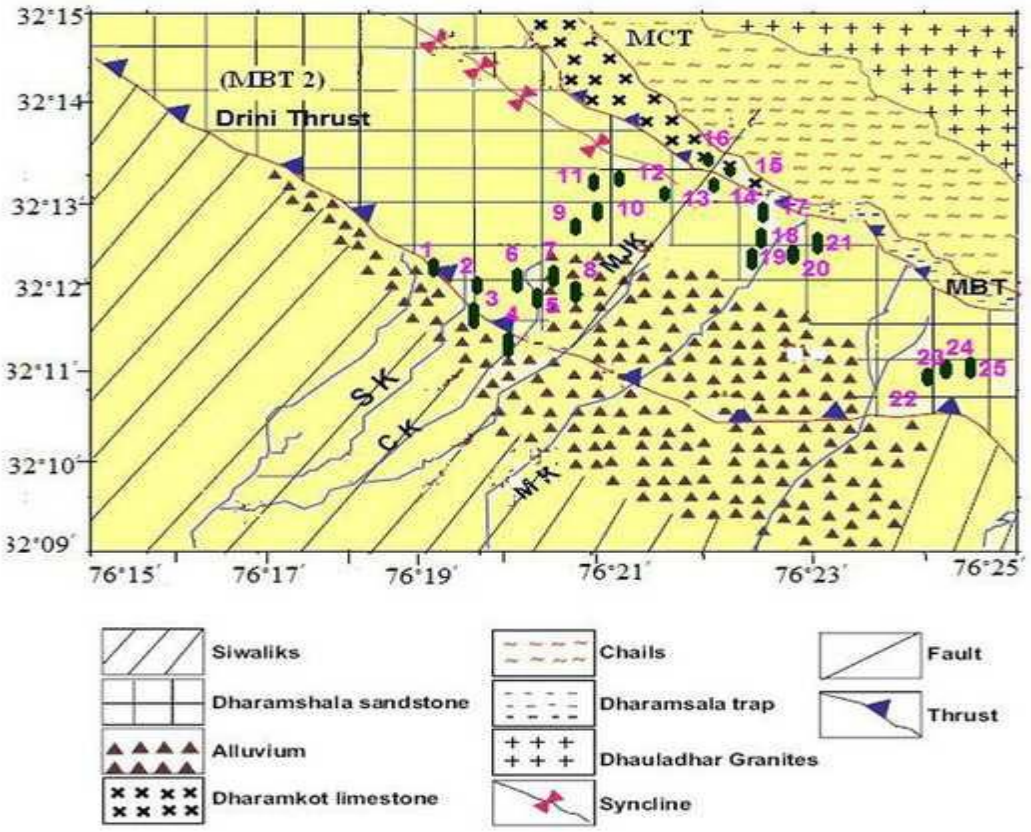

Figure 22: Geological map showing the locations of radon- thoron discriminators installed in the study area and tectonic features (MBT = Main Boundary Thrust, MCT = Main Central Thrust) and drainage systems (SK =

Sarah Khad, CK = Churan Khad, MJK = Manjhi Khad, MK = Manuni Khad, DK = Darun Khad) (modified after Mahajan et al., 1997).

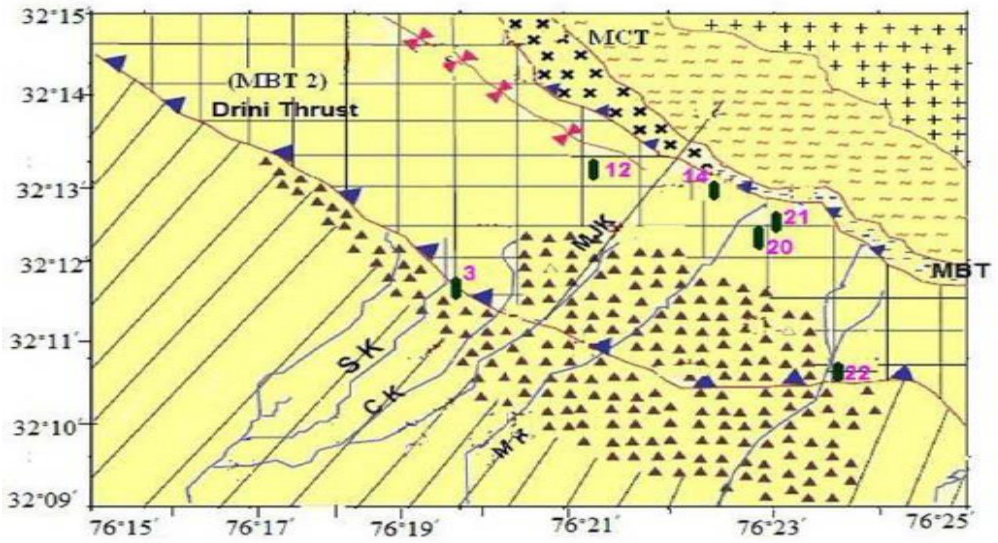

Figure 23: Map showing the places where the value of radon is more than average + standard deviation.

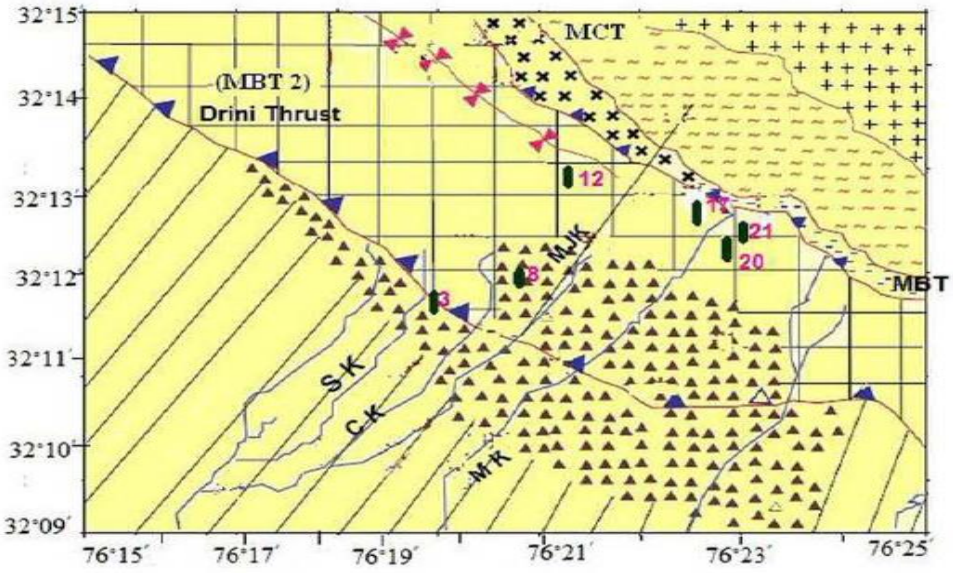

Figure 24: Map showing the places where the value of thoron is more than average + standard deviation**.**

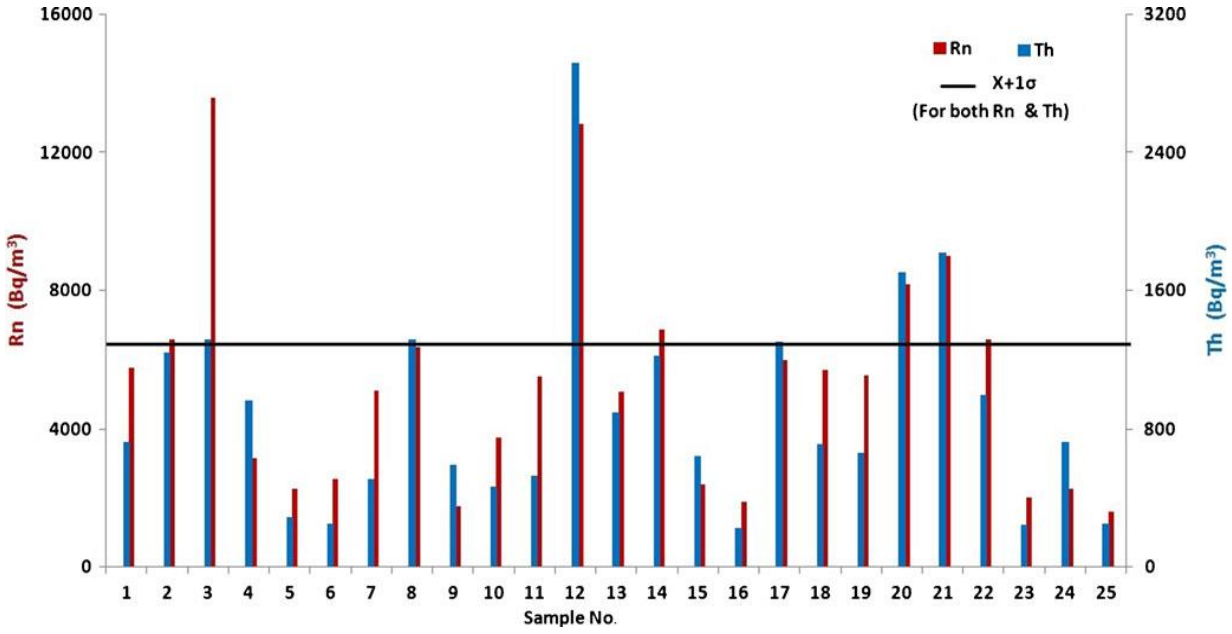

Fig. 25: Map showing the places where the value of radon-thoron is more than average + standard deviation

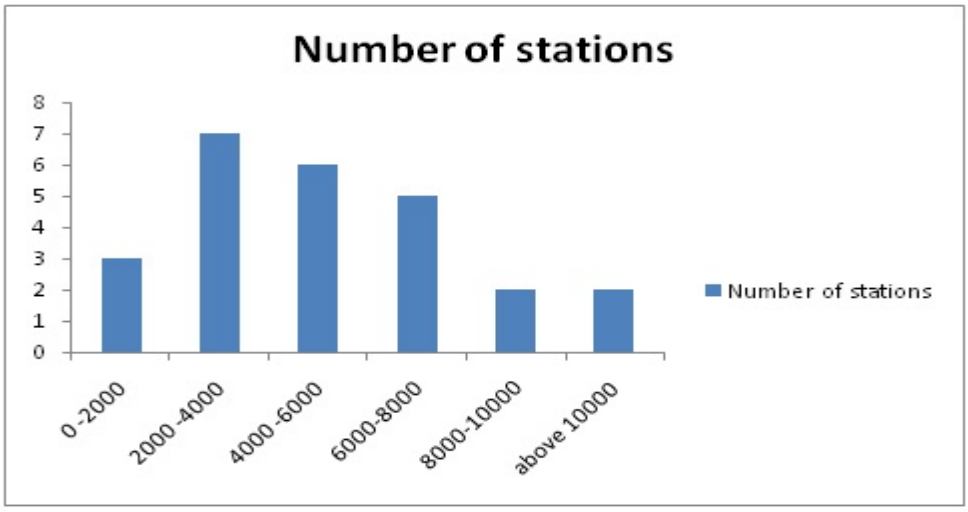

Figure 26: showing frequency of stations in different range of Radon concentration in Bq/m^3

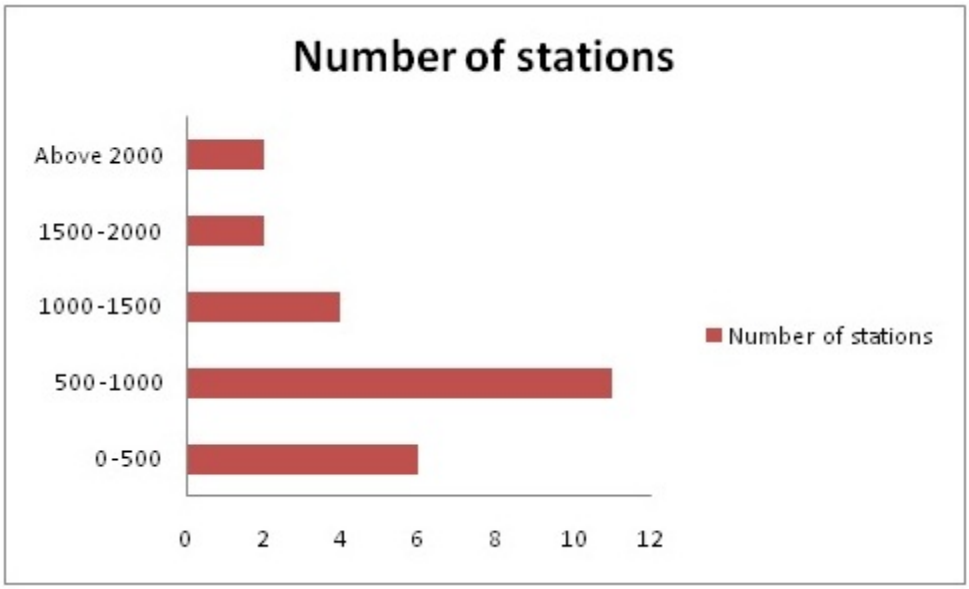

Figure 27: Showing frequency of stations in range of different Thoron concentrations in Bq/m^3

3.3 Conclusions

An economical and simple method has been evolved to measure soil gas radon–thoron simultaneously using discriminator deploying LR-115 films. In Dharamsala areas, recorded soil gas radon concentration varies from 1593 to 13570 Bq/m3 with an average value of 5292 Bq/m3 whereas recorded soil gas thoron concentration varies from 223 to 2920 Bq/m3 with an average value of 901 Bq/m3. The anomalous value of radon–thoron has been observed near to the faults in the region, i.e., main boundary thrust (MBT, MBT2) and also along the drainage system in the study area. The presence of neotectonic faults/lineaments in the region has made it tectonically active. Based on the preliminary results of the present study and from the previous studies, it is suggested that the detailed studies of radon–thoron along with other noble gases will be fruitful for such kind of studies

CHAPTER 4

SOIL GAS RADON THORON MONITORING IN ACTIVE REGION OF MANDI

4.1 Introduction

Himalayan mountains are one of the most seismically active fault zones in the world. The monitoring of soil gases like hydrogen, helium, radon- thoron, methane, carbon dioxide profiles in these zones may provide useful information before the seismic activities. Anomalous changes in the subsurface soil gas concentrations may be used as tectonic activities precursor according to the dilitancy-diffusion model for earthquake occurrence [Scholz et al., 1973]. Moreover the soil gas monitoring has been developed as the effective tool in understanding the gas transportation mechanisms in the seismically active zones and many other fields of geosciences. However, the precursor predictions may not be accurate, but may be helpful to study the under soil activities [Han et al., 2014] and is considered as precursor for various deportation processes, such as to discover fault interfaces and uranium- thorium ores [Quattrucchi et al., 2000]. Improved permeability of soils along active faults customarily favours the gas escape, hydraulic conductivity (for ground water and thermal fluids), however the thermal conductivity of the soil decreases with increase in the porosity and permeability of soil because the pore filling fluids have lower value of coefficient of thermal conductivity [Poelchau et al., 1997]. The movement of radon in rocks and through rocks within the earth mainly depends on lithology, compaction, porosity and fractural/tectonic features [Choubey et al., 1997; Gunderson et al., 1998]. The presence of various fault systems and thrusts in any region provides secondary porosity for upward migration of thermal fluids. The thermal gradient may be diluted if fresh water is mixed in up flow of thermal fluid [Sharma, 1977; Shanker, 1988; Cinti et al. 2009].

The measurement of various soil gases for earthquake monitoring and prediction of active faults zones has been reported by various researchers. [Etiope and Lombardi, 1995; Igarashi et al, 1995; Ciotoli et al., 1998; Guerra and Lombardi, 2001; Al-Tamimi and Abumurad, 2001; Chyi et al., 2005; Fu et al. 2005; Singh et al., 2005, Kumar et al., 2009, 2012, 2013a, 2013b; Pereira et al., 2010; Singh et al., 2010; Sac et al., 2011; Yang et al., 2011; Li et al., 2013; Walia et al., 2013; Koike et al., 2014; Han et al., 2014, Jaishi et al., 2014; Jashank, 2014; Georgy et al., 2015; Piersanti et al., 2015]. Measurement of natural radon in soil is very important to determine because it helps in monitoring changes in natural background activity with time as a result of any radioactivity release [Darko et al.,

2015]. The soil gas and water radon has been measured using alpha guards in some areas of Punjab and Himachal Pradesh for health risk assessments [Bajwa et al., 2003; Walia et al., 2003].

Chandrasekharam et al., [2005] and Walia et al., [2005] have conducted studies along Parvati and Beas valley of the Himachal Pradesh including geothermal sub-province mainly on the famous thermal springs of Manikaran and Kasol with an objective to check the suitability of geothermal resources for electric power production. Other study by various authors [Choubey et al., 1997, 2007; Virk and Walia , 2000; Walia et al., 2003] focused on radon monitoring in waters and soils for health hazard assessment and earthquake prediction research. Some research papers have reported the geochemistry [Gupta, 1996] and isotopic data study [Giggenbach et al., 1983] of the thermal waters.

The present studies dealt with radon-thoron measurements in soils, measurement of radon exhalation rates and radium contents of Mandi district, Himachal Pradesh, NW Himalaya, India using the passive detectors LR -115 type 2 films and measurement of porosity of soil samples from 71 sampling sites (detail of technique is discussed in chapter 2). The technique used is cost effective, easily applicable and less disturbed by different environmental conditions.

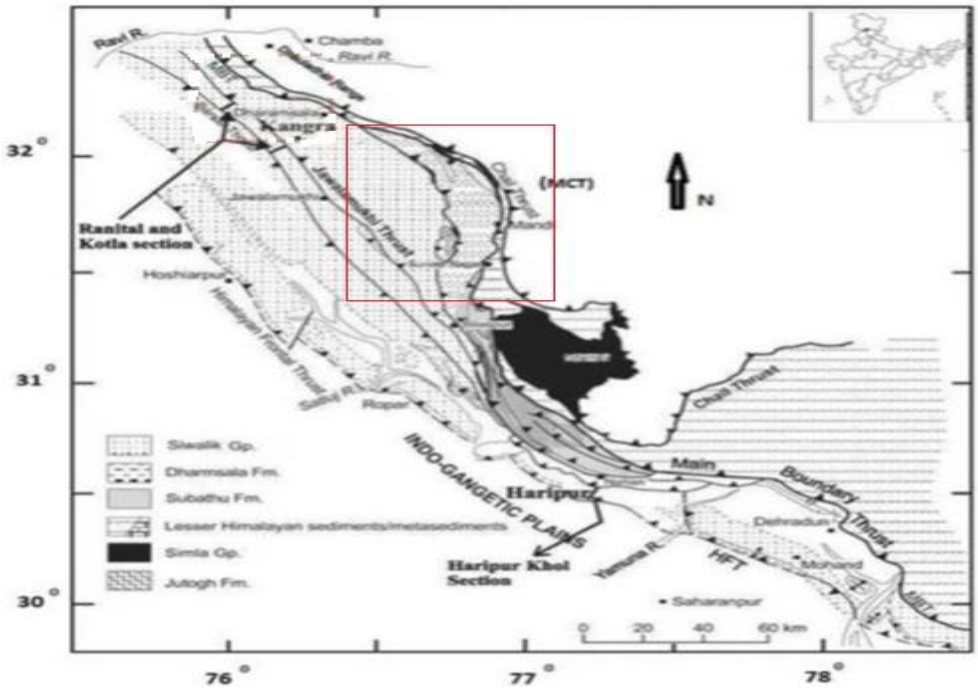

Figure 28: Geology of the study area.

The statistical variation in measurement of radon concentration is larger in summer than in winter [Szabo et al., 2013] keeping in view this fact, study was performed in January and February, 2015 (Figure 28 & 29).

The porosity η of the soil is calculated using following formula $\eta=1-\rho_{bulk}/\rho_{particle}$ [Morgan et al., 2005].

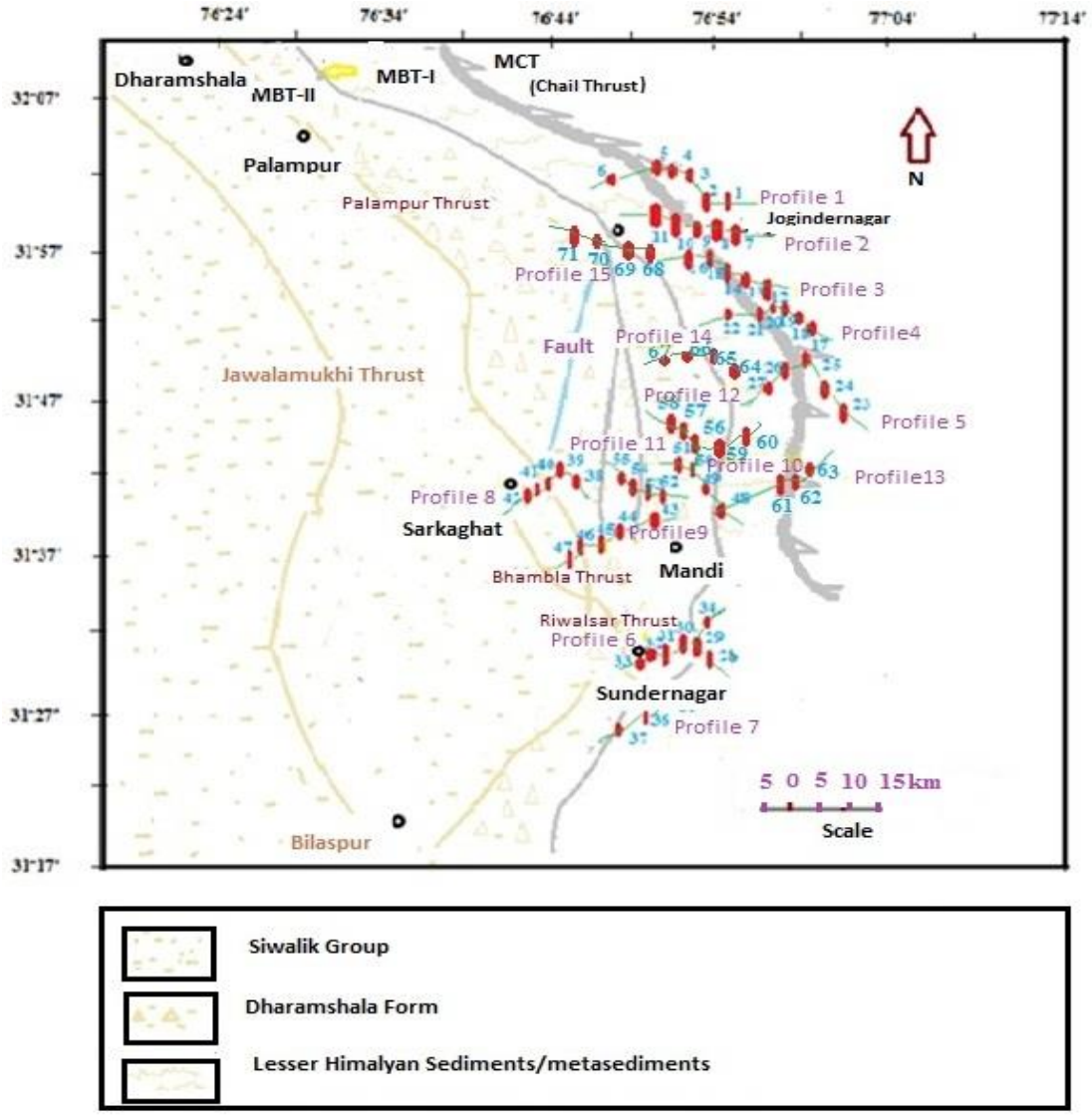

Figure 29: The position of the detectors along with different faults and thrust systems in the study area.

4.2 Results and Discussion

The radon and thoron concentration along with exhalation rates, radium contents, porosity and radon production rate per unit volume recorded at 71 locations (Figure 29) in the study area are shown in the Table numbered 6 and 7.

Table 6: Radon- Thoron concentration in soil at different places in Mandi region

S.N.	Place	Radon conc. in Bq/m^3	Thoron conc. in Bq/m^3	Latitude	Longitude	Height
1	Tikkan	3273	957	N 31°58.08′	E 76°53.43′	1652
2	Tikkan	4353	1387	N 31°58.16′	E 76°53.82′	1701
3	Barot	19970	5950	N 32°00.46′	E 76°51.74′	1825
4	Bardhan	16183	4123	N 31°59.92′	E 76°51.79′	1763
5	Bardhan	12740	1490	N 31°59.49′	E 76°52.20′	1769
6	Near Jogindernagar	4459	2491	N 31°58.32′	E 76°46.02′	1410
7	Gumma	1067	873	N 31°57.48′	E 76°51.48′′	1540
8	Ghatasni	1733	1527	N 31°57.31′	E 76°53.46′	1906
9	Jhatingni	8447	3447	N 31°56.82′	E 76°52.98′	2037
10	NearJogindernagar(towards Mandi)	3337	747	N 31°59.03′	E 76°49.70′	1467
11	Galu	9370	2048	N 31°58.79′	E 76°49.82′′	1529
12	Padhar	2370	1649	N 31°52.44′	E 76°55.48′′	1371
13	Kotropi	3940	697	N 31°54.90′	E 76°53.06′′	1298
14	Near Nagan	5813	2463	N 31°54.87′′	E 76°53.97′′	1259
15	Ghatasni	3983	360	N 31°56.67′′	E 76°52.36′′	1617
16	Near Lani	2353	1877	N 31°55.06′	E 76°51.86′′	1163

17	Below Kunnu	893	367	N 31°51.06′	E 76°55.36′	1188
18	Shingar	3417	290	N 31°50.96′	E 76°54.07′	1364
19	Sarwahan	1340	296	N 31°52.62′	E 76°55.53′	1464
20	Below Padhar	3498	453	N 31°50.01′	E 76°48.12′	1387
21	Above Padhar	3180	373	N 31°52.33′	E 76°55.65′	1415
22	Chehar	1040	37	N 31°50.91′	E 76°55.00′	1223
23	Near Mahar	4830	3827	N 31°45.98′	E 76°56.53′	934
24	Pakhari	10017	77	N 31°47.09′	E 76°56.21′	1052
25	Drang	5655	2060	N 31°50.46′	E 76°56.06′	1236
26	Nomile	4740	3650	N 31°49.20′	E 76°55.79′	1203
27	Below nomile	5648	4366	N 31°46.13′	E 76°53.85′	1154
28	Near pung Sundernagar	2770	1647	N 31°30.33′	E 76°54.50′	909
29	Pung Sundernagar	4277	1323	N 31°30.81′	E 76°52.08′	981
30	Near Phafalani	3600	3247	N 31°31.07′	E 76°51.57′	1090
31	Churar	4323	693	N 31°30.95′	E 76°51.33′	1080
32	Nagalth	4140	1290	N 31°30.08′	E 76°50.74′	1286
33	Nagalth	2030	600	N 31°30.05′	E 76°50.64′	1358
34	Nolakha	3570	3337	N 31°34.14′	E 76°54.47′	814
35	Harabag	4923	338	N 31°30.07′	E 76°52.42′	877
36	Jarol	1647	600	N 31°27.13′	E 76°51.46′	684
37	Towards Salapar	2004	525	N 31°25.81′	E 76°48.12′	646
38	Near Maseran	8017	4867	N 31°41.43′	E 76°45.61′	1348
39	Nonu Ropri	4600	3923	N 31°44.13′	E 76°44.19′	1084
40	Sarkaghat	3970	2907	N 31°42.04′	E 76°44.14′	940

41	Near Girl Hostel G C Sarkaghat	10052	353	N 31°41.10′	E 76°43.76′	861
42	Barchhawar	14123	6970	N 31°40.82′	E 76°43.11′	863
43	9km from Riwaksar towards Mandi	1983	1050	N 31°38.50′	E 76°52.26′	1082
44	Between Kalkhar and Riwalsar	10336	1797	N 31°37.11′	E 76°49.46′	1329
45	Ambla galu	1027	980	N 31°35.95′	E 76°48.41′	1298
46	NearUpper Bhambla(towards Mandi)	7300	2033	N 31°35.86′	E 76°45.59′	1215
47	Lower Bhambla	5003	1867	N 31°35.11′	E 76°44.56′	993
48	5km before Kotli on NH-70	2406	1180	N 31°41.29′	E 76°54.58′	1099
49	1 km before Kotli	1516	983	N 31°42.76′	E 76°54.29′	1141
50	At Sai Galu	1473	1353	N 31°45.27′	E 76°53.27′	1185
51	At Kotli	1880	1863	N 31°45.58′	E 76°52.23′	1224
52	Above Riwalsar about 4 km	7807	5820	N 31°38.39′	E 76°50.04′	1474
53	Near Durgapur	2920	1440	N 31°39.60′	E 76°49.46′	1543
54	Near Bhadarwar	4340	3847	N 31°40.76′	E 76°47.32′	1028
55	Near Rakhota	3353	3290	N 31°40.39′	E 76°47.16′	1043
56	Kotli to Jogindernagar about 2 km	3000	54	N 31°46.27′	E 76°52.12′	1208
57	Near Koon	867	684	N 31°45.65′	E 76°51.56′	1202
58	Kotli to Dharampur raod about 3 km	993	167	N 31°45.30′	E 76°51.60′	1171

59	Near pattan towards kasan	3430	1604	N 31°44.50′	E 76°54.76′	1196
60	Near bariyara	2674	1572	N 31°46.88′	E 76°55.05′	1178
61	1 km behind ronde on Mandi to kamand road	3620	937	N 31°44.78′	E 76°56.80′	1071
62	1km behind katindi	1680	1707	N 31°44.93′	E 76°57.53′	1189
63	2 km from Katindi jal Bhawan toward drang	1574	907	N 31°46.09′	E 76°58.03′	1368
64	Malog	4322	1234	N 31°49.32′	E 76°55.44′	1101
65	Ropa	3425	654	N 31°51.42′	E 76°32.72′	1087
66	Chhahri	2232	1087	N 31°51.31′	E 76°50.72′	991
67	Near panchyatan	2465	1543	N 31°50.12′	E 76°39.42′	970
68	Near Basi power station	5678	2466	N 31°57.01′	E 76°47.66′	936
69	Machhayal	5376	1489	N 31°56.20	E 76°47.83′	878
70	Near balakrupi	3456	987	N 31°59.12′	E 76°46.53′	1197
71	2km from balakrupi towards chontra	4566	1123	N 32°00.62′	E 76°45.33′	1232

Table 7: The radon and thoron concentrations along with exhalation rates (Area and Mass exhalation rates), radium contents, porosity and radon production rate per unit volume at sampling positions

Location No.	**Area exhalation rate (Bqm^{-2} h^{-}**	**Mass exhalation rates ($Bq\ kg^{-1}h^{-1}$)**	**Radium contents ($Bq\ kg^{-1}$)**	**Radon concentration(Bq/m^3) as measured in soil**	**Thoron concentration(Bq/m^3) as measured in soil**	**Porosity**	**Amount of radon available for transport to**

	[1])						the surface (radon production rate per unit volume) (Bqm^{-3} h^{-1})
1	1.140	0.050	5.34	3273	957	0.36	0.0146
2	0.854	0.038	4.11	4353	1387	0.38	0.0115
3	1.670	0.074	7.98	19970	5950	0.39	0.0217
4	1.403	0.062	6.65	16183	4123	0.39	0.0182
5	1.328	0.059	6.26	12740	1490	0.39	0.0176
6	1.769	0.078	8.20	4459	2491	0.40	0.0216
7	1.507	0.066	6.97	1067	873	0.32	0.0190
8	1.014	0.045	4.77	1733	1527	0.31	0.0117
9	1.079	0.048	5.28	8447	3447	0.38	0.0152
10	1.723	0.076	8.19	3337	747	0.36	0.0228
11	1.009	0.044	4.71	9370	2048	0.38	0.0122
12	2.076	0.092	9.33	2370	1649	0.38	0.0240
13	2.110	0.093	9.96	3940	697	0.36	0.0269
14	1.035	0.046	4.81	5813	2463	0.42	0.0127
15	1.643	0.073	7.41	3983	360	0.37	0.0185
16	0.863	0.038	3.97	2353	1877	0.41	0.0106
17	1.782	0.079	8.25	893	367	0.31	0.0225
18	0.914	0.040	4.37	3417	290	0.35	0.0119
19	1.976	0.087	9.53	1340	296	0.33	0.0268
20	1.254	0.055	5.60	3498	453	0.31	0.0141
21	1.285	0.057	6.37	3180	373	0.24	0.0186
22	1.043	0.046	5.01	1040	37	0.34	0.0139
23	0.976	0.043	4.52	4830	3827	0.43	0.0123
24	1.171	0.052	5.67	10017	77	0.31	0.0163
25	1.698	0.075	8.35	5655	2060	0.27	0.0232
26	1.784	0.079	8.66	4740	3650	0.31	0.0250

27	1.316	0.058	6.29	5648	4366	0.5	0.0179
28	0.675	0.030	3.18	2770	1647	0.38	0.0085
29	1.650	0.073	7.71	4277	1323	0.41	0.0199
30	1.658	0.073	8.02	3600	3247	0.32	0.0229
31	2.635	0.116	12.41	4323	693	0.39	0.0332
32	0.881	0.039	4.21	4140	1290	0.35	0.0119
33	1.494	0.066	7.04	2030	600	0.39	0.0189
34	2.524	0.111	11.73	3570	3337	0.41	0.0297
35	1.556	0.069	7.12	4923	338	0.32	0.0186
36	1.578	0.070	7.20	1647	600	0.34	0.0187
37	1.433	0.063	6.63	2004	525	0.32	0.0167
38	1.355	0.060	6.61	8017	4867	0.45	0.0196
39	1.864	0.082	8.99	4600	3923	0.42	0.0254
40	1.420	0.063	6.88	3970	2907	0.4	0.0192
41	1.627	0.072	7.37	10052	353	0.36	0.0186
42	1.521	0.067	6.94	14123	6970	0.5	0.0180
43	2.005	0.089	9.06	1983	1050	0.39	0.0237
44	2.075	0.092	9.57	10336	1797	0.4	0.0257
45	0.934	0.041	4.39	1027	980	0.38	0.0117
46	2.061	0.091	9.44	7300	2033	0.41	0.0247
47	1.538	0.068	6.99	5003	1867	0.4	0.0181
48	0.896	0.040	4.26	2406	1180	0.36	0.0118
49	2.204	0.097	10.44	1516	983	0.37	0.0285
50	1.984	0.088	9.72	1473	1353	0.32	0.0276
51	1.422	0.063	6.74	1880	1863	0.37	0.0184
52	1.255	0.055	5.81	7807	5820	0.48	0.0152
53	1.563	0.069	7.19	2920	1440	0.39	0.0192
54	1.705	0.075	7.88	4340	3847	0.43	0.0204
55	1.443	0.064	6.79	3353	3290	0.4	0.0181
56	1.152	0.051	5.35	3000	54	0.29	0.0142

57	1.113	0.049	5.07	867	684	0.36	0.0131
58	1.197	0.053	5.59	993	167	0.31	0.0151
59	0.778	0.034	3.66	3430	1604	0.39	0.0098
60	1.443	0.064	6.88	2674	1572	0.38	0.0195
61	0.644	0.028	3.11	3620	937	0.36	0.0088
62	1.369	0.060	6.72	1680	1707	0.39	0.0192
63	1.202	0.053	5.73	1574	907	0.36	0.0162
64	1.160	0.051	5.46	4322	1234	0.39	0.0146
65	1.422	0.063	6.67	3425	654	0.4	0.0183
66	1.572	0.069	7.49	2232	1087	0.37	0.0210
67	1.239	0.055	5.71	2465	1543	0.43	0.0147
68	3.317	0.15	15.41	5678	2466	0.41	0.0408
69	0.918	0.041	4.41	5376	1489	0.37	0.0123
70	1.304	0.058	6.27	3456	987	0.34	0.0175
71	1.118	0.049	5.17	4566	1123	0.38	0.0135

Table 8: Values of various soil parameters in different profiles (as shown in Figure no. 29)

Sr. No.	Profile	Porosity (average)	Average Area Exhalation rates	Average Radium Contents	Average value(Bq/m^3)		Standard deviation value(Bq/m^3)	
					Radon	Thoron	Radon	Thoron
1	1 to 6	0.39	1.36	6.42	10163	2733	7111	1947
2	7 to 11	0.35	1.27	5.98	4791	1728	3862	1094
3	12 to 16	0.39	1.55	7.10	3692	1409	1431	865
4	17 to 22	0.35	1.46	6.81	2221	303	1267	143
5	23 to 27	0.36	1.39	6.70	6178	2796	2190	1746
6	28 to 34	0.38	1.65	7.76	3530	1734	856	1126
7	35 to 37	0.33	1.52	6.98	2858	488	1797	135
8	38 to 42	0.43	1.56	7.36	8152	3804	4165	2443
9	43 to 47	0.40	1.72	7.89	5130	1545	3826	492
10	48 to 51	0.36	1.63	7.79	1819	1345	432	377
11	52 to 55	0.43	1.49	6.92	4605	3599	2216	1803
12	56 to 60	0.35	1.14	5.31	2193	816	1184	744
13	61 to 63	0.37	1.07	5.19	2291	1184	1152	453
14	64 to 67	0.40	1.35	6.33	3111	1130	958	370
15	68 to 71	0.38	1.66	7.82	4769	1516	993	668

The average concentration of radon and thoron gases in the study area has been found to be 4541Bq/m^3 and 1778Bq/m^3within a range of 867-19970Bq/m^3 and 37-6970 Bq/m^3, respectively. In order to identify possible threshold values of anomalous radon and thoron concentration, various statistical methods have been used by different authors in the past (Guerra et al., 2001; Walia et al., 2005; Fu et al., 2005). In the present context, statistical threshold values of gas anomalies are fixed at average (μ) plus one standard deviation (σ). Figure no. 30 and 31 shows the variation of radon and thoron concentration (Bq/m^3) at different sampling locations in comparison to average (μ) and average+standard deviation value (μ+σ). The anomalous value of radon has been observed at 8 locations (3, 4, 5, 11, 24, 41, 42 & 44). The locations 3, 4, 5, 11 & 24 are close to MCT and locations 41 & 42 are close to MBT-II. The location 44 is close to local fault in the study area. The anomalous value of thoron has been observed in 12 locations (3, 4, 9, 23, 26, 27, 34, 38, 39, 42, 52 & 54). The locations 3, 4, 9, 23 & 26 are close to MCT and location 27 is close to MBT-I. Whereas locations 39 & 42 are close to MBT-II and locations 34, 38, 52 & 54 are close to the local fault in the study area. Anomalies in measurement of radon and thoron concentration are more along and across MCT than MBT and any fault system. More anomalies have been found in measurement of thoron concentrations. It may be due to shallower gas source in the study area [Yang et al., 2005; Kumar et al., 2013b].

The area and mass exhalation rates of radon have been calculated for each site and have been reported in Table 7. The average value of area and mass exhalation rates have been found to be 1.46Bq/m^2 h and 0.064Bq/kg h with a variation of 0.644Bq/m^2 h and 0.028Bq/kg h, respectively at location number 61 to 3.317Bq/m^2 h and 0.15Bq/kg h respectively at location number 68. The radium content of the soil has been ranged between 3.11- 15.4Bq/kg with an average value for the area as 6.84Bq/kg.

The porosity of the soil has been found to vary with a minimum (0.24) at location 21 to a maximum of 0.5 at two locations 27 and 42 with an average of 0.37 at five locations labelled with numbers 15, 49, 51, 66, 69. The correlation factor of 0.59 has been observed between radon and thoron concentration of the study area and a good

correlation (0.64) between thoron and porosity has also been detected. Similar kind of correlation has been reported by Al Jarallah et al., [2005] in a study related to construction materials (especially granite) used in Saudi Arabia.

In this study very less correlation (0.03) between porosity and amount of radon available for transport to the surface has been recorded. However, at the sampling sites 51, 62 and 65 the values of radium contents, porosity and amount of radon available for transport to the surface recorded are 6.74 Bq kg^{-1}, 0.37, 0.0184 Bqm^{-3} h^{-1}, 6.72 Bq kg^{-1}, 0.39, 0.0192 Bqm^{-3} h^{-1} and6.67 Bq kg^{-1}, 0.4, 0.0183 Bqm^{-3} h^{-1} respectively. For sampling sites 17 and 18 these values are 8.25 Bq kg^{-1}, 0.31, 0.022 Bqm^{-3} h^{-1}5 and 8.02 Bq kg^{-1}, 0.32, 0.0229 Bqm^{-3} h^{-1} and at sampling sites 57 and 71 values are 5.17 Bq kg^{-1},0.38, 0.0135 Bqm^{-3} h^{-1} and 5.07 Bq kg^{-1},0.36, 0.0131 Bqm^{-3} h^{-1}. These observations shows that if the radium contents of some soil samples are comparable then with the porosity of the soil radon transport factor to surface will increase. Also, if there is secondary porosity in any region due to presence of fault systems then permeability/ emanation factor of the soil will increase, which will further increase the radon transport to surface [Cinti et al., 2009; Ciotoli et al., 2016].

The average value of radon, thoron along with average exhalation rates, average radium contents and average porosity in different profiles (as shown in fig 29) has been reported in table 8. Profiling 1, 2, 3, 4, 5 and 13 has been made along and across the main central thrust (MCT) and profiling 6, 7, 8, 9, 10, 11, 12, 14 and 15 has been made along and across MBT and local faults in the study area. The radon has been found to vary in the range of 1680-12740 Bqm^{-3} with an average of 6253 Bqm^{-3} along the MCT. The concentration of radon and thoron at MBT has varied in the range of 1516-7300 Bqm^{-3} with an average value of 3980 Bqm^{-3} and 338-3847 Bqm^{-3} with an average value of 1621 Bqm^{-3}, respectively. The values of radon and thoron are found to be highest along the thrust. Similar observations have been recorded for the MBT and local faults in the region. The concentration of radon and thoron decreases as the observer moves up or down across the thrust. The radon and thoron concentrations have been observed to decrease with the distance from the thrust with few exceptions. The radon and thoron concentrations have been detected to increase with a movement from Chail thrust (MCT) to MBT in the Jogindernagar region that may be attributed to the geological stress and

strain in this region. The concentrations of radon and thoron along the MBT have been found lesser than that of the MCT. This may be due to the reason that MCT is under more geological stress and strain as compared to the MBT.

The average values of soil radon measured along the MCT (Main central thrust) in the profiles 1, 2, 3, 4, 5 and 13 have been recorded as 10163Bq/m^3, 4791Bq/m^3, 3692Bq/m^3, 2221Bq/m^3, 6178Bq/m^3, 2291Bq/m^3 whereas the average thoron concentration in the same profiles has been observed as 2733Bq/m^3, 1728Bq/m^3, 1409 Bq/m^3, 303Bq/m^3, 2796Bq/m^3, 1184Bq/m^3.. The profile 1 has exceptionally high average values because the presence of sling zones along this profile. The radon concentrations have been noticed to decrease from Jogindernagar to Mandi along MBT-1 due to the decrease in porosity of the soil. The same trend has been observed when the observer has moved along the profile 8, 11, 10 that may be attributed to the cross presence of other faults systems.

The decreasing trend of radon and thoron concentrations has been observed along the route followed through the profile 15, 3 and 4 that may be due to the higher radon exhalation rates, radium contents and more or less due to porosity of soil in the area of profile 15 than in soil of profiles 3 and 4. The slight elevation in the concentration along the sampling sites of profile 6 and 7 has been spotted that may have been caused by the presence of secondary fault systems (Sundernagar fault)in the vicinity of Sundernagar [Mahajan et al., 2010] and may be due to high porosity in the soil of profile 6 (0.38) and profile 7 (0.33) and relatively high values of radon exhalation rates1.65Bq/m^2 h (in profile 6) and 1.52Bq/m^2 h (in profile 7) and high values of radium contents 7.76Bq/kg (in profile 6) and 6.98Bq/kg (in profile 7).

The results also shows that the MBT and MCT of Himalayan region is more active than Turkish faults as reported by Sac et al., [2011] as the values of soil radon concentration measured are more as compared to the values measured near the fault in the western Turkey. However the values of soil radon concentration observed in the present study have been found to be lower as compared to the values measured in complex tectonic and seismic Tangshan area of Northern China (where earthquake Ms 7.8 was occurred in 1976) as reported by Li et al., [2013]. The average values of radon and thoron concentration in Dharamshala near MBT and MCT in Himachal Pradesh were 5992

Bq/m^3 and Thoron values of 901Bq/m^3 [Kumar et al., 2013b]. The trend in observed value of radon in Dharamshala region of Himachal Pradesh are similar to the present study, however the thoron values in Mandi region are found to be almost double than in Dharamshala region.

The values of Radon concentration are decreasing by factor of 1.01 to 2.56 on both side of MCT and MBT, while Thoron concentrations are decreasing by factor of 1.01 to 1.5 on moving distance of 2 to 3 km from MBT and MCT, with exceptions at some stations towards Palampur thrust (Table no. 9), this may be due to the fact that there exist numbers of local faults in between MBT and MCT.

The present study may also be helpful to study other natural features of study area like geothermal potential and ground water reservoirs, since high thermal energy flow with good thermal gradient have been observed by various researchers in NW Himalaya. This heat flow may be due the melting and reductions of intrusive granites near to MBT and MCT in Mandi area and presence of uranium, thorium and potassium contents in the soil texture [Rao et al., 1976; Das et al., 1979; Walia et al., 2005]. These reductions in basic strata of area may create faults which are the cause of secondary porosity and hence increase in the gases like Radon and thoron along with thermal energy fluids with a path of flow of water to the surface. The Beas valley, Uhl valley and region from Jogindernagar to Mandi have potentially good source of ground water. Thus elevated levels of radon and thoron gases in seismically active and faulty area may be used detect secondary porosity, so the monitoring of these radio nuclides will further help to study the other gases transport through porous medium of the soil.

Table 9: Average values of radon- thoron concentration at Relative distance from MBT and MCT

Average values along MCT				**Average values along MBT**		
Sr. No.	**Serial no. of detectors as in figure**	**Radon concentration (Bq/m^3)**	**Thoron concentration (Bq/m^3)**	**Serial no. of detectors as in figure**	**Radon concentration (Bq/m^3)**	**Thoron concentration (Bq/m^3)**
1	Monitoring station no. 5,9,14,21,25,62	6253	1923	Monitoring station no. 69,65,59,49,34,29,36,35,37,54,46	3801	1521

	very near to MCT			Very near to MBT		
2	Above serial no. 1(towards District Kullu) station no. 6,10,16,22,26,61	6158	1297	Above serial no. 1(towards District Kullu and MCT) 68,64,60,48,28,53,45	3113	1502
3	Next nearest stations above serial no.2 from chail thrust	2401	1661			
4	nearest Station from chail thrust (towards MBT) no.i. e. Below MCT 4,8,13,20,24,63	3258	1623	70,66,56,50,30,55,47(these Stations were below MBT towards Palampur thrust)	3159	1698
5	Next nearest stations below chail thrust(towards MBT) from serial no. 4	5217	2186	71,67,57,51 (these Stations were below MBT towards Palampur thrust, next to above stations	2445	1303

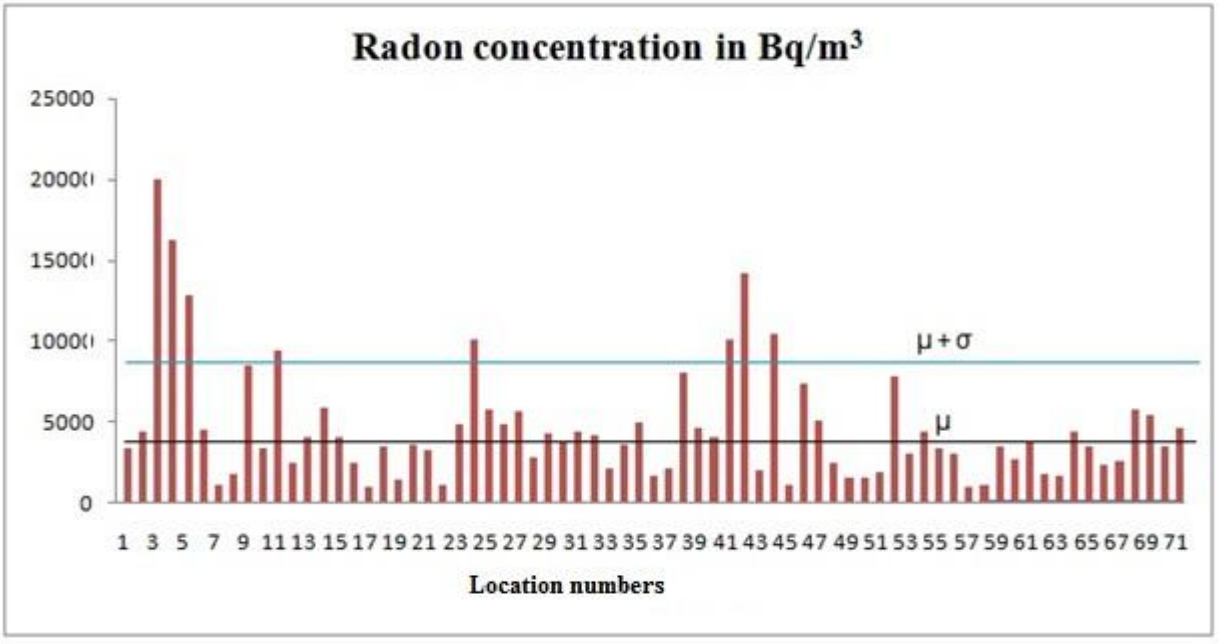

Figure 30: Values of radon concentration (Bq/m^3) at different measuring stations in comparison to average (μ) and average+ standard deviation value (μ+σ).

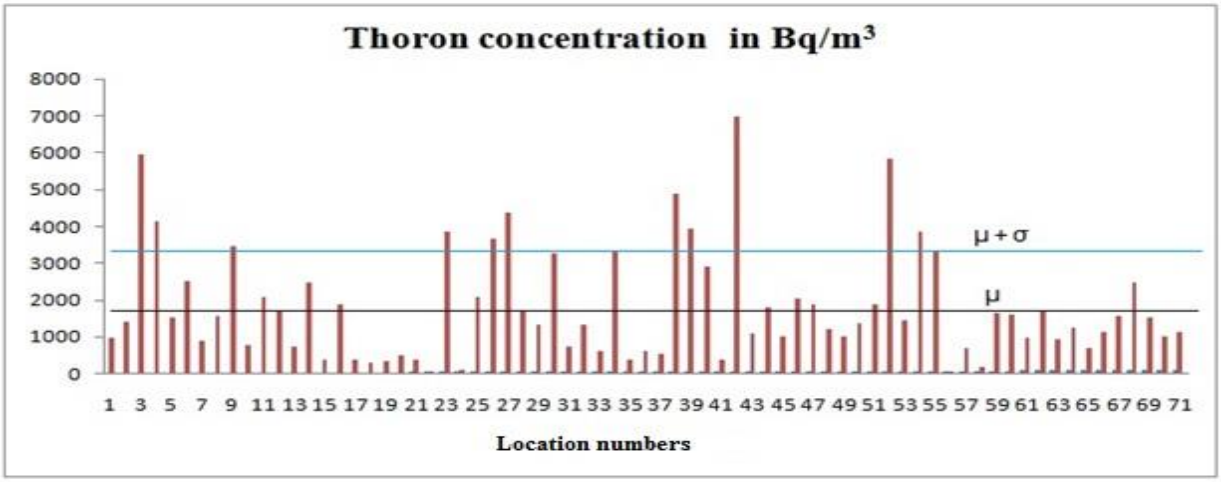

Figure 31: Values of thoron concentration (Bq/m^3) at different measuring stations in comparison to average (μ) and average+ standard deviation value (μ+σ).

4.3 Conclusions

The radon-thoron measurement in soil, measurement of radon exhalation rates and radium contents of Mandi district, Himachal Pradesh, NW Himalaya, India have been carried out using passive detectors LR-115 type-2 films. The anomalous values of radon-thoron have been reported along and around MCT, MBT and local faults in the study area. Radon concentration along MCT have been found higher than that along MBT, this may be due to the reason that MCT is under more geological stress and strain as compared to MBT. More anomalies have been recorded in the measurement of thoron concentration. The thoron concentrations values are very low at some places; this may be due to presence of deeper source in earth at these places. Good correlation between porosity and thoron has been recorded in this study, which shows presence of local fault in the area. Also it has been found that area exhalation rates, mass exhalation rates depend up on the radium contents of the soil. The porosity and seepage of radon and thoron may be helpful to study ground water potential and its reservoir in any region. The elevated levels of radon and thoron at certain places can be associated to the presence of secondary porosity in the soil texture. Secondary porosity due to fracturing of basic strata may provide the easy pathway for upward movement of geothermal fluids.

CHAPTER 5

INDOOR RADON CONCENTRATIONS IN THE DWELLINGS OF THE STUDY AREA (ALONG ACTIVE FAULTS)

5.1 Introduction

Due to chemically inertness radon which inhaled is also exhaled. Being metal (such as lead, bismuth, and polonium) radon progeny, however, are chemically active. The radioactive active elements decayed from radon and its progeny impacts the health of people adversely. The alpha particles decay from radon and its isotopes along with other particles beta, and gamma. They do not penetrate deep in the body in spite of the fact that they have very high energy but they can do considerable damage to cells at surfaces of respiratory organs. The decay elements from radon will stick to bodies with which they come into contact such as particulates in the air, furniture and room surfaces and during inhalation about 30% of the radon and its progeny elements come in contact with air passageways in the lung and adsorb to the surface of associated organs [Mclaughlin, 1989]. Similarly during ingestion of food (including water) these elements diffuse through the walls of the gut to lungs of human beings, thus they can also affect some cells in the stomach wall (because of ingestion). However, they are mixed in food so good part of radiation is absorbed so this causes less exposure to stomach and other digestive organs (the quantity of water consumed in a day is much less than the quantity of air that is breathed). Since radon exists in the environment mainly in the gaseous phase hence people are mainly exposed to radon through inhalation of air. Background levels of radon in outer environment are quite low (because of convection of radon due to other gases) but indoor locations may have higher levels of radon in air may be higher, exposure to these higher levels of radon through breathing air is a cause to lung diseases. The prolonged exposure of radon increases the chances of developing lung cancer, which may be appeared after several years of exposure. Although radon is radioactive, it radiates a small quantity of gamma radiation, as a result of which the evidences of harmful effects from exposure to radon radiation without actual contact with radon compounds are very less. It is not known whether radon can cause health effects in other organs besides the lungs. The effects of radon, which is found in food or drinking water, are unknown. Various researchers have contributed in field of measurement and continuous monitoring of the radon gas around the world, in India and too many places in the Himachal Pradesh [Singh et al. 2001, 2005a, 2005b; Kant et al, 2009; Akota et. al, 2011; Gupta et. al, 2011;

Tchorz and solecki, 2011; Zaher, 2011; Kumar et al, 2013]. They have reported the fluctuations in radon concentration in different climatic conditions and seasons.

The study area is lying near Dhauladhar range - Shiwaliks of north west Himalaya India (it includes the Sarkaghat, Mandi, Sundernagar, Jogindernagar, Palampur and Dharamshala in Himachal Pradesh). The region is bounded by two major fault systems MCT (Main Central Thrust) and MBT (Main Boundary Thrust). The radon concentration levels were measured in fifty randomly selected houses in Dharamshala-Palampur and Jogindernagar region and forty houses in Mandi district of Himachal Pradesh using the LR-115 Type –II SSNTD. More over the region under study is seismically active, so the study of the radon level in this area becomes very significant [Dwivedi etal, 1996a, 1996b, 2001]. The recording chemical etching and counting of tracks was similar as already discussed in material and method part of thesis and by researchers Kumar et al., [2013, 2015], Singh etal., [1997], Amrani and Cherouati, [1999] in their study.

The Purpose of study is to measure the radon concentration level in study area and to find the possible connection between the radon concentration, major fault systems of areas and to health of residents.

5.2 Results and discussion

Mandi-Region

The values of radon concentrations in forty houses in Mandi District of Himachal Pradesh are reported in Table 10 and shown in Figure no. 32.

Table 10: Radon concentration along MCT and MBT in Mandi district of Himachal Pradesh

S.no	Name of place	Construction materials used in houses	Radon Concentration(Bq/m^3)
1	Barot	Mud Based	97.22
2	Barot	Dwelling	322.78
3	Barot	Wooden and concrete	127.22
4	Barot	Concrete based	398.33

5	Barot	Concrete based	44.44
6	Tikkan	Concrete based	48.89
7	Tikkan	Concrete based	292.78
8	Jhatingni	Mud and granite	124.44
9	Jhatingni	Mud and granite	107.78
10	Mohar dhar	Mud house	133.33
11	Mohar dhar	Mud and granite	92.78
12	Mohar dhar	Concrete House	124.44
13	Chipnu near Mandi	Concrete House	133.33
14	Chipnu near Mandi	Concrete House	160.00
15	Mandi	Concrete House	138.33
16	Mandi	Concrete House	67.78
17	Mandi	Concrete House	113.33
18	Malori	Mud House	117.22
19	Malori	Mud House	213.33
20	Lunapani	Concrete House	65.56
21	Baggi	Mud House	137.22
22	Pali near baggi	Concrete House	137.22
23	Pali	Mud House	140.00
24	Sundernagar	Concrete House	126.11
25	Harabag	Concrete House	128.89
26	Harabag	Concrete House	60.56

27	Harabag	Mud House	161.67
28	Ropari	Concrete House	42.22
29	Bhubwana	Mud House	71.67
30	Bhubwana	Mud House	143.33
31	Kangu	Concrete House	170.00
32	Kangu	Dwelling	150.00
33	Slapper	Concrete House	76.11
34	Slapper	Concrete House	156.67
35	Sundernagar	Concrete House	375.56
36	Sundernagar	Concrete House	253.33
37	Sundernagar	Mud House	109.44
38	Sundernagar	Concrete House	42.78
39	Sundernagar	Concrete House	49.44
40	Lunapani	Concrete House	62.22

The houses were selected randomly from different area of Mandi district in Himachal Pradesh situated at a few kms away from each other. The lowest value concentration was found to be 42.22 Bq/m^3 whereas the highest concentration was found to be 398.33Bq/m^3. The highest value was observed in the house of participant number 4 was due to poor ventilation, lifestyle and the accumulation of dust in the room due to the closeness of the house to the roadside which are usually considered as important sources of radon in buildings. Whereas the lowest value was found in the house number 28. Although at most of locations the indoor radon concentrations were within the ICRP action level and they were higher than the reference level set by the USEPA for the USA (ICRP). Construction material used in houses was same (concrete and cement blocks) but their finishing was done using different materials, this factor may also differ from room

to room. One of the factors explaining the high levels of radon these houses were poorly ventilated due to the relatively narrow openings. Windows are opened only when honors of houses are in the house and since most of the them were out of houses for their daily routine work so they leave the house early and come back late in the night. Also, most of the houses in the present study areas serve as both living rooms and bed rooms for the residents. This may also be the reason to accumulate the high radon concentration levels since most of the house hold items are kept in one room making the room non-spacious for inflow of air. The various dwellings and their corresponding radon concentrations are represented graphically.

The average concentration of radon in sample houses was 138 $Bq/m^{3.}$ This value of the radon is somewhat in comparison with the value of radon as suggested by other researchers in Himachal Pradesh [Mamta Gupta etal., 2011].The concentration of Radon in sample houses were large than the average expected value because the region under study is having large no. of faulty structure where Radon concentration is more. Also the uranium contents in the soil of Mandi District is large [Mithilesh Sharma etal., 2000]. The concentration in ventilated houses were below 80 Bq/m^3 and poorly ventilated house were <200 Bq/m^3. Higher value of Radon concentration is measured along fault and seismic zones, in dwellings where there is very less ventilation. The current investigation shows that survey points 2 and 4 located at Barot in Mandi (H.P) have values of radioactivity 322.78 Bq/m^3 and 398.33 Bq/m^3. Survey points 7, 31 and 35 representing Tikkan, Kangoo and Sundernagar have values of radon concentration levels of 292.78 Bq/m^3, 170.00 $Bq/m^3$and 375.56 Bq/m^3 respectively. The houses made of mud and wood found to be having more level of radon concentration as compared to well ventilated houses made of concrete reinforced steel structures.. In addition, the radon gas also emanates from the gaps in ground prone to displacement of actual positions of tectonic plates, where the chance of earthquake catastrophes is more.

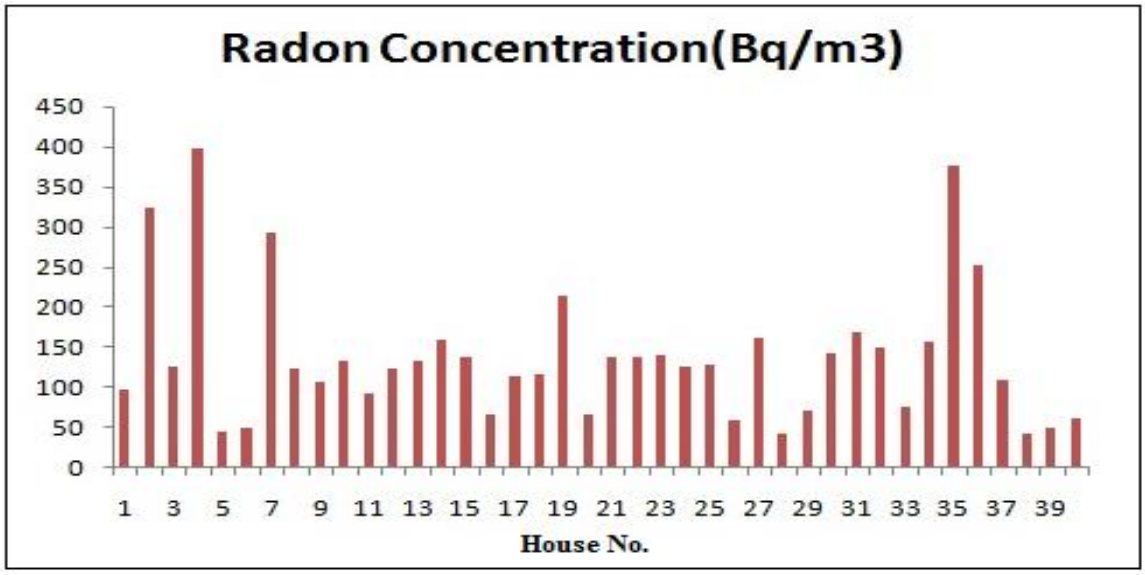

Figure 32: Radon concentration levels in forty houses of study area (Mandi)

Dharamshala region

The values of radon concentrations in fifty houses in Dharamshala-Palampur and Jogindernagar region of Himachal Pradesh are reported in table 11 and shown in figure no. 34.

Table 11 : Radon concentration in the dwellings of Dharamshala-Palampur and Jogindernagar region of Himachal Pradesh

House no.	Locations	Construction materials used in houses	Radon Concentration(Bq/m^3)
1.	Aganjar Mahadev	Concrete based	159
2.	Mohli-I	Wooden and Concrete based	49
3.	Mohli-II	Wooden and Concrete based	37
4.	Chakban	Wooden and Concrete based	29
5.	Lunta	Wooden and Concrete based	30
6.	Darnu-I Below road	Wooden and Concrete based	23
7.	Darnu-II Below road	Wooden and Concrete based	42
8.	Khanyara-I	Wooden and Concrete based	55
9.	Khanyara-II	Wooden and Concrete based	57

10.	Upper Khanyara	Concrete based	113
11.	Khanyara (Near Manjhi micro Project	Concrete based	135
12.	Darnu-I Above road	Concrete based	81
13.	Darnu-II Above road	Concrete based	92
14.	Dari	Concrete based	68
15.	Narwana Khas-I	Concrete based	116
16.	Narwana Khas-II	Concrete based	119
17.	Andrad (Narwana)	Wooden and Concrete based	38
18.	Narwana (home)	Concrete based	69
19.	Near ITI	Concrete based	117
20.	Upper Barol-I	Concrete based	69
21.	Upper Barol-II	Concrete based	129
22	Sakoh-I	Concrete based	57
23.	Chalian Near Jawahar Nagar	Concrete based	51
24.	Chilghari	Concrete based	77
25.	Sakoh Near Radio colony	Concrete based	115
26.	Yol cant	Concrete based	48
27.	Near Chamunda	Concrete based	41
28.	Palampur	Wooden and Concrete based	65
29.	Palampur	Wooden and Concrete based	47
30.	Palampur	Concrete based	43
31.	Near neugal pul	Concrete based	64
32.	Near neugal pul	Concrete based	129
33.	Dagbaar	Concrete based	41
34.	Dagbaar	Concrete based	54
35.	Near Sai University	Concrete based	64
36.	Near Palampur CSIR lab	Concrete based	93
37.	Padyakhal	Concrete based	55
38.	Near Sacha suada	Concrete based	77

39.	Near Nagri	Concrete based	42
40.	Paprola	Concrete based	52
41.	Paprola	Concrete based	114
42.	Baijnath	Concrete based	51
43.	Baijnath	Wooden and Concrete based	41
44.	Baijnath	Concrete based	69
45.	Near Para billing station	Concrete based	51
46.	Delu Gadiyara	Concrete based	122
47.	Near Chauntra	Concrete based	48
48.	Between Harabag and Joginderngar	Concrete based	52
49.	Jogindernagar	Wooden and Concrete based	24
50.	Jogindernagar	Concrete based	141

Indoor radon concentration in the study area is found to vary from 23.3Bq/m^3 to 158.8 Bq/m^3 with the average value of 71.1 Bq/m^3, which is higher than world average of 40 Bq/m^3 (UNSCEAR, 2000), but well below the recommended action level of 200 Bq/m^3 as suggested by ICRP (ICRP, 1993). Maximum number of houses which were monitored with radon concentration more than the world average except house no. 3, 4, 5, 6, 17 and 49. The values of radon concentration monitored in house(s) no. 1, 10, 11, 15, 16, 19, 21, 25, 32, 41, 46 and 50 were more than 100 Bq/m^3. No house was found with radon concentration more than 200 Bq/m^3.The lesser values of radon concentration are because of the well ventilation in sample houses, the radon concentration which was measured more than 100 Bq/m^3, because of life style of owner of houses and these houses remained closed most of during study period.

These values are lesser than the values monitored by other researchers Sharma et al., [1998)], Singh et al., [1998, 2001], Kumar et al., [2013], Gupta et al., [2011] in Himachal Pradesh and Punjab.

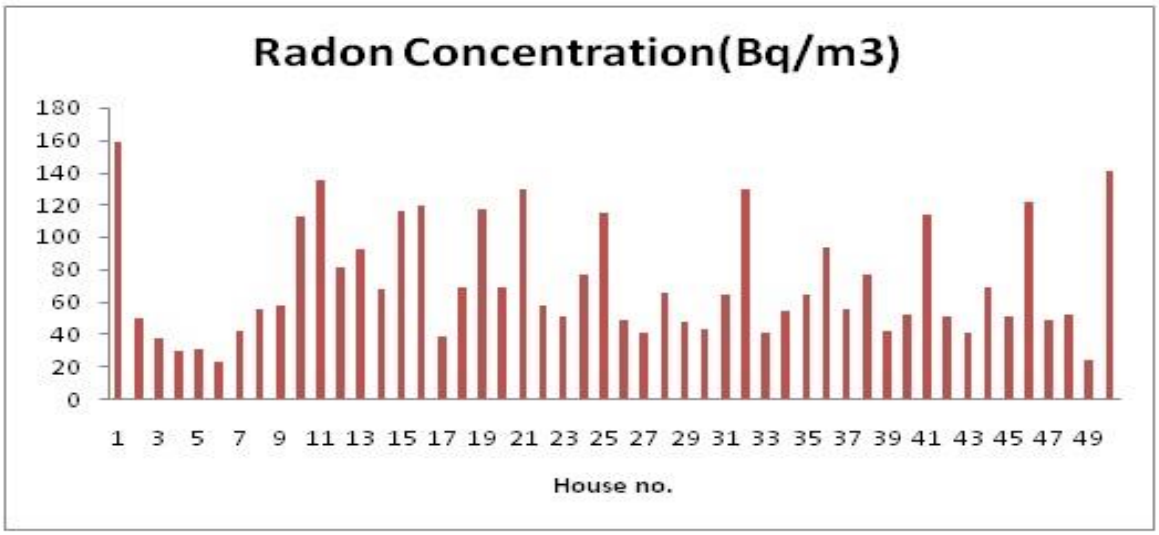

Figure 33: Radon concentration levels in fifty houses of study area (Dharamshala-Palampur-Jogindernagar)

5.3 Conclusions

The average indoor radon concentration measured in the dwellings of Dharamshala region (Dharamshala-Palampur- Jogindernagar) is found to be 71.1 Bq/m^3 with range of 23.3 Bq/m^3 to 158.8 Bq/m^3, whereas the values of indoor radon concentrations for Mandi region are found to vary from 42.22 Bq/m^3 to 398.33Bq/m^3 with an average of 138Bq/m^3. In both regions this value was more than world average of 40 Bq/m^3 [UNSCEAR, 2000]. But the value of Radon concentration was less than action level 200 Bq/m^3 [ICRP, 1993]. The accumulation concentration level in dwellings depends upon the types of construction material used and ventilation level.

CHAPTER 6

CONTINOUS RADON MONITORING AND HEALTH RISK ASSESSMENTS

6.1 Introduction

Over the past few decades, investigations throughout the world provide enough evidence that significant variations of radon concentration (both in soil-gas as well as indoor levels) may occur in association with major geophysical events such as volcanic eruptions and earthquakes [Hartmann and Levy, 2005; Kumar et al., 2013a, 2013b; Martinelli et al., 1995; Singh et al., 2010; Walia et al., 2013; Yang et al., 2011]. Radon distribution may also be correlated to the tectonic fault lines and geothermal heat flow zones in some regions of world [Etiope and Martinelli, 2002; Walia et al., 2008; Kumar et al., 2014; Khattak et al., 2014]. In spite of being used as a marker for geophysical activities, its indoor levels has been measured by different techniques due to its carcinogenic effects of human body [Kávási et al., 2010; Kovacs 2010; ICRP 2011]. The World Health Organization (WHO) had drawn the attentions of world towards health effects from residential radon exposures. In continuation with its work, in 2005 WHO established some projects about the international radon exposure aimed to identify, make and develop effective strategies of reducing the health impact from radon exposure and to raise public awareness about the consequences of long term exposures to radon [WHO, 2009]. The measurement of exposure from radon is relatively simple to perform and essential to assess radon concentration in homes since the studies in Europe, North America and Asia provide strong evidences of correlation between increases in the cancer risks with proportional increase in concentration of radon [WHO, 2009]. The underlying prone risk to lung cancer for active smokers was estimated higher than for lifelong non-smokers, whereas the potential for risk to both smoker and non smoker groups increase by 16% for every 100Bq/m^3 of radon exposure at home. There are evidences for lung cancer below 200Bq/m^3 for prolonged exposure [ICRP, 2011]. During inhalation process radon gas, alpha particles emitted from its decay interact with biological tissue in the lungs, leading to DNA damage hence increase chances of mutation of the biological cells available for the development of cancer. The results of pooled residential radon studies in the North America [Krewski et al., 2006], Europe [Darby et al. 2006], and China [Lubin et al., 2004] have reported statistically significant increase (ranging from 8% to 18%, depending on the method of analyses) in lung cancer risk at 100 Bq/m^3. The radon concentrations are affected by air pressure and pathways in

the home, depending upon the construction and the ventilations. Like present study the fluctuations in radon concentration in different climatic conditions and seasons at different places around the world are reported by many authors (Singh et al., 2001, 2005a, 2005b, Kant et al., 2009, Akota et al., 2011). The radon concentration is generally expressed in units of Bq/m^3 whereas radon dose is the energy absorbed by unit mass of absorber (human organ like lung) from radon and its progeny atoms. The Radon exposure is generally expressed in the unit of mSv [ICRP, 1991, 1993] whereas in mines or homes, the exposure is traditionally measured in working level (WL) and the cumulative exposure in working level month (WLM); 1 WL in presence of short-lived any of ^{222}Rn progeny (^{218}Po, ^{214}Pb, ^{214}Bi, and ^{214}Po) and its combination in 1 liter of air that releases 1.3×10^5MeV of potential alpha energy; one WL is equivalent to 2.08×10^{-5} joules per cubic meter of air (J/m^3). 1WL for 170 hours equals 1WLM cumulative exposure. Passive detectors (Viz. Solid state nuclear Track Detector) are cheap and easy to install so can be used in remote areas. Since SSNTD's give the results of radon concentration for prolonged integration exposure hence they are widely used for large scale surveys. Numerous measurements of radon activity concentrations in different countries have been published in recent years [UN-SCEAR, 2000; Kávási et al., 2010].

The present study will, therefore, focus on the radon monitoring using SSNTDs in the houses of Mandi District (which is second largest district in term of population (out of 12) according to the 2011 census), Himachal Pradesh, India for health hazard assessment(technique is detailed in chapter 2) . Moreover the region (Figure 34) under study is seismically active and comes under Zone IV and Zone V, so the study of the radon level in this region becomes very important [Dwivedi et al., 1996a, 1996b, and 2001]. The study may help the residents to take measures to reduce the radon level in their homes.

6.2 Climate and description of the houses

Mandi district falls in the high hill temperate, mid-hills, sub-humid and wet agro climatic zone of Himachal Pradesh. In this district major rainfall occurs in the month

span of June to September followed by January to March whereas least rainfall occurs in the month of November followed by December, October and April. Lower areas of the district experience hot summer, low to high degree of snowfall in winter and moist during rainy season. Some areas of district usually have heavy snowfall from January to March. .

Most of the houses chosen for the study (about 80%) are made of concrete, the rest of the house are made of mud, granite and wood with metal sheet coverage on the top. The houses that were chosen for continuous study were of approx. size of 3.5m x 4 m with height of 2.75m to 3m. In most of the houses there were only one door and window of size approx. of 1.75 m^2 and a 1.9m^2.

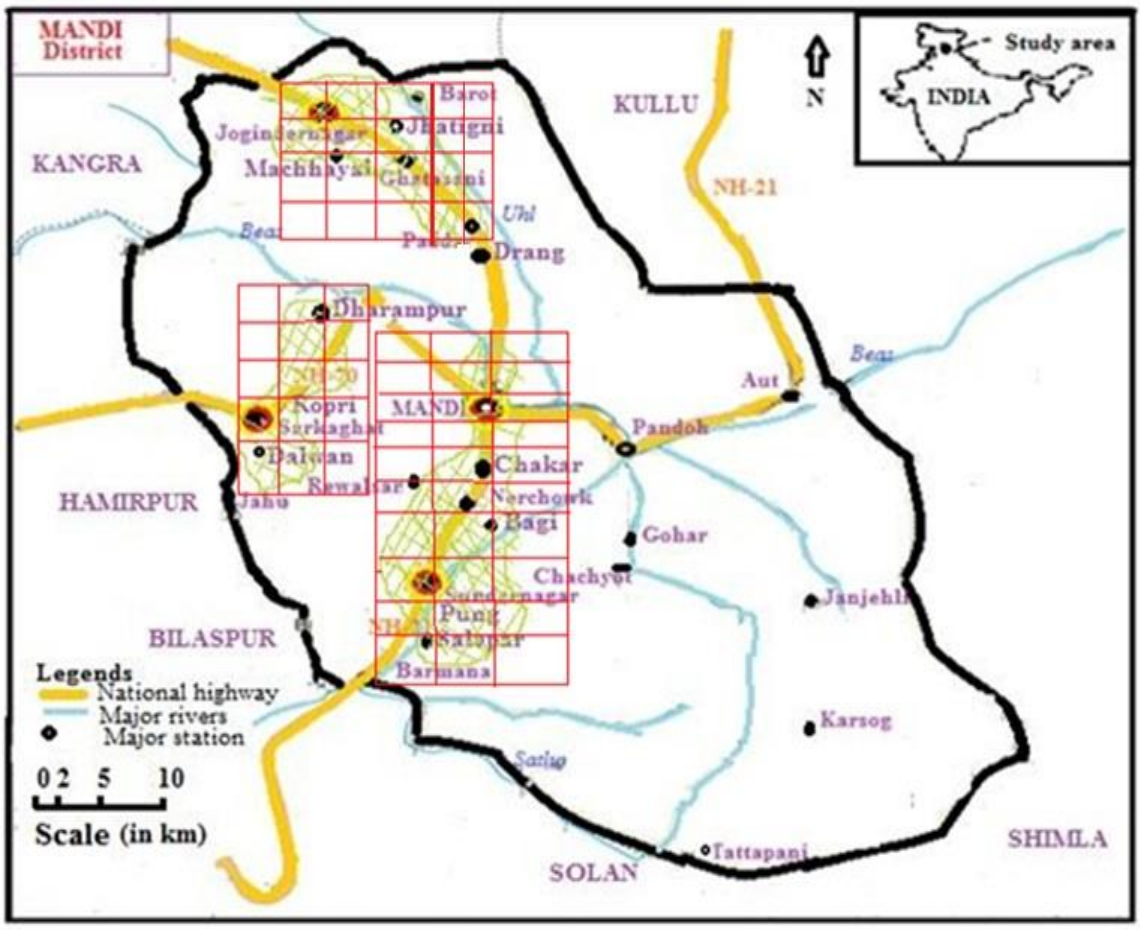

Figure 34: Map showing the location of study area in three different regions Sarkaghat, Mandi- Sundernagar and Jogindernagar of Mandi district,

Himachal Pradesh, India.

6.3 Results and discussion

The observed values of indoor radon concentration in three different regions Sarkaghat, Mandi-Sundernagar and Jogindernagar of Mandi district, Himachal Pradesh, India are reported in tables 12, 13 & 14 respectively. The indoor radon concentration varies from 17±5Bq/m^3 to 533± 41Bq/m^3 with the average for the whole year (annual average) of 94Bq/m^3. Houses of Sarkaghat were having average indoor radon concentration for whole year 101 Bq/m^3. Mandi-Sundernagar region was observed with average radon concentration of 125 Bq/m^3, whereas the average value of Jogindernagar region was 56 Bq/m^3. The comparative values of indoor radon concentration to the world average indoor radon value of 40Bq/m^3 [UNSCEAR, 2000] are shown in Figure 35. The average value of radon concentration for time duration October- December, January- March, April-June and July-September for different areas of Mandi district of Himachal Pradesh are shown in Figure 36. The maximum radon concentration was recorded in January- March (winter season). This may be due to less ventilation in cold season [Akbari et al., 2013]. However, fairly large values in July-September (rainy season) are found may be attributed to the increased porosity of the soil during the rainy season (figure 37). It is found that there is a very less difference in the average value of the indoor radon concentration from October to December, 2012 and July to September, 2013. However, there were about 10% changes in the value of equilibrium equivalent radon concentration (EERC) from winter season (January, 2013 to March, 2013) to the summer season (April, 2013 to June, 2013). It means that variation in indoor radon concentration is less affected by changes in temperature, humidity and atmospheric pressure, but is also affected mostly by ventilation condition of the house.

The radon exposure is determined on the basis of ICRP adopted, conversion convention model [Raghavayya, 1994; Chen, 2005]. The average value of the observed annual effective dose was found to be 1.72mSv in a Sarkaghat region (table 12). Mandi-Sundernagar region was observed with an annual effective dose of

2.14mSv (table 13). Whereas the value of the annual effective dose in Jogindernagar region was 0.97mSv (table 14). The average annual effective doses for three regions are shown in figure 38. The total mean annual estimated effective dose received by the public of the study area was 1.61mSv. The average annual estimated effective dose is less than the recommended action level 3-10mSv/y [ICRP, 1993]. However, there are some houses in different region of the study area where the value of annual estimated dose is close to or more than the recommended action level. The indoor radon concentrations observed in the study areas were less than the action level 200Bq/m^3 [ICRP, 1993] except for, one house in Sarkaghat region and two houses in Mandi-Sundernagar region. The indoor radon concentration recorded more than action level in the one house of Sarkaghat region was region was 533±41Bq/m^3 (table 12). Whereas the indoor radon concentration recorded more than action level in the two houses of Mandi – Sundernagar region were 224±49Bq/m^3 and 417±112Bq/m^3 respectively (table 14). Higher values of indoor radon concentration in these houses may be attributed to the building material and low ventilation rate [Akbari et al., 2013]. These dwellings were constructed using the mud and granite stones with only two windows which were not opened for maximum of the times. Further, the radon concentration was found to be below 100Bq/m^3 for most of the houses in the study area. This may be attributed to the maximum residing time of the population at home with good ventilation conditions.

It has been also observed the values of indoor radon concentration were usually high in the Mandi-Sundernagar region. This may be attributed to the high uranium content in the soils of this region [Sharma et al., 2000] and low ventilation conditions.. These values are incomparable to the values reported in Himachal Pradesh and Punjab by Sharma et al., [1998] and Singh et al., [1998] but less than the values reported by Singh et al., [2001] and more than the values obtained by Kumar and Chauhan, [2014] in the northern part of Haryana state of India. The values of radon concentration in the dwellings of Hamirpur district, Himachal Pradesh [Mehra and Bala, 2014] are comparable to the values reported in this study with some exceptions (high level of the uranium content in soil). Moreover, the region also has a number of thermal springs, and a uranium mineralisation zone with high values of radon, uranium and deep

originated gases which can be possible radon carriers [Walia et al., 2005; Cinti et al., 2009]. However, the present study area is far away from these features and not influenced by it.

Table 12: Indoor radon concentration, WLM and annual effective dose observed in Sarkaghat region of district Mandi, Himachal Pradesh.

House no.	Radon concentration (Bq/m^3)					Radioactivity in mSv/y	WLM/ Year	Exposure ($mJhm^{-3}$)
	Oct-Dec, 2012	Jan-March, 2013	April-June, 2013	July-Sept, 2013	$\mu \pm \sigma$ (Average ± Stdev)			
1	194	165	141	173	168±22	2.89	0.74	2.62
2	96	109	103	121	107±11	1.84	0.47	1.67
3	118	104	112	116	113±6	1.94	0.50	1.75
4	62	43	47	54	52±8	0.89	0.23	0.80
5	65	40	51	98	64±25	1.09	0.28	0.99
6	36	32	38	32	35±3	0.59	0.15	0.54
7	38	29	33	49	37±9	0.64	0.16	0.58
8	44	18	27	36	31±11	0.54	0.14	0.49
9	78	144	167	92	120±42	1.78	0.45	1.61
10	524	592	498	519	533±41	9.17	2.35	8.31
11	38	58	42	38	44±10	0.76	0.19	0.69
12	82	98	101	96	94±8	1.6	0.42	1.47
13	42	48	46	42	45±3	0.77	0.20	0.69
14	32	36	41	36	36±4	0.62	0.16	0.57
15	39	41	38	50	42±5	0.72	0.18	0.65

Table 13: Indoor radon concentration, WLM and annual effective dose in Mandi – Sundernagar region of district Mandi, Himachal Pradesh

House no.	Radon concentration (Bq/m^3)					Radioactivity in mSv/y	WLM /year	Exposure ($mJhm^{-3}$)
	Oct-Dec, 2012	Jan-March, 201	April-June, 2013	July-Sept, 2013	$\mu \pm \sigma$ (Average ±Stdev)			
1	86	9	81	102	92±10	1.5	0.40	1.4
2	54	5	51	56	53±2	0.9	0.23	0.8
3	163	127	113	122	131±22	2.2	0.58	2.0
4	78	7	64	64	70±7	1.2	0.31	1.0

5	89	100	91	99	95±6	1.6	0.42	1.4
6	44	4	42	48	46±3	0.7	0.20	0.7
7	207	293	180	214	224±49	3.8	0.98	3.4
8	87	124	108	117	109±16	1.8	0.48	1.7
9	99	107	91	97	99±7	1.6	0.43	1.5
10	158	133	114	121	132±19	2.2	0.58	2.0
11	52	9	79	76	75±17	1.2	0.33	1.1
12	99	124	111	110	111±10	1.9	0.49	1.7
13	97	133	128	147	126±21	2.1	0.56	1.9
14	126	160	158	167	153±18	2.6	0.67	2.3
15	162	138	134	136	143±13	2.4	0.63	2.2
16	82	6	53	64	67±12	1.1	0.29	1.0
17	92	113	102	120	107±12	1.8	0.47	1.6
18	74	117	109	131	108±24	1.8	0.47	1.6
19	127	213	190	218	187±42	3.2	0.82	2.9
20	47	6	52	65	58±10	0.9	0.25	0.9
21	105	137	123	168	133±27	2.2	0.59	2.0
22	158	137	151	177	156±17	2.6	0.69	2.4
23	152	140	147	157	149±7	2.5	0.66	2.3
24	135	126	117	119	124±8	2.1	0.55	1.9
25	62	129	131	152	119±39	2.0	0.52	1.8
26	79	6	48	51	60±14	1.0	0.26	0.9
27	311	162	136	126	184±86	3.1	0.81	2.8
28	49	4	35	36	41±6	0.7	0.18	0.63
29	180	190	166	174	178±10	3.0	0.78	2.7
30	568	437	320	345	417±112	7.1	1.84	6.5

Table 14: Indoor radon concentration, WLM and Annual effective dose observed in Jogindernagar region of district Mandi, Himachal Pradesh

House no.	Radon concentration (Bq/m^3)					Radioactivity in mSv/y	WLM /year	Exposure ($mJhm^{-3}$)
	Oct-Dec, 2012	Jan-March, 2013	April-June, 2013	July-Sept, 2013	$\mu \pm \sigma$ (average ±stdev)			
1	54	48	36	54	48±8	0.83	0.21	0.75
2	164	174	156	182	169±11	2.90	0.74	2.63
3	19	49	14	21	26±16	0.44	0.11	0.40
4	32	37	28	33	33±4	0.56	0.14	0.51
5	40	29	26	36	33±6	0.56	0.14	0.51
6	23	30	54	61	42±18	0.72	0.18	0.65
7	21	23	12	19	19±5	0.32	0.083	0.29
8	101	92	78	98	92±10	1.59	0.41	1.44
9	42	42	21	24	32±11	0.55	0.14	0.51

10	31	43	34	30	35±6	0.59	0.15	0.54
11	83	95	56	65	75±18	1.29	0.33	1.17
12	44	63	66	54	57±10	0.98	0.25	0.88
13	11	23	16	19	17±5	0.30	0.08	0.27
14	38	40	30	42	38±5	0.65	0.17	0.59
15	114	132	93	105	111±16	1.91	0.49	1.73
16	40	57	33	42	43±10	0.74	0.19	0.67
17	31	36	27	28	31±4	0.52	0.13	0.48
18	168	203	130	180	170±30	2.93	0.74	2.65
19	26	29	19	24	25±4	0.42	0.11	0.38
20	29	31	33	34	32±2	0.55	0.14	0.49

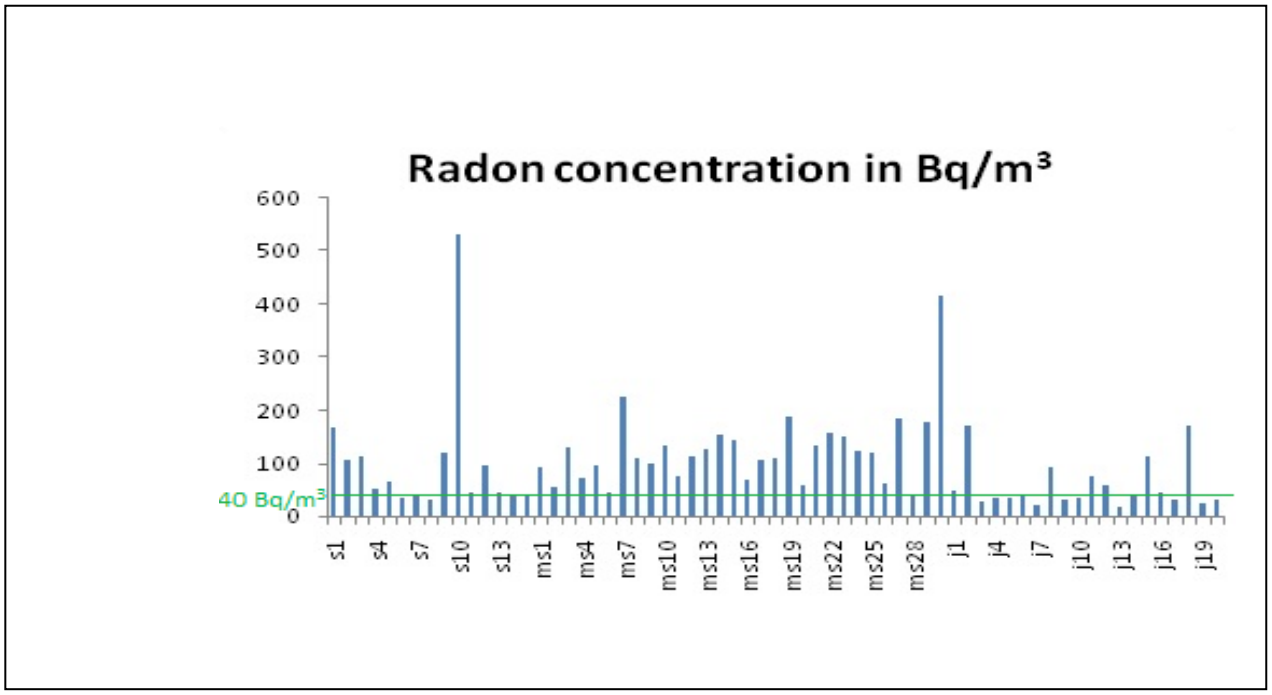

Figure 35: Average value for Indoor radon concentration in sixty five dwellings (where s for Sarkaghat, ms for Mandi- Sundernagar and J for Jogindernagar) of study area compared to the world average value of 40Bq/m^3 [UNSCEAR, 2000].

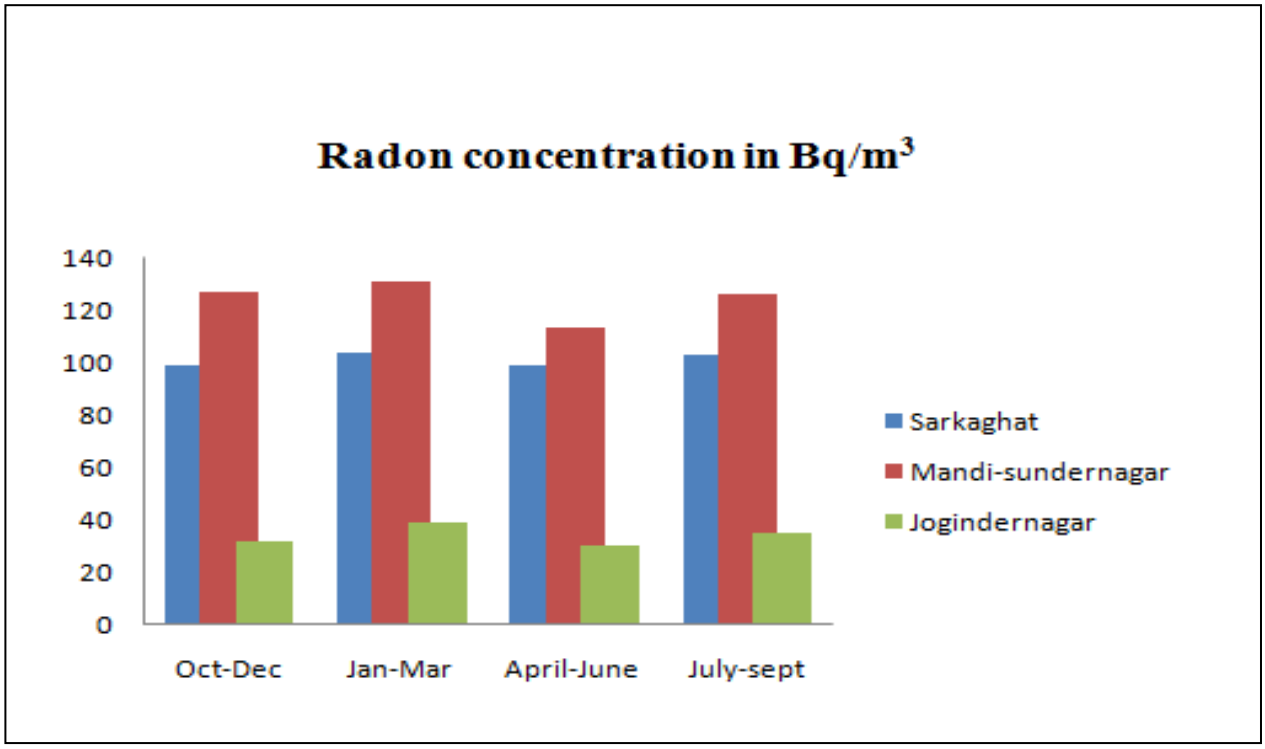

Figure 36*:* Average value of indoor radon concentration (in different seasons) for different areas of Mandi district of Himachal Pradesh.

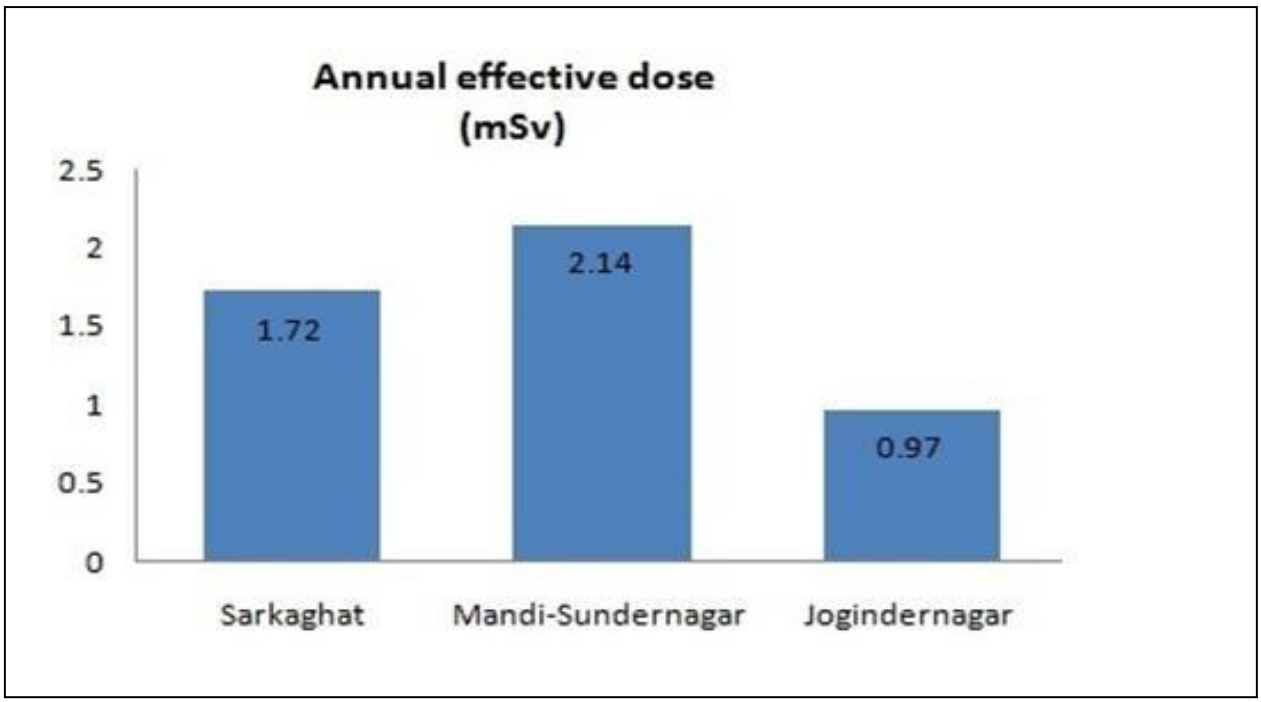

Figure 37: Showing the level annual effective dose (mSv) in different areas of Mandi district of Himachal Pradesh

6.4 Conclusions

1. The peoples of study area are living in higher radon concentration than the world average of 40 Bq/m^3, but less than the reference level 300 Bq/m^3 [ICRP, 2007], depending upon time of exposure these concentration may affect the public health [ICRP,2011].

2. There were about 10% changes in the Maximum value of equilibrium equivalent radon concentration (EERC) from winter season (January, 2013 to March, 2013) to minimum value in the summer season (April, 2013 to June, 2013).

3. The seasonal variation in radon equilibrium equivalent concentration is affected mostly by ventilation condition in different seasons along with changes in temperature, humidity and atmospheric pressure.

4. The difference in the average value of observed radon equilibrium equivalent concentration in different parts of the study area may be due to differences in radioactive contents of the soil.

CHAPTER 7

RADON EXHALATION RATES AND THEORETICAL MODELING

7.1 Introduction

The radon measurement is very significant for health assessment as well for geological tracing. The concentration of different gases in soil like CO_2 and CH_4 affect the diffusion of ^{222}Rn, therefore Radon exhalation rates may be helpful to study various gaseous transport Processes [Zhou etal., 2008]. The radon escapes from the soil by plant transpiration and diffusion through soil pores. The radon emanation fluxes from land areas are approximately 100 times more than ocean mass fluxes, even the vegetation areas are having more flux rates (difference in the porosity or permeability of the soil). Similarly the radon fluxes are also differ in snow bound areas (precipitation may clock the pores of soil i.e. reduction in porosity) [Feichter and Crutzen, 1990; Schery and Gaeddert, 1982; Strong and Levins, 1982; Schery et al., 1984]. The emanation of the radon from surface is known to be function of Radium contents, soil temperature, porosity, depth, moisture and type of vegetation in their decreasing importance [Pearson and Jones, 1966]. Radon emanation rates may also be affected by air pressure [Schery and Gaeddert, 1984]. The world wide radon emanation rates are approximately 1 atom $cm^{-2}s^{-1}$ [Lambert et al., 1982]. Various climate model are devised using radon emanation of (a) Source strength of 1 atom $cm^{-2}s^{-1}$ (60S to 60 N) and 0.5atom $cm^{-2}s^{-1}$ (60 N to 70 N) (b) Source strength a function of air temperature 3.2×10^{-16} kg $m^{-2}d^{-1}$ when Temperature T_k <273K and 1.0×10^{-16} kg $m^{-2}d^{-1}$ when $T_k \leq$ 273K [Rind and Lerner, 1996]. The latitudinal distribution of radium contents decreases linearly with latitude in northern hemisphere [Masayoshi et al., 2008]. These researches showed that radon is global environmental Tracer. Therefore the study of ^{222}Rn exhalation rates can also be used develop various theoretical models explaining various phenomenon like Pollutions and Green house effect [Rogers et al., 1991; Sakashita et al., 1994; Genthon and Armengaud, 1995; Schery et al., 1995; Chino and Yamazawa, 1996; Taguchi et al., 2002; Zhou et al., 2008]. By measuring radon exhalation rates for various types of soil one can estimate the Indoor radon and thoron concentrations by developing a appropriate model using similar conditions as may be in real situation [Kumar et al., 2014; Chauhan et al., 2014]. The present study is based on the measurement of radon exhalation rates in 96 sites of active Kangra and Mandi region of Himachal Pradesh, NW Himalaya India using solid state nuclear track detectors (Figure 38 & 39). A theoretical model is developed based on Roger model, Schery model and some previous researches to calculate the radon exhalation rates. For this purpose the simple second order equations were

solved based on boundary conditions and conditions used in our study.

7.2 Theoretical basis

The radon Diffusion flux ($Bqm^{-2}s^{-1}$) through big radius path in single phase is

$$\mathbf{F = -D_i \frac{dC}{dx}}$$

[Fick, 1855; Crank, 1975]

Where C = Radon concentration (Bqm^{-3}) and D_i = Diffusion coefficient (m^2s^{-1}) however soil moisture can greatly affect the Rn Diffusion. According to Rogers model at soil-gas interface the balance equation for Rn concentration is given by

$$\frac{dC}{dt} = D_i \, d^2C/dx^2 - [g/v\ p\ (1\text{-}m)]\ P \frac{dC}{dx} - \lambda\ C + [R\ p\ \lambda\ \varepsilon\ /p\ (1\text{-}m)] - [R\ m\ \lambda\ /(1\text{-}m)\ K] + T_{la} - T_{as} \quad \textbf{.....(1)}$$

[Roger et al., 1991]

g = Bulk material air permeability (m^2)

v = Viscosity of air

m = moisture saturation in pores

P = gas pressure in pores

λ = Radon decay constant(s^{-1})

R = R_a concentration in dry solid material (Bq kg^{-1})

ρ = Bulk dry density (kg m^{-3})

ε = Rn emanation coefficient in pore air phase

T_{la} = Transfer factor of Rn from pore liquid to air ($Bqm^{-2}s^{-1}$)

T_{as} = Transfer factor of Rn from pore air to solid surface ($Bqm^{-2}s^{-1}$)

K = Radon Equilibrium distribution coefficient solid to pore liquid (m^3kg^{-1})

The first term in above equation is the Rn diffusion in the pore space, second term represent the convection of Rn by pore air the convection velocity of pore air so we may write V dC/dx = - [g/v p (1-m)] P dC/dx -ve sign is used because convection velocity increases the radon exhalation rates. third term account for the radioactive decay of Rn , fourth term is Rn source for pore air and fifth term describe the correction term for Rn dissolved in the pore air since in present study we use dry soil in closed container so fourth and fifth terms are negligible. Sixth and seventh term

represent Rn transfer from pore water and its loss to surface particle. Now equation (1)becomes

$$\frac{dC}{dt} = D_i \frac{d^2C}{dx^2} + V\frac{dC}{dx} - \lambda C + T$$

..... (2)

Where (T_{la} - T_{as}) = T.

The steady state equation for radon transport using diffusion and convection processes can be written as:

$$D_i \frac{d^2C}{dx^2} + V\frac{dC}{dx} - \lambda C + T = 0$$

..... (3)

In our study we have considered the homogenous pore and uniformly distributed uranium and radium in the soil.

Equation **(3)** represents the Darcy's law whose general solution is given as

$$C = a_1 \exp\left[\frac{-V+\sqrt{V^2+4\lambda D_i}}{2D_i}\right]x + a_2 \exp\left[\frac{-V-\sqrt{V^2+4\lambda D_i}}{2D_i}\right]x + \frac{T}{\lambda}$$

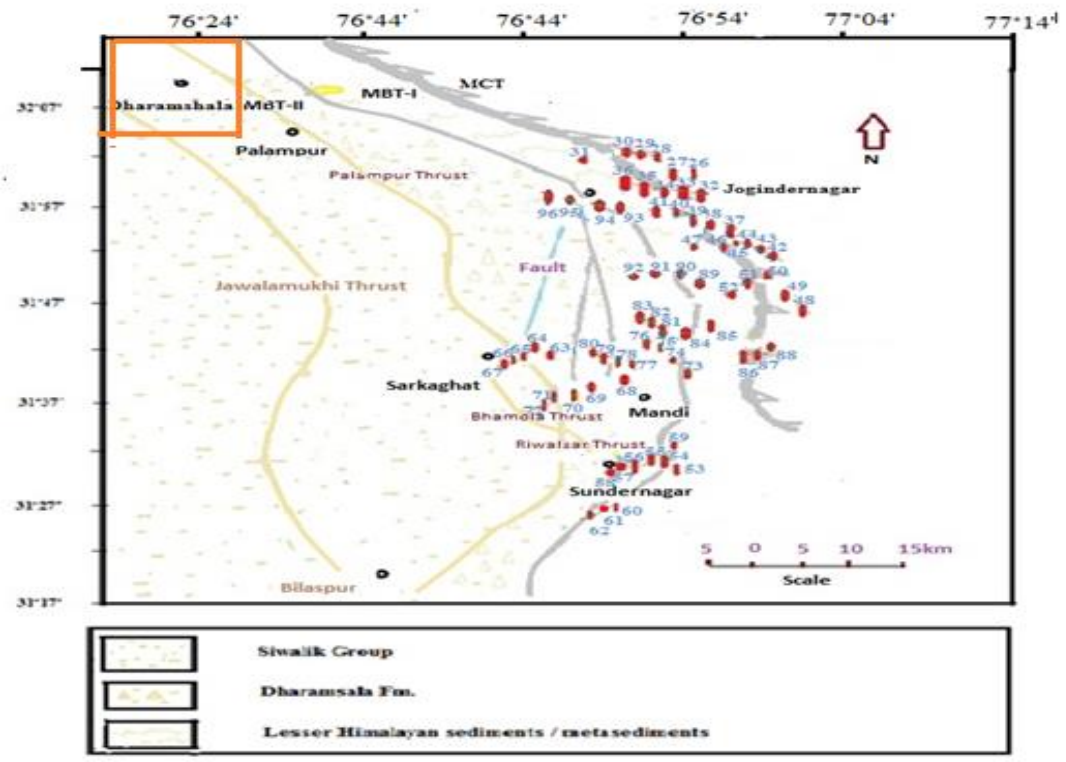

Figure 38: Sampling sites in Mandi district of Himachal Pradesh

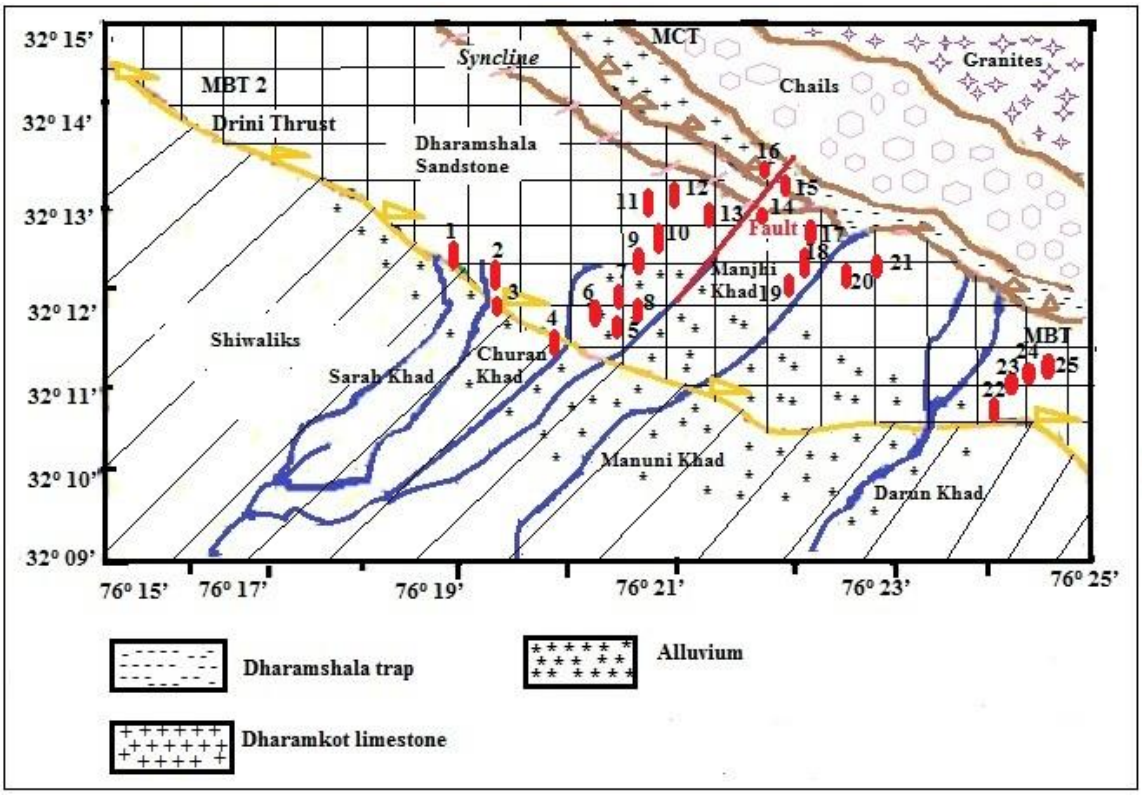

Figure 39: Sampling sites in Dharamshala region inset of figure 15 in red square [Kumar et al., 2013]

7.3 Theoretical modeling:

For calculation of C following conditions were considered

1. when $x \rightarrow \infty$, C should not be infinite
2. at surface – air interface radon exhalation rate must be equal in both direction i.e. towards surface side and towards air side.
3. when $x \rightarrow 0$, $C \rightarrow 0$
4. when $x \rightarrow \infty$, C approaches be infinite because of first part of equation (4) hence only possible solution is

$C = a_2 \exp\left[\frac{-V-\sqrt{V^2+4\lambda Di}}{2Di}\right] x + \frac{T}{\lambda}$ when $x \rightarrow 0$, $C \rightarrow 0$ so $a_2 = -\frac{T}{\lambda}$ Using these conditions

$\mathbf{C = \frac{T}{\lambda}[1- exp\{\frac{-V-\sqrt{V^2+4\lambda Di}}{2 Di}\}x]}$ for maximum value of C, $T = \lambda C_{max} = \lambda C_{Ra} \rho \varepsilon / \eta$ where C_{Ra} = Soil activity (Bq kg^{-1}), ε = Radon emanation coefficient, η = effective porosity and ρ is the density of the soil. In the present the radon exhalation rate is measured by LR-115 type-II detector in seal container, so we consider V = 0, hence value of C may be written as

$$\mathbf{C = \frac{T}{\lambda}[1- exp(-\sqrt{\frac{\lambda}{Di}})x]}$$

Using above equation in fick law the radon exhalation rate may be

$$\mathbf{F \propto T\sqrt{Di\,\lambda}[exp(-\sqrt{\frac{\lambda}{Di}})x]}$$

(proportionality sign is used, since many factors used in Roger model are ignored)

However on the basis of radon exhalation rates experimentally measured at 96 different sites the proposed value of exhalation rate is $\mathbf{F = 0.1\,\eta^2\,T\sqrt{Di\,\lambda}[exp(-\sqrt{\frac{\lambda}{Di}})x]}$ in Bq m^{-2} s^{-1}, where x is the distance between source and detector and η is porosity of soil.

7.4 Results and discussion

The values of measured and estimated Exhalation rates are tabulated in Table no. 15 and 16

Table 15: Measured exhalation rates in the study area

S.N.	Radon concentration (Bq/m^3)	Area exhalation rate (Bq $m^{-2}h^{-1}$)	Mass Exhalation rate (Bq $kg^{-1}h^{-1}$)	Radium Contents (Bq kg^{-1})
1	2246	1.178	0.052	5.66
2	2213	1.161	0.051	5.59
3	2231	1.171	0.052	5.57
4	4996	2.622	0.116	12.20
5	2144	1.125	0.050	5.28
6	2586	1.357	0.060	6.46
7	4930	2.587	0.114	12.10

8	2860	1.501	0.066	6.44
9	2282	1.198	0.053	5.43
10	2909	1.527	0.067	6.89
11	4658	2.445	0.108	11.46
12	3732	1.959	0.086	9.26
13	3007	1.578	0.069	7.42
14	1431	0.751	0.033	3.62
15	1398	0.734	0.032	3.28
16	6020	3.159	0.139	14.33
17	2376	1.247	0.055	5.94
18	4070	2.136	0.094	10.21
19	3950	2.073	0.092	9.94
20	2360	1.239	0.055	5.77
21	2400	1.260	0.056	5.83
22	3459	1.815	0.080	8.69
23	3500	1.837	0.081	9.02
24	2675	1.404	0.062	6.63
25	2784	1.461	0.065	6.91
26	2173	1.140	0.050	5.34
27	1627	0.854	0.038	4.11
28	3183	1.670	0.074	7.98
29	2674	1.403	0.062	6.65
30	2530	1.328	0.059	6.26
31	3371	1.769	0.078	8.20
32	2871	1.507	0.066	6.97

33	1932	1.014	0.045	4.77
34	2056	1.079	0.048	5.28
35	3284	1.723	0.076	8.19
36	1922	1.009	0.044	4.71
37	3955	2.076	0.092	9.33
38	4020	2.110	0.093	9.96
39	1973	1.035	0.046	4.81
40	3130	1.643	0.073	7.41
41	1644	0.863	0.038	3.97
42	3395	1.782	0.079	8.25
43	1742	0.914	0.040	4.37
44	3766	1.976	0.087	9.53
45	2389	1.254	0.055	5.60
46	2449	1.285	0.057	6.37
47	1988	1.043	0.046	5.01
48	1860	0.976	0.043	4.52
49	2231	1.171	0.052	5.67
50	3236	1.698	0.075	8.35
51	3399	1.784	0.079	8.66
52	2507	1.316	0.058	6.29
53	1286	0.675	0.030	3.18
54	3144	1.650	0.073	7.71
55	3160	1.658	0.073	8.02
56	5020	2.635	0.116	12.41
57	1678	0.881	0.039	4.21

58	2846	1.494	0.066	7.04
59	4810	2.524	0.111	11.73
60	2965	1.556	0.069	7.12
61	3007	1.578	0.070	7.20
62	2731	1.433	0.063	6.63
63	2582	1.355	0.060	6.61
64	3551	1.864	0.082	8.99
65	2706	1.420	0.063	6.88
66	3100	1.627	0.072	7.37
67	2899	1.521	0.067	6.94
68	3820	2.005	0.089	9.06
69	3953	2.075	0.092	9.57
70	1780	0.934	0.041	4.39
71	3927	2.061	0.091	9.44
72	2930	1.538	0.068	6.99
73	1707	0.896	0.040	4.26
74	4200	2.204	0.097	10.44
75	3780	1.984	0.088	9.72
76	2710	1.422	0.063	6.74
77	2391	1.255	0.055	5.81
78	2978	1.563	0.069	7.19
79	3249	1.705	0.075	7.88
80	2750	1.443	0.064	6.79
81	2196	1.152	0.051	5.35
82	2120	1.113	0.049	5.07

83	2280	1.197	0.053	5.59
84	1482	0.778	0.034	3.66
85	2749	1.443	0.064	6.88
86	1227	0.644	0.028	3.11
87	2609	1.369	0.060	6.72
88	2290	1.202	0.053	5.73
89	2210	1.160	0.051	5.46
90	2710	1.422	0.063	6.67
91	2996	1.572	0.069	7.49
92	2360	1.239	0.055	5.71
93	6320	3.317	0.15	15.41
94	1749	0.918	0.041	4.41
95	2484	1.304	0.058	6.27
96	2130	1.118	0.049	5.17

Table 16: The estimated exhalation rates, calculated using proposed model based on Rogers model

S.N.	X (distance between source and detector) in cm	Density of soil ($x10^3$ Kg/m^3)	Porosity	Emanation rates	Estimated radon-exhalation rates on the basis of proposed model ($Bq\ m^{-2}s^{-1}$) $x10^{-4}$	Experimental value of exhalation rates ($Bq\ m^{-2}s^{-1}$) $x\ 10^{-4}$
1	5.71	1.76	0.34	0.20	3.20	3.27
2	5.72	1.77	0.34	0.20	3.18	3.23
3	5.65	1.68	0.36	0.22	3.50	3.25
4	5.45	1.46	0.45	0.24	8.96	7.28
5	5.58	1.59	0.39	0.22	3.40	3.13
6	5.66	1.69	0.37	0.22	4.20	3.77

7	5.56	1.57	0.40	0.23	8.26	7.19
8	5.10	1.19	0.54	0.26	5.08	4.17
9	5.39	1.41	0.47	0.24	4.08	3.33
10	5.36	1.38	0.48	0.25	5.39	4.24
11	5.57	1.58	0.39	0.22	7.34	6.79
12	5.62	1.64	0.38	0.22	6.0	5.44
13	5.59	1.61	0.39	0.22	4.84	4.38
14	5.73	1.78	0.32	0.21	2.05	2.09
15	5.31	1.33	0.50	0.25	2.57	2.04
16	5.39	1.41	0.47	0.25	11.21	8.78
17	5.66	1.69	0.37	0.22	3.86	3.46
18	5.68	1.73	0.35	0.21	6.13	5.93
19	5.70	1.75	0.34	0.21	5.87	5.76
20	5.54	1.55	0.38	0.22	3.53	3.44
21	5.50	1.51	0.42	0.23	4.02	3.50
22	5.69	1.73	0.34	0.21	5.07	5.04
23	5.84	1.95	0.26	0.19	4.11	5.1
24	5.61	1.63	0.38	0.22	4.27	3.90
25	5.62	1.64	0.38	0.22	4.47	4.06
26	5.57	1.58	0.40	0.23	3.67	3.17
27	5.72	1.77	0.33	0.21	2.38	2.37
28	5.68	1.72	0.35	0.21	4.77	4.64
29	5.63	1.65	0.37	0.22	4.22	3.90
30	5.60	1.62	0.39	0.23	4.29	3.69
31	5.51	1.52	0.42	0.23	5.69	4.91

32	5.50	1.51	0.43	0.24	5.13	4.19
33	5.59	1.3	0.51	0.25	3.73	2.82
34	5.81	1.91	0.28	0.20	2.67	3.00
35	5.65	1.68	0.36	0.22	5.15	4.79
36	5.55	1.56	0.38	0.22	2.90	2.80
37	5.34	1.37	0.48	0.25	7.24	5.77
38	5.61	1.63	0.38	0.22	6.41	5.86
39	5.51	1.52	0.42	0.23	3.33	2.88
40	5.36	1.38	0.47	0.24	5.45	4.56
41	5.47	1.48	0.44	0.24	2.93	2.40
42	5.50	1.51	0.43	0.24	6.07	4.95
43	5.68	1.72	0.35	0.21	2.61	2.54
44	5.73	1.78	0.33	0.21	5.55	5.49
45	5.31	1.34	0.50	0.25	4.43	3.48
46	5.89	2.04	0.24	0.19	2.8	3.57
47	5.71	1.76	0.34	0.21	2.98	2.90
48	5.50	1.51	0.43	0.24	3.33	2.71
49	5.76	1.82	0.31	0.21	3.18	3.25
50	5.84	1.94	0.27	0.19	3.92	4.72
51	5.77	1.83	0.31	0.21	4.87	4.96
52	5.68	1.72	0.35	0.22	3.93	3.65
53	5.60	1.62	0.38	0.22	2.03	1.87
54	5.55	1.56	0.41	0.22	5.12	4.58
55	5.75	1.81	0.32	0.21	4.61	4.61
56	5.60	1.62	0.39	0.22	8.15	7.32

57	5.68	1.72	0.35	0.22	2.63	2.45
58	5.60	1.62	0.39	0.22	4.62	4.15
59	5.52	1.53	0.41	0.22	7.64	7.01
60	5.44	1.45	0.45	0.24	5.27	4.32
61	5.42	1.44	0.47	0.24	5.52	4.38
62	5.50	1.52	0.41	0.22	4.3	3.98
63	5.80	1.88	0.33	0.21	4.07	3.76
64	5.73	1.79	0.32	0.21	5.11	5.18
65	5.76	1.85	0.30	0.20	3.61	3.94
66	5.38	1.40	0.47	0.24	5.49	4.52
67	5.42	1.44	0.46	0.24	5.21	4.23
68	5.37	1.39	0.48	0.25	7.14	5.57
69	5.48	1.49	0.44	0.24	7.11	5.76
70	5.59	1.61	0.39	0.22	2.87	2.59
71	5.44	1.45	0.45	0.24	6.98	5.72
72	5.41	1.43	0.46	0.24	5.22	4.27
73	5.65	1.67	0.36	0.22	2.66	2.49
74	5.63	1.65	0.37	0.22	6.63	6.12
75	5.82	1.89	0.28	0.20	4.86	5.51
76	5.63	1.65	0.37	0.22	4.27	3.95
77	5.50	1.51	0.43	0.23	4.10	3.49
78	5.47	1.48	0.44	0.24	5.31	4.34
79	5.49	1.50	0.43	0.23	5.52	4.74
80	5.59	1.61	0.39	0.22	4.43	4.01
81	5.52	1.53	0.41	0.23	3.65	3.20

82	5.41	1.43	0.46	0.24	3.78	3.09
83	5.55	1.56	0.41	0.23	3.88	3.32
84	5.60	1.62	0.39	0.22	2.41	2.16
85	5.67	1.71	0.36	0.22	4.40	4.01
86	5.74	1.80	0.32	0.21	1.78	1.79
87	5.83	1.90	0.28	0.20	3.38	3.80
88	5.67	1.71	0.36	0.22	3.67	3.34
89	5.59	1.61	0.39	0.22	3.56	3.22
90	5.57	1.58	0.40	0.23	4.58	3.95
91	5.66	1.69	0.37	0.22	4.87	4.37
92	5.48	1.49	0.43	0.23	3.98	3.44
93	5.52	1.53	0.41	0.23	10.5	9.21
94	5.71	1.76	0.34	0.21	2.62	2.55
95	5.72	1.77	0.34	0.21	3.75	3.62
96	5.50	1.51	0.43	0.23	3.65	3.11

The experimentally measured exhalation rates for the soil samples in the study area (at different 96 sites) are tabulated in Table 15. The average values of Area Exhalation rate =1.50±0.52 Bq $m^{-2}h^{-1}$ and Mass exhalation rate= 0.0661±0.022 Bq $kg^{-1}h^{-1}$where as average radium contents were found to be 7.03±2.39 Bq kg^{-1}. The minimum value of the exhalation rate is 0.644 Bq $m^{-2}h^{-1}$ at station no. 61 and its maximum value is 3.317 Bq $m^{-2}h^{-1}$ at station no. 93, with corresponding values of radium contents of 3.11 Bq kg^{-1} and 15.41 Bq kg^{-1}**.** The radon exhalation rates were found to increase with the radium contents. The slightly higher values of radium contents were found at station no. 7,16,18,74 and 93. The values for exhalation rates as observed by authors in study area are slightly more than the values as observed by Kumar and Singh [2004] for soil samples from Una (Himachal Pradesh) and Amritsar

(Punjab). These exhalation rates are also very high than the radon exhalation rates from cement samples from various companies in Himachal Pradesh [Kumar and Singh, 2004]. The exhalation rates measured by authors are less than the rates reported by Chauhan [2011] in soil samples from Aravali hills and soil sample from area of Santhal, Pargana and Jharkhand reported by Singh et al., [2010]. However the measured values of radium contents and radon exhalation rates in soil samples from Dharamshala region in present study are comparable to the result reported for these values by Duggal et al., [2015] from northern Rajasthan, India. Moreover radium contents of the soil are sufficiently less than recommended action level 370Bq kg^{-1} and less than world average 36Bq kg^{-1} OECD [1979]. A new data set related to properties of soil in the study area is also developed .The densities of the soil calculated in this study are some similar to results of a study by Gupta et al., [2010].

A new data set related to properties of soil in the study area is also developed .The densities of the soil calculated in this study are some similar to results of a study by Gupta et al., [2010].

The theoretical value of the radon exhalation rate are calculated using empirical formula suggested by authors as:

$\mathbf{F} = 0.1\,\eta^2\,\mathbf{T}\sqrt{\mathbf{Di}\,\boldsymbol{\lambda}}\,\mathbf{[exp\,(-\sqrt{\frac{\lambda}{Di}}\,)}\boldsymbol{x}\mathbf{]}$ Where Di is the radon diffusion coefficient, Di is calculated on the basis of its Temperature dependence $\mathbf{Di= (T_k/273)^{0.75}\,D_0}$ [Schery et al., 1995]. D_0 is the ^{222}Rn diffusion coefficient in Air $=1.1\times 10^{-5}$ m^2s^{-1} and T_k (nearly 303K in our case) the average temperature of the soil during experiment. So $D_i=1.13 \times 10^{-5}$ m^2s^{-1}. The porosity η of the soil is calculated using following formula $\eta=1-\rho_{bulk}/\rho_{particle}$ [Morgan et al., 2005]. The radon emanation coefficient for different type of soil were estimated by the data provided elsewhere by [Nazaroff etal., 1988]. Average estimated exhalation rate= 3.89×10^{-4} Bq $m^{-2}s^{-1}$ whereas average measured value of exhalation rates=3.52×10^{-4} Bq $m^{-2}s^{-1}$. Both values were well correlated to 0.96. By extending the radon measurement at different depths, seasons for a long time monitoring the radon convective velocity can be calculated [Feichter and Crutzen, 1990; Yakovlena, 2005] using formula $C = \mathbf{a_2\,exp\,[\frac{-V-\sqrt{V^2+4\,\lambda\,Di}}{2\,Di}]}\,\boldsymbol{x} + \frac{\mathbf{T}}{\boldsymbol{\lambda}}$ and thus the present work can be extended to develop a radon transport model in different seasons along different faults.

7.5 Conclusions

1. The radium contents in the study area are sufficiently less than permissible limit, so soil of region can be used as construction material for buildings and other structures.
2. The radium contents, area exhalation rate and mass exhalation rate show a good Positive correlation of 0.997.
3. Very less correlation between soil emanation rate and porosity with exhalation rates shows that exhalation rates are mildly depends up on these two quantities.
4. The model developed is correlated to about 0.96 to its experimental counterpart.
5. Difference in the theoretical and experimental results at certain sites may be due to error in measurement of various other factors like Soil density, Porosity and emanation rates.
6. Certainly more data is required to check the validity of model.

CHAPTER 8

RADON LEVEL IN THE WATER SAMPLES

8.1 Introduction

The high level of radioactive constituents of drinking water can result from presence of natural radioactive elements, contamination which is added to water through technological processes (Industries), radioactive wastes from nuclear laboratories/ reactors and radioactive transmutations. Various research studies explore the evidences that radiation exposure from mild to middle level dose for long term exposure may increase chances of mutation of cells to cancer in both human and animals. The maximum recommended reference dose level for absorbed effective dose is equal to 0.1mSv/y, it means that no bad health effects are expected on consumption of water below this limit. Radon concentration in water is mainly due to porosity, permeability, soil exhalation rates and radium contents of the soil beneath water source or rocks related to source area. Since life time of radon is considered to long relative to other isotopes so it has sufficient time to diffuse through the crakes in rocks or through fractured rocks in to ground water resources [Samuelsson and Peterson, 1984]. Hence ground water contains high radon concentration than surface water. It is expected that mean value of radon concentration in water is 0.4Bq/l in public water supply and about 20Bq/l in ground water resources. The average inhalation dose from drinking water should exceed 0.025mSv/y and in case for ingestion 0.002mSv/y so these values are very less as compared with the inhalation doses received from radon and its progeny [UNSCEAR, 2000]. US-NAS [1999] reports an approximate 1:100 risk of cancer from consumption of drinking water to cancer caused by indoor radon. World health organization [WHO, 2011] set a limits of 0.5Bq/l in case of radium content for safe consumption and the allowed maximum concentration level for Rn^{222} in water in 500Bq/m^3 [WHO, 2004]. Precautions should be made if radon concentration of drinking water for public water supplies exceeds 100Bq/l. Since radon comes from the decay of radium therefore water may also be transporter of radium contents. According to USEDA [2000] ^{226}Rn Radium behaves chemically similar to calcium in bone so its large contents in body may cause bone cancer and soft tissue cancer in developing children.

For making radon free water so to its safe consumption aeration systems should be implanted, these aeration plants have efficiency of 99%. However in order to obtain the radon free water fill the container with ordinary tap water and close it undisturbed for about 4 weeks, this time will sufficient to take away the dissolved radon in water.

The modeling for radon seepage through faults and fractures may be helpful to estimate the quantity and quality of the ground water. Using this type of study one can make correlation between major fault systems and radon anomalies in water including its health effects on population consuming water from resources. The study was performed with an objective to measure radon concentration in the water sample from Mandi – Dharamshala Region. For this purpose was comprised of radon concentration measurement in forty water samples from different water resources collected from the study area using RAD7 detector(methodology is discussed in chapter 2).

8.2 Results and discussion

The Longitude and Latitude of the location have been listed in Table 17 and table 18 along with the radon concentrations in water, radium contents of soil and annual effective doses.

Table 17: Measured values of radon concentration in water

.

Sr. No.	Location (from which sample is taken)	Latitude	Longitude	Height	Radon Concentration (Bq/m^3)	Radon Concentration (Bq/l)
1	Sarkaghat	N 31°42.095′	E 76°44.166′	958m	11400	11.4
2	Fatehpur	N 31°38.0093′	E 76°44.038′	892m	7780	7.78
3	Upper Bhambla	N 31°36.0323′	E 76°45.3705′	929m	22700	22.7
4	Kalkhar	N 31°36.1004′	E 76°49.6550′	1297m	4250	4.25
5	Galma	N 31°36.2190′	E 76°52.7699′	877m	18300	18.3
6	Nagchala	N 31°37.6677′	E 76°56.3609′	774m	5570	5.57
7	Near Katoula	N 31°43.8133′	E 76°56.5432′	920m	18200	18.2
8	Drang	N 31°50.4621′	E 76°56.0611′	1236 m	5700	5.7
9	Near Jogindernagar	N 31°59.0311′	E 76°49.7023′	1467 m	1830	1.83
10	Sukh Bag	N 32°01.2229′	E 76°43.3477′	1313 m	7530	7.53
11	Radabhakar	N 32°03.3764′	E 76°39.1007′	1050 m	3480	3.48
12	Mohan ghati	N 32°01.8088′	E 76°41.4065′	1216 m	3980	3.98
13	Ghata	N 32°02.0090′	E 76°40.5680′	1239 m	3680	3.68
14	Baijnath	N 32°03.3764′	E 76°39.1007′	1050 m	4530	4.53
15	Paprola	N 32°04.4306′	E 76°35.9276′	1099 m	3790	3.79
16	Between paprola and Palampur	N 32°05.5771′	E 76°34.6722′	1189 m	3510	3.51
17	Neugalpul	N 32°06.6645′	E 76°29.2555′	1096 m	5950	5.95
18	Near chamuda	N 32°07.9165′	E 76°28.9476′	1258 m	7520	7.52

19	Between yol cant and chamunda	N 32°09.6910′	E 76°24.4096′	1057 m	3880	3.88
20	Yol cant	N 32°09.9561′	E 76°23.6815′	1121 m	2890	2.89
21	Sidhwari	N 32°11.3220′	E 76°21.5194′	1169 m	1950	1.95
22	Aghanjar Mahadev (khanyara)	N 32°12.6556′	E 76°22.3278′	1409 m	1510	1.51
23	Shila chowk	N 32°11.8699′	E 76°20.5835′	1151 m	2280	2.28
24	Near Swarawatinagar Dharmshala	N 32°12.0163′	E 76°20.1789′	1142m	4560	4.56
25	Near Hotel Pavalian	N 32°12.8589′	E 76°21.2988′	1295m	3400	3.4
26	Near circuit house	N 32°12.1607′	E 76°19.2482′	1208 m	3620	3.62
27	Near Balrupi (Jogindernagar)	N 31°59.0478′	E 76°47.2839′	1150 m	2560	2.56
28	Bassi	N 31°57.0111′	E 76°47.658′	936 m	2920	2.92
29	Machhayal	N 31°56.2011′	E 76°47.8330′	878 m	4210	4.21
30	Makridi	N 31°52.9697′	E 76°47.0204′	1322m	4230	4.23
31	Basai	N 31°52.0595′	E 76°45.7236′	1377m	3150	3.15
32	Between basai and kandapattan	N 31°50.2729′	E 76°46.7697′	883 m	7590	7.59
33	Dharmpur	N 31°48.7345′	E 76°46.2071′	647 m	8340	8.34
34	Logni	N 31°46.4445′	E 76°44.0097′	781 m	5540	5.54
35	Parchhu	N 31°44.7592′	E 76°43.4927′	811m	8460	8.46
36	Parsada	N 31°43.6735′	E 76°43.7333′	921m	3540	3.54
37	Jamsai	N 31°42.6708′	E 76°44.1802′	985m	11400	11.4
38	Naunu	N 31°43.798′	E 76°44.125′	945m	3760	3.76
39	Pung-Sundernagar	N 31°30.3321′	E 76°54.5011′	909 m	5210	5.21
40	Near Durgapur	N 31°39.6010′	E 76°49.4611′	1543 m	2510	2.51

Table 18: Measured values of annual effective doses and radium contents

Sr. No.	Annual Effective Dose in mSv/y (Due to intake of water)	Annual Effective Dose in mSv/y (Due to inhalation of water borne radon)	Radium Contents (Bq/kg) in the Soil of Water Resource
1	0.042	0.0702	8.78
2	0.028	0.0479	7.23

3	0.083	0.1398	14.73
4	0.016	0.0262	9.35
5	0.067	0.1127	13.57
6	0.020	0.034	5.56
7	0.067	0.112	13.78
8	0.021	0.0351	6.35
9	0.0067	0.0113	8.21
10	0.028	0.0464	7.47
11	0.013	0.0214	3.17
12	0.015	0.0245	3.28
13	0.014	0.0227	4.11
14	0.017	0.0279	4.05
15	0.014	0.0233	3.79
16	0.013	0.0216	4.01
17	0.022	0.0279	5.68
18	0.028	0.0463	5.57
19	0.014	0.0239	5.54
20	0.011	0.0178	3.23
21	0.007	0.0120	2.97
22	0.0056	0.009	5.65
23	0.0083	0.0140	3.63
24	0.017	0.02809	6.41
25	0.012	0.0209	6.43
26	0.013	0.0223	6.66
27	0.0094	0.0157	6.28
28	0.011	0.0179	5.41
29	0.015	0.0259	4.43
30	0.015	0.0261	4.99
31	0.012	0.0194	3.13
32	0.028	0.0468	7.88
33	0.031	0.0514	5.58
34	0.02	0.0341	5.33
35	0.031	0.0521	8.55
36	0.013	0.0218	3.44
37	0.042	0.0702	7.88
38	0.014	0.0231	7.44
39	0.019	0.0321	6.18
40	0.0092	0.0154	7.31

The Average value of radon concentration in water from study area 5.93Bq/l with maximum of 22.7Bq/l and minimum of 1.51Bq/l. The average absorbed dose received by the people of study area is 0.022mSv/y with maximum of 0.083mSv/y and minimum of 0.0056mSv/y. The Annual effective dose due to inhalation and ingestion is calculated using appropriate conversion coefficient [Badhan et al., 2010]. Whereas the radium contents in the study area have average value 6.326Bq/kg.The radon concentration is maximum at station no. 2 upper Bhambla with radium contents of 14.73Bq/kg and minimum value is at sample taken from a water spring situated new Aghanjar Mahadev above H P university region centre Khanyara with value of radon concentration and radium contents of 1.51Bq/l and 5.65Bq/kg. The other elevated values are at station no. 1Sarkaghat, 2 Fatehpur, 3 Galma, 7Near Katola (above Mandi), 33 Dharampur and 37 Jamsai. Since the average inhalation dose from drinking water should exceeds 0.0025mSv/y and in case for ingestion 0.002mSv/y. The result of our study shows 0.022mSv/y is the average dose received by the people of area and from inhalation point of view these values are less however in view of ingestion this value is very large. This much dose could not be actually received by the people of area because when water from resources is utilized for house hold tasks it comes in contact with the air and much amount of radon is removed from the water. The values reported in paper are more than the values measured by Abojassim [2013] in Kufa city/Iraq in samples of drinking water using similar technique [Abojassim, 2013]. When results are compared with study of radon level measured by Singh et al., [2010] in some area of Punjab and Himachal Pradesh, higher values of radon concentrations in Water sample were reported by authors may be due to presence of water resources near to major fault systems of the Himalaya area.

The correlation coefficient between the radium contents of the study area and radon concentration of the water sample is found to be 0.83. This shows that radon concentration in water strongly depends up on the radium contents of the study area.

8.3 Conclusions

1. Radon concentration in water depends up on the radium contents of the soil where water resource is situated**.**
2. The dose absorbed by the people of study area is within permissible limit.
3. With the aeration process the radon concentration in water can be reduce to permissible limit.

4. When results were compared with results of similar studies in area shows that the radon concentration may be large in water source of faulty zones.
5. The results may vary by using some another techniques.

(SUMMARY)

RADON ANOMALIES AND FAULT SYSTEM OF STUDY AREA

The study was performed in most tectonically active area in vicinity of MBT (Main Boundary thrust) and MCT (Main central thrust) from Mandi to Dharamshala including Sarkaghat, Sundernagar, Jogindernagar and Palampur in NW Himalayas, Himachal Pradesh, India. The main aim of the study was to establish possible connection between main fault systems in the study area with leakage of soil gases like radon and thoron. Due to possibility of higher radon and thoron leakage in these faulty areas, an indoor study in houses of residents of area along these major faults with continuous monitoring for one year at selective sites was also performed. Since radon concentration in soil depends upon its parent radium so radium contents and radon exhalation rates were also measured at the monitoring locations. Since many researchers in literature had shown the possible leakage of radon from parent rock through the liquid phase in their pores therefore radon concentrations from water samples from selective locations were also calculated. An attempt is also made to develop a model on the basis of Roger and Schery model to explain the theoretical basis of radon exhalation rates. In Mandi area near to Parvati and Beas valley there exit many geothermal resources of water, so possible connection of these sources with soil gas leakage, porosity and permeability of the soil was also made. These porosity and permeability of the soil- rocks are also related to the Ground water potential of the study area.

On the basis of observations made during different types of studies following overall conclusions were made:

Soil gas study

The anomalies were found in the values of radon–thoron near to the faults in the region, i.e., main boundary thrust (MBT, MBT2) and also along the drainage system in the study area. The presence of neotectonic faults/lineaments in the region has made it tectonically active. Radon concentration in soil profiling along MCT are found higher than that along MBT, i.e. MCT is under more geological stress and strain as compared to the MBT. Anomalies in measurement of radon and thoron concentration are more along and across MCT than MBT and any fault system. Greater anomalies are found in measurements of thoron concentrations may be due to the presence of local fault system. Thoron concentration values are very less at some places, maybe due to the presence of source deeper in earth at these places.

Higher will be density of the cross fault and thrust systems more will be radon concentration. Good correlation in porosity and thoron shows presence of local fault at shallow position in the area. The porosity and seepage of radon and thoron may be helpful to study ground water potential and its reservoir in any region. The elevated levels of radon and thoron at certain places can be associated to the presence of secondary porosity in the soil texture. Secondary porosity due to fracturing of basic strata may provide the easy pathway for upward movement of geothermal fluids.

Indoor Radon monitoring

The peoples of study area are living in higher radon concentration than the world average of 40 Bq/m^3. There were about 10% changes in the Maximum value of radon equilibrium equivalent concentration in winter season (January to March) to minimum value in the summer season (April to June). The seasonal variation in radon equilibrium equivalent concentration is affected mostly by ventilation condition in different seasons along with changes in temperature, humidity and atmospheric pressure. The difference in the average value of observed radon equilibrium equivalent concentration in different parts of the study area may be due to differences in radioactive contents of the soil.

Radon concentrations in water

Radon concentration in water was found to be depending up on the radium contents of the soil where water resource is situated**.** The dose absorbed by the people of study area due to inhalation and ingestion was found to be within permissible limit. When results were compared with results of similar studies in area shows that the radon concentration may be large in water source of faulty zones.

Radon exhalation rates and modeling to explain its theoretical basis

The radium contents in the study area are sufficiently less than permissible limit, so soil of region can be used as construction material for buildings and other structures. The radium contents, area exhalation rate and mass exhalation rate show a good Positive correlation of 0.997. Very less correlation between emanation coefficients and porosity with exhalation rates shows that exhalation rates are mildly depends up on these two quantities. The model developed is correlated to about 0.96 to its

experimental counterpart. Difference in the theoretical and experimental results at certain sites may be due to error in measurement of various other factors like Soil density, Porosity and emanation rates.

Future Perspectives

The soil gas study in Dharamshala- Mandi region of NW Himalayas, Himachal Pradesh, India is carried out using solid state nuclear track detector (LR-115 type II) films. The technique used is a cost effective and efficient for Seismotectonic studies. But to study the radon migration (especially through convection) the other carrier gases (CO2, CH_4, N_2, H_2, He) must be needed to monitored along with the radon.

The correlations of radon anomalies in soil and water will further be affected by the pressure, rainfall, humidity, wind velocity and uranium contents. So while making any correlation these parameters need to be kept in mind. Even for radon-thoron a continuous and comprehensive monitoring is needed which may include its spatial variation, variation in indoor radon levels prior and after any seismic activity and variations in levels of radon and its progeny in water. All these features may be included in the model to validate it universally.

Limitation of the Study

1. The study is limited to region of Mandi District and Dharamshala belt of Himachal Pradesh and outside of these areas the results and outcomes may vary.
2. The variation in the Radon gas may also be affected by difference in the traces of Uranium and other radioactive elements in the soil.
3. The study is limited to the measurement of the radon gas, but the other factor like variation in Helium may further be helpful in estimation of fault line and forecast of earthquake in study area [Walia et al., 2008].
4. The study is based on the measurement of the contents of Radon gas in which we are using LR-115 films and RAD7 detector, by using other techniques there maybe variation in result

BIBLIOGRAPHY

Abd El-Zaher M., (2011) Seasonal variation of radon level and radon effective doses in the Catacomb of Kom EI-Shuqafa, Alexandria, Egypt. Pramana. J Phys 77: 749–757.

Abojassim A. A., (2013) Radon concentrations measurement for drinking water in Kufa city/Iraq using Active detecting method. Advances in Physics theories and Applications vol.26, 30-35.

Akbari K., Mahmoudi J., Ghanbari M., (2013) Influence of indoor air conditions on radon concentration in a detached house, Journal of Environmental Radioactivity 116: 166-173

Al- Azmi D., (2009) The use of soil gas a radon source in radon chambers. Radiation Measurement 44,306-310.

Al-Jarallah M., F. Ur-Rehman, M.S. Musazay, A. Aksoy (2005) Correlation between radon exhalation and radium contents in granite samples used as construction material in Saudi- Arabia. Radiat. Meas., 40(2), 625-629.

Al- Tamimi M. H., Abumurad K. M., (2001) Radon concentration along faults in north of Jordan. Radiation measurement 34,397-400.

Amrani D., Cherouati D. E., (1999) Radon exhalation rate in building materials using plastic track detectors. Journal of Radioanalytical and nuclear chemistry. vol. 242, no. 2, 269-271

Anderson P., Clavensjo B., Akerblom G., (1983) The effect of the ground on the concentration of radon and gamma radiation indoors. *Swedish council for Building research (In Swedish) Report* R9: 1-442.

Andrews J.N., Hussain H., Batchelor A.S., Kwakwa K., (1986) ^{222}Rn solution by circulating fliud in a hot dry rock, geothermal reservoir. Applied geochemistry, vol 1,pp 647-657.

ASC: Seismicity of Himachal Pradesh, India.

Axelson O., (1995) Cancer risks from exposure to radon in homes, Environ. Health Persp. 103(2), 37-33.

Bajwa B.S., N. Sharma, V. Walia, H.S. Virk (2003) Measurements of natural radioactivity in some water and soil samples of Punjab state, India. Indoor and Built Environment, 12, 357-361

Balducci O., Bigazzi G., Cioni R., Leonardi M., Meletti C., Norelli P., Pescia A., Taddeucci G., (1994) Monitoring of ^{222}Rn in soil gas of Garfaganana(Tuscany) aimed at earthquake prediction. Annali Di Geofisica. Vol XXXVII,n.5.september 1994.

Balokhra J.: The wonderland HIMACHAL PRADESH.

Barooah D., Barman S., Phukan S., (2013) Study of environmental radon exhalation, radium and effective dose in Dilli Jeypore coalfield, India using LR-115(II) nuclear track detectors. Indian Journal of pure and applied Physics Vol.51, October 2013, pp 690-695.

Beck L.S., Gingrich J.E., (1976) Track etch orientation survey in the cliff Lake area, Northern Saskatchewan; Canadian Int. Min and Met. Bull. 69,104-109.

Bochicchio F., Foreastiere F., Abeni D., Rapiti E.,(1998) Epidemiologomic studies on lung cancer and residential exposure to radon in Italy and other countries. Radiat. Prot. Dosim 78(1),33-38.

Census of India (2001) Primary census abstract of total population -2001,series-3,table-A_5,primary census abstract, Himachal Pradesh, Himachal Pradesh: Directorate of census operations(Delhi :Govt. of India,2005).

Chandrasekharam D., Alam M.A., Minissale A., (2003) Geothermal resource potential of Himachal Pradesh, India. International geothermal conference, Reykjavik, Sept, 2003 session # 4, 15-20 p.

Chandrasekharam D., Alam M.A., Minissale A., (2005) Geothermal Discharge at Manikaran Himachal Pradesh, India. Proceedings world geothermal congress, 2005 Antalya, Turkey, 24-29 April 2005.

Chandrasekharam D., Chandrasekhar V., (2008) Geothermal resources in India: Possibilities for direct use in the Himalayas. Presented at the workshop for decision makers on direct heating use of geothermal resources in Asia, Organised by UNU-GTP, TBLRREM and TBGMED, in Tianjin, China, 11-18 May, 2008.

Chauhan R.P.,(2011) Radon exhalation rates from stone and soil samples of Aravali hills in India. Iran. J. Radiat. Res. 9(1),57-61.

Chauhan N., Chauhan R. P., Joshi M., Agarwal T. K., Aggarwal P., Sahoo B. K., (2014) Study of indoor radon distribution using measurement and CFD modeling. Journal of Environmental Radioactivity. 136, 105-111.

Chen J., (2005) A Review of Radon Doses. Radiation Protection Bureau, Health Canada. Radiation Protection 22 (4):27-31.

Chen J., Moir D., (2010) An updated assessment of radon exposure in Canada. Radiat Prot Dosim 140:166–170.

Chino M., Yamazawa H., (1996) Development of an atmospheric ^{222}Rn concentration model using a hydrodynamic meteorological model: three dimensional research purpose model. Health Physics 70, 50-63.

Choubey, V.M., K.K. Sharma, R.C. Ramola (1997) Geology of radon occurrence round Jari in Parvati Valley, Himachal Pradesh, India. J Environ. Radioact., 34(2), 139-147.

Choubey, V.M., P.K. Mukherjee, B. S. Bajwa, V. Walia (2007) Geological and Tectonic Influence on Water-Soil-Radon Relationship in Mandi – Manali Area, Himanchal Himalaya. Environmental Geology, 52, 1163-1171.

Cinti, D., Pizzine L., Voltattorni N., Quattrocchi F., Walia V., (2009) Geochmistry of thermal fluids along faults segments in the Beas and Parvati Valley (north-west Himalaya Himachal Pradesh) and Sohana town (Haryana), India. Geochemical journal, 43,65-76.

Ciotoli, G., M. Guerra, E. Lombardi, E. Vittori (1998) Soil gas survey for tracing seismogenic faults: A case study in the Fucino basin, central Italy. J.Geophys. Res., 103, 23781–23794.

Ciotoli, G., A. Sciarra, L. Ruggiero, A., Annunziatellis, S. Bigi, (2016) Soil gas geochemical behaviour across buried and exposed faults during the 24 August 2016 Central Italy earthquake. Annals of Geophysics, 59, fast track 5, 2016; DOI: 10.4401,ag-7242.

Crank, J. (1975) The Mathematics of diffusion 2nd Ed. New York: Oxford University Press.

Darby S., Hill D., Auvinen A., Barros-Dios J. M., Baysson H., Bochicchio F., Deo H., Falk R., Farchi S., Figueiras A., Hakama M., Heid I., Hunter N., Kreienbrock L., Kreuzer M., Lagarde F., Mäkeläinen I., Muirhead C., Oberaigner W., Pershagen G., Ruosteenoja S., Rosario A., Tirmarche M., Tomášek L., Whitley E., Wichmann H. E., Doll R., (2006) Residential Radon and Lung Cancer: Detailed Results of a Collaborative Analysis of Individual Data on 7,148 Subjects with Lung Cancer and 14, 208 Subjects without Lung Cancer from 13 Epidemiological Studies in Europe. Scand J Work Environ Health 32(1):1-83.

Darko G., Faanu G., Akoto O., Acheampong A., Goode E.J., Gyamfi O., (2015) Distribution of natural and artificial radioactivity in soils, water and tuber crops, Environ.Monit.and Assess., 187, 339.

Das G.R.N., Parthasarthy T. N., Taneja P.C., (1979) Uranium mineralisation in the politic schists in the Kullu Himalaya and its probable origin. Proc. Indian Sci. Acad.37,267-276.

Dhar S., Singh S., Dogra M., Kochhar N., (2002) Geological Significance of radon in Eco-system of Dharamshala area, Himachal Pradesh, India; Natural Hazards and

their mitigations (special, Bulletain of IGA, PU, Chandigarh, 35(2) 139-147.

District census hand book (2011) of Kullu and Mandi District.

Dongarra G., Martinelli G., (1993) Migration process of radon towards the earth surface: Implications for the prediction of seismic and volcanic events. Proceedings of scientific meeting on seismic protection. ATTI colloquio sulla Orotezione seismic Venice, 12-13 July, 1993, Palazzo Balbi, Regione Veneto.

Durrance E. M., (1986) Radioactivity in geology, Principles and applications. Ellis Horwood Limited, Chichester, England.

Dwivedi K. K., Srivastava A., Ghosh S., Sinha D., Laldawngliana C., Lalramagzami R., Sexena A., (1995) Measurement of Indoor radon in some dwelling in Aizawal, Journal of indoor Air International 4(6):362-364.

Dwivedi K. K., Ghosh S., Srivastava A., Lalramagzami R., Laldawngliana C., Sinha D., Ramachandran T. V., (1996) Measurement of Potential alpha energy exposure (PAFE) of radon and its progeny in northeastern India. Radiation measurement 26(2): 291-296.

Dwivedi K. K., Mishra R., Tripathy S.P., Kulshreshtha A., Sinha D., Srivastava A., Deka P., Bhattacharji B., Ramachandran T. V., Nambi K. S. V., (2001) Simultaneous determination of radon, thoron and their progeny in dwellings. Radiation measurement 33(1): 7-11.

Duggal V., Rani A., Mehra R., Ramola R.C., (2013) Assessment of natural radioactivity levels and associated dose rates in soil samples from Northern Rajasthan, India. Radiation protection dosimetry pp 1-6. Doi : 10.1093/rpd/nct199.

Durrani S. A., Ilic R., (1997): Radon measurement by Etch Track Detectors, World Scientific Publishing Singapore.

Durridge Co., "RAD7 detector user Manual", 2009

Durridge Co., "RAD7 RAD H_2O Radon in Water accessory owner's Manual", 2009

Eappen K. P., Mayya Y. S., (2004) Calibration factors for LR-115(Type-II) based radon thoron discriminating dosimeter. Radiation measurement 38, 5-17.

Etiope G., Martinelli G., (2002) Migration of carrier and trace gases in the geosphere: an overview.Phys. Earth Planet. Int. 129(3-4); 185-204.

Feichter J., Crutzen P.J., (1990) Parameterisation of vertical tracer transport due to deep cumlus convection in a globel transport model and its evalustion with 222-radon measurements. Tellus 42B, 100-117.

Feichter J., Crutzen P.J. (1990) Parameterization of vertical tracer transport due to deep cumulus convection in a global transport and its evaluation with ^{222}Rn measurements. Tellus, 42B, 100-117.

Fick A., (1855) Ueber diffusion. Annln Phys, 170:59-86 (German).

Fleischer R. L., Prince P.B., Walker R.M., (1975) Nuclear Tracks in solids. Univ. of calf. press Berkeley.

Fleischer R. L., (1980) Isotopic disequilibrium of uranium: Alpha – recoil damage and preferential solution effects. Science 207, 979-981.

Fu C.C., Yang T.F., Walia V., Chen C.H.,(2005) Reconnaissance of soil gas composition over buried faults and fractured zone in southern Taiwan; Geochem.J. 39,427-439.

Gansser A., (1964) Geology of Himalayas; Interscience,New York.

Ghosh P. C., Soundararajan M., (1984) A Technique for discrimination of radon and thoron in soil gas using soil state Nuclear track detectors(SSNTD). Nucl.Tracks 9,23-27.

Ghosh D., Deb A., Sengupta R., Patra K.K., Bera S., (2007) Pronounced soil – radon anomaly- Precursor of recent earthquake in India. Radiation measurement 42, 466-471.

Geology and Mineral Resources of Himachal Pradesh (2012) Miscellaneous Publication no. 30: Part-17, Geology and mineral resources of the states of India, Geological Survey of India.

Georgy, C., Z. Rafael, B. Ivan (2015) Radon monitoring in groundwater and soil gas of Sakhalin Island, J Geosci.and Environ.Protect.,3(5), 48-53.

Genthon C., Armengaud A., (1995) Radon-222 as a comparative tracer of transport and mixing in two general circulation models of atmosphere. Journal of geophysics research 100 (02), 2849-2866.

Gingrich J.E., Fisher J.C.,(1976) Uranium exploration using track- etch method. In: exploration for uranium ore deposits; IAEA, Vienna 213-227.

Giggenbach, W.F., R. Gonfiantini, B.L. Jangi, A.H. Truesdell (1983) Isotope and chemical composition of Parvati valley geothermal discharges, North west Himalaya, India, Geothermics 12, 199-222.

Goto M., Moriizumi J., Yamazawa H., Iida T., Zhou W., (2008) Estimation of global radon exhalation rate distribution. AIP conference proceedings volume 1034 issue 1.

Grammakov A.G., (1936) On the influence of some factors in the spreading of radioactive emanations under natural conditions. Zhur, Geofiziki, 6: 123-148.

Guerra M., Lombardi S.,(2001) Soil gas method for tracing neotectonic faults in clay Basins: The Pisticci fields (southern Italy); Tectonophysics 339,511-522.

Gupta, G.K. (1996) Hydrogeology and hydrochemistry of Beas valley geothermal system, Kullu district Himachal Pradesh, Geol survey of India 45, 249-256.

Gupta R. D., Arora S., Gupta G. D., Sumberia N. M., (2010) Soil Physical variability in relation to soil erodibility under different land uses in foothill of Shiwaliks in NW India. Tropical Ecology 51(2):183-197.

Gupta M., Mathur A. K., Sonkawade R. G., Verma K. D. (2011) Monitoring of indoor radon and its progeny in dwellings of Delhi using SSNTD's. Pelagia Research Library, Advances in Applied science Research, 2(5):421-426 ISSN: 0976-8610, CODEN (USA)-AASRFC.

Han X., Li Y., Du J., Zhou X., Xie C., Zhang W., (2014) Rn and Co_2 geochemistry of soil gas across the active fault zone in the capital area of china. Nat. hazards earth syst. Sci., 14,2803-2815,2014.

Hartmann J., Levy J. K., (2005) Hydro geological and Gas geochemical Earthquake Precursors – A Review for Application. Natural Hazards 34:279–304.

Hernandez P., Nemesio P., Salazar J., Reimer M., Notsu K., Wakita H., (2004) Radon and helium in soil gas at Canadas Caldera, Tenerife, Canary Island, Spain Journal of volcanology and geothermal research 131, 59-76. Doi: 10.1016/So377-0273(03)00316-0.

Horton C.W., Rogers F.T., (1945) convection currents in porous medium. J.Appl. Phys, Vol 16. Pp 367-370.

ICRP (1991) International commission on Radiological Protection. "Recommendations of the International commission on Radiological Protection," ICRP publication 60. Annals of the ICRP 21.

ICRP, (1993) International commission on Radiological Protection. "Protection Against Radon-222 at Home and at work," ICRP publication 6 . Annals of the ICRP 23.

Jaishi H. P., Singh S., Tiwari R. P., Tiwari R. C., (2014) Analysis of soil radon data in earthquake precursory studies. Annals of Geophysics, 57,5,2014,S0544; doi 10.4401/ag-6513.

Jashank, M., Gupta S.J., Nair J., (2014) Development of Radon Gas Sensor to Monitor: The Precursors of Earthquake. IOSR J. of Engg., 4, 10-15.

Jonsson G.,(1997) Soil radon survey in radon measurement by etched track detectors.

Appl. Rad. Prot. Earth Sci. Environ.(World scientific Singapore), 179-188.

Kalsi P. C., Ramaswami A., Manchanda V. K., (2005) Solid state Nuclear track Detectors and their applications.

Kant K., Rashmi, Sonkawade R. G., Sharma G. S., Chauhan R. P., Chakarvarti S .K., (2009) Seasonal variation of radon, thoron and their progeny levels in dwellings of Haryana and western Utter Pradesh. Iran. J. Radiat.7 (2): 79-84.

Kavasi N., Somlai J., Szeiler G., Szab´o B., Schafer I., Kov´acs T., (2010) Estimation of effective doses to cavers based on radon measurements carried out in seven caves of the Bakony Mountains in Hungary. Radiat. Meas., 45: 1068–1071.

Khattak N.U., Khan M. A., Shah M.T., (2014) Radon concentration in drinking water sources of the region adjacent to a tectonically active Karak Thrust, southern Kohat Plateau, Khyber Pakhtunkhwa, Pakistan. J Radioanal Nucl Chem. 302:315–329.

Kies A., Massen F., (1999) Radon concentrations under a dam reservoir, Proc. 5th Int. conference on Rare-gas geochemistry, Debrecan Hungary.

Kies A., Massen F., Toshen Z., (2002) Influence of Variable stress on underground radon concentration. *Geofisica International*, 41, 3,325-329.

Kitto M., (2014) Radon Testing in schools in New York state : a 20-year summary, Journal of Environmental radioactivity 137(2014) 213-216.

Koike K., Yoshinaga T., Ueyama T., Asaue H., (2014) Increased radon-222 in soil gas because of cumulative seismicity at active faults. Earth planet and space 2014, 66-57.

Kovacs T., (2010) Thoron measurements in Hungary, Radiation Protection Dosimetry. 141(4): 328-334.

Krewski D., Lubin J. H., Zielinski J. M., Alavanja M., Catalan V. S., Field R.W., Klotz J. B., Létourneau E.G., Lynch C. F., Lyon J. L., Sandler D.P., Schoenberg J.B., Steck D. J., Stolwijk J.A., Weinberg C., Wilcox H. B., (2006) A combined analysis of North American case-control studies of residential radon and lung cancer. Journal of toxicology and Environmental Health. Part A 69(7):533-97.

Kumar A., Singh S., (2004) Radon exhalation studies in Building materials using Solid state nuclear Track detectors. Pramana-J.phys.,vol 62, No.1, 143-146.

Kumar A., Walia V., Yang T.F., Hsien C. H., Lin S. J., Eappen K. P., Arora B.R., (2013a) Radon-thoron monitoring in Tatun volcanic areas of northern Taiwan using LR-115 alpha track detector technique: Pre Calibration and Installation. Acta

Geophysica 61(4):958-976.

Kumar G., Kumar A., Walia V., Kumar J., Gupta V., Yang T.F., Singh S., Bajwa B.S., (2013b) Soil gas radon -thoron monitoring in Dharamshala area of North-West Himalayas, India using solid state nuclear track detectors. Journal of Earth System Science 122 (5): 1295-1301.

Kumar A., Arora V., Walia V., Bajwa B.S., Singh S., Yang T.F., (2014) Study of soil gas radon variations in the tectonically active Dharamshala and Chamba regions, Himachal Pradesh, India. Environmental Earth Sciences 72:2837-2847.

Kumar A., Chauhan R.P., (2014) The radon concentration also depend upon the uranium contents of the soil, Journal of Geochemical Exploration 143: 155–162.

Kumar A, Chauhan R. P., Joshi M., Sahoo B. K., (2014) Modeling of indoor concentration from radon exhalation rates of building materials and validation through measurements. Journal of Environmental radioactivity 127 (2014) 50-55.

Kumar G., Kumar A., Kumar M., Walia V., Prasher S., Tuccu M. A. , (2016) Indoor radon monitoring in the Mandi district of Himachal Pradesh, India, for health hazard Assessment. Radioprotection, 51(1), 47-50. DOI: 10.1051/radiopro/2015024.

Labrecque J. J., (2002) Simple and rapid methods for onsite determination of radon and thoron in soil-gases for seismic studies; J. Radioanal. Nucl. Chem. 254 439–444.

Lambert G., Polion G., Sanak J., Ardoun B., Buisson A., Jegou A., Le Roulley J.C., (1982) Appilcation altitude exchanges in troposphere- stratosphere. Annals Geophys, 48, 497-531.

Lehmann B. E., Lehmann M., Neffel A., Tarakanov S.V., (2000) Radon-222 monitoring of soil diffusivity. Geophys Res Lett. 22: 3917-3920. Doi 10.1029/1999GL008469.

Li Y., Du J., Wang X., Zhou X., Xie C., Cui Y., (2013) Spatial variations of soil gas geochemistry in Tangshan area of northern china. Terr. Atmos.Ocean.Sci., Vol.24.No 3,323-332.

Lubin J. H., Wang Z. Y., Boice J. D., Xu Z. Y., Blot W. J., Wang L. D., Kleinerman R. A., (2004). Risk of lung cancer and residential radon in China: pooled results of two studies. Int J Cancer 109:132-137.

Mahajan A. K., Kumar S., Chabak S.K., (1997) Local gravity anomaly and geotectonics in the Dharamshala and Palampur area, North west Himalaya; J. Geol. Soc. Ind. 50, 75-89.

Mahajan A. K., Virdi N.S., (2000) Preparation of Landslides Hazard Zonation Map of

Dharamshala Town and adjoining area, district Kangra (H.P.) Project Report, H.P. Government, 45(p).

Martinelli G., Al barello D., Mucciarelli M., (1995) Radon emmisions from Mud volcanoes in Northeren Italy: Possible connection with local seismicity. Geophys. Res. Lett. 22: 1989-1992.

Masayoshi G., Moriizumi J., Yamazawa H., Iida T., Zhou W., (2008) The natural radiation Environment- 8th International symposium. American Institute of Physics 978-0-7354-0559-2/08.

Mc Laughlin J. P., (1989) Aspects of Radon and its decay products in indoor air .In: Workshop on Radon monitoring and radio protection, Environmental radioactivity and earth sciences, ICTP, Trieste, Itlay,51-69.

Mehra R., Badhan K., Sonkawade R.G., (2010) Radon Activity Measurements in drinking water and its indoors of dwelling using RAD7. Tenth Radiation Physics and Protection conference 27th- 30th Nov, 2010, Nasar city-Cairo, Egypt.

Mehra R., Bala P., (2014) Estimation of annual effective dose due to Radon level in indoor air and soil gas in Hamirpur district of Himachal Pradesh. Journal of Geochemical Exploration 142:16-20.

Morgan R.P.C., (2005) Soil erosion and conservation 3rd edn, Blackwell Publishing Ltd. USA.

Nazaroff W. W., Nero A.V.,(1988) Radon and its decays products in indoor air, John Wiley & sons, New York,74.

OECD (1979) Exposure to radiation from the natural radioactivity in building materials report by a group of experts of the OECD nuclear agency OECD Paris France.

Okabe S., (1956) Time variation of the atmospheric radon content near the ground surface with the relation to some geophysical phenomenon. Mem.coll.sci.univ. Kyoto ser. A28 (2), 99-115.

Papastefanou C., (2007) Measuring radon in soil gas and groundwaters: a review; Annals of Geophysics. 50: 569-578.

Pearson J. E., Jones G. E., (1966) Soil concentration of emanating radium-226 and the emanation of radon from soil and plants. Tellus,18;655-662.

Pereira, A.J.S.C.,M.M.Godinho,L.J.P.F.Neves (2010). On the influence of faulting on small-scale soil-gas radon variability: A case study in the Iberian Uranium Province, J. Environ.Radioact., 101, 875–882.

Piersanti A., Cannelli V., Galli G., (2015) Long term continous radon monitoring in a

seismically active area. Annals of geophysics, 58,4,2015,S 0437. Doi: 10.4401/ag-6735.

Poelchau, H.S., D.R. Baker, T.H. Hantschal, B. Horsefield, B.C. Wygrala (1997) Basin simulation and the design of the conceptual basin model. In: Welre DH, Horsefield B, Baker DR(eds) Petroleum and Basin evaluation. Springer Berlin, pp 36-41.

Popit A., Vaupatic J., Dolenec T., (2005) Geochemical and geophysical monitoring of thermal waters in the Slovenia in relation to Seismic activity. Annals of geophysics, 45, N.1.

Quattrucchi F., Di Stefano G., Pizzino L., Pongetti F., Romeo Scarloto G., Sciacca P., Urbini U. G., (2000) Geochemi C; al Monitoring system II Prototype (GMS II)installation at the " Aqua Difesa" well, within the Etna Region : First data. J. Volcanol. Geotherm. Res., 101, 273-306.

Raghavayya M., (1994) Safety standards for exposure to radon Bulletin. Radiat. Prot.17 (3&4): 1-4.

Ramola R.C., (2011) Survey of radon and thoron in homes of Indian Himalaya. Radiation Protection Dosimetry 46, 1-3, 11-13 doi 10.1093/ rpd/nc095.

Rao R.U.M.,. Rao G.V., Hari N., (1976). Radioactive heat generation and heat flow in the Indian shield. Earth Planet Sci. Lett. 30, 57-64.

Ravi Shanker (1988). Heat flow of india and discussion on its geological and economic significance. Ind. Min. 42,89-110.

Rind D., Lerner J., (1996) Use of on line tracers as a diagnostic tool in general circulation model development1. Horizontal and 2. Vertical Transport. J. Geophys. Res, 101(12): 667-683.

Rogers V. C., Nielson, K.K., (1991) Multiphase radon generation and transport in porous materials, Health Phys., 60, 807.

Ryzhakova N.K., Yakovleva V.S. (2003) A technique for determination of the radon flux density from the earth's surface. RF Patent n0. 2212688, September 2003 (in Russian).

Sac M. M., Harmansah C., Camgoz B., Sozbilir H., (2011): Radon monitoring as the earthquake precursor in fault line in western Turkey. Ekoloji 20,79,93-98.

Sahoo B.K., Sapra B.K., Gaware J.J., Kanse S.D., Mayya Y.S., (2011) A model to predict radon exhalation from walls to indoor air, based on the exhalation from building material samples J. Sci. Total Environ 409(13), 2635-2641.

Saidu, Abdourahimi, Tchuente Y F, Siaka, Bouba O (2014) Indoor radon measurement in the uranium regions of Poli and Lolodorf Cameroon. Journal of Environmental radioactivity 136 (2014) 36-40.

Sakashita T., Murakami T., Iida, T., Ikebe, Y., Suzuki, K., Chino, M., (1994) A numerical model of three dimensional transport with application to the transport of ^{222}Rn. Journal of Atmospheric electricity 14,57-62.

Samuelsson C., Peterson H., (1984) "Exhalation of ^{222} Rn from Porous Materials" Radiation Protection Dosimetry, 7(1), 95-100.

Schery S. D., Gaeddert D. H., (1982) Measurement of the effect of cyclic atmosphere pressure variation on the flux ^{222} Rn from soil. Geophys. Res. Letts., 9: 835-838.

Schery S. D., Gaeddert D. H., Wilkening M. H., (1984) Factors affecting exhalation of radon from gravelly sandy loam. J. Geophys. Res 89: 7299-7309.

Schery S.D., Wasiolok M. A., (1998) Modeling Radon flux from the earth's surface In: proceedings of seventh Towa university International symposium, Fukuoka, Japan pp 207-217 ISBN 98102-3443-0.

Sharma N., Virk H.S., (1998) Indoor levels of radon/thoron daughters in some dwellings of Punjab. In: Proceedings of XIth National symposium, Guru Nanak Dev University Press, Amritsar pp.259-262.

Sharma M., Sharma Y.C., Basu B., Chhabra J., Gupta R.K., Singh J., (2000) Uranium mineralization in the sandstones of Dharamshala, Tileli area Mandi district, Himachal Pradesh, India. Current Science 78(7):897-899.

Singh, A.K., P. J .Jojo, A.J. Khan, R. Prasad and T.V. Ramachandran(1997) Calibration of track detector and measurement of radon exhalation rates from soil sample, Radiat. Prot. Environ.,20,129.

Singh S., Singh B., Kumar J., (1998) Uranium and radon measurements in the environs of Himachal Himalayas—an application of solid state nuclear track detectors. Proceedings of the XIth National Symposium SSNTD, Guru Nanak Dev University Press, Amritsar, India, pp. 69–78.

Singh S., Singh B., Kumar A., (2001) Measurement of indoor radon levels in dwellings and estimation of uranium in environmental samples from Una district, Himachal Pradesh, using passive detector technique. Radiat. Prot. Environ. 24 (1-2):445–449.

Singh S., Mehra R., Singh K., (2005a) Seasonal variation of indoor radon in dwellings of Malwa region, Punjab. Atmospheric Environment 39 (2005): 7761-

7767.

Singh S., Kumar M., Mahajan R., (2005b.) The study of indoor radon in dwellings of Bathinta district, Punjab, India and its correlation with Uranium and radon exhalation rate in soil. Radiation measurement 39:535-542.

Singh, S., D.K. Sharma, S. Dhar. and S.S. Randhawa (2006) Geological significance of soil gas radon: A case study of Nurpur area, district Kangra, Himachal Pradesh, India,Radiat. Meas., 41(4), 482–485.

Singh S., Kumar A., Bajwa B.S., Mahajan S., Kumar V., Dhar S., (2010) Radon Monitoring in Soil Gas and Ground Water for Earthquake Prediction study in NW Himalaya, India. Terr. Atmos. Ocean Sci. 21(4): 685-695.

Singh, B., S. Singh,B.S. Bajwa, J. Singh, A. Kumar (2011) Soil gas radon analysis in some areas of Northern Punjab, Environ. Monit. and Assess., 174, 209-217.

Singh P., Singh P., Sahoo B.K., Bajwa B.S., (2016) A study of Uranium and radon levels in drinking water sources of a mineralized zone of Himachal Pradesh, India. Journal of Radioanalytical and nuclear chemistry. 309, 541-549 DOI 10.1007/s10967-015-4629-9.

Stoulos S., Manolopoulou M., Papastefanou C., (2003) Assessment of natural radiation exposure and radon exhalation from Buliding materials in Greece. J. Environ. Radioact. 69, 225-240.

Strong K.P., Levins D.M., (1982) Effect of moisture content on radon emanation from uranium ore and tailing. Health Phys.,42: 27-32.

Sun K., Guo Q., Zhuo W. (2004) Feasibility for mapping radon exhalation rate from soil china. Journal of Nuclear science and Technology. Vol .41, no. 1, 86-90.

Taguchi, S., T. Iida, J. Moriizumi, (2002) Evaluation of the atmospheric transport model NIRE-CTM-96 by using measured radon-222 concentration Tellus 54B,250-268.

Tanner A. B., (1964) Radon migration in ground: review. In Jas Adams and WM Lowder (Editors), Natuarl radiation environment. University of Chicago press, Chicagi,III, pp 161-190.

Tanner A. B., (1980) Radon migration in the ground: A supplementary review. In The Natural Radiation Environment III. (Eds. T.F. Gesell and W.M. Lowder), National Technical Information service, Springfield, VA. CONF-780422, 5-56.

Tommasino L., (1990) Radon Monitoring by alpha track detection, In: Proc. Int. workshop on radon monitoring in radioprotection environment, Radioactivity and

earth science, Tammasino etal.(eds) Trieste, 1981, world scientific, Singapore, 123-132.

Toutain J. P., Boubron J. C., (1999) Gas geochemistry and Seismotectonic: a review, Tectophysics, 304, 1-24.

Thamos D. M., (1988) Geochemical precursors to seismic activity, Pure Appl. Geophys, 126,241-266.

UNSCEAR (2000) United Nations scientific committee on effects of Atomic Radiation sources and effects of Ionizing Radiation. Report to General Assembly, New York.

USEPA- United states Environmental Protection Agency, (2000) National Primary Drinking water regulations; Radionuclide's: Final Report .

Valentina S.Y.,(2005) A theoretical method for estimating the characteristics of radon transport in homogeneous soil. Annals of Geophysics, vol. 48,1,195-198.

Vaupotic J., Gregoric A., Kobal L., Zveb P., Kozok K., Mazur J., Kochowska E., Grzadziel, (2010) Radon concentration in soil gas and radon exhalation rate at the Ravne fault in NW Slovenia. Nat. Hazards Earth syst. Sci.,10,895-899,2010.

Virk H.S., V. Walia (2000) Radon/ Helium monitoring in thermal springs and earthquake prediction, Publ. of the centre of advanced study in Geol. 7.106-107.

Walia, V., B.S. Bajwa, H. S. Virk (2003) Radon monitoring in ground water of some areas of Himachal Pradesh and Punjab states, India. Jour. of Environment Monitoring, 5, 122-125

Walia, V., H.S. Virk, T.F. Yang, S. Mahajan, M. Walia and B.S. Bajwa (2005) Earthquake prediction studies using radon as a precursor in NW- Himalaya India: a case study. Terr. Atmos. Ocean. Sci.,16(4) 775-804.

Walia V., Mahajan S., Kumar A., Singh S., Bajwa B.S., Dhar S., Yang T. F., (2008) Fault delineation study using soil-gas method in Dharamshala area, NW Himalayas, India. Radiat. Meas. 43: S337-S342.

Walia V., Yang T.F., Lin S.J., Kumar A., Fu C., Chiu J.M., Chang H.H., Wen K.L., Cheng C.H., (2013) Temporal variation of soil gas compositions for earthquake surveillance in Taiwan. Radiat Meas 50:154–159.

World Health Organization (2004) third ed. Guidelines for drinking water quality.

World Health Organization (2009) Handbook on Indoor Radon.

World Health Organization (WHO), (2011) Guidelines for drinking water quality.

Yakovelena V. S.,(2005) A theoretical method for estimating the characteristics of radon transport in homogeneous soil. Annals of Geophysics, vol. 48,1,195-198.

Yakovelena V. S.,(2005) A theoretical method for estimating the characteristics of radon transport in homogeneous soil. Annals of Geophysics, vol. 48,1,195-198.

Yang, T.F., V. Walia, L. L. Chyi, C.C. Fu, C.H. Chen, T.K. Liu, S. R. Song, C.Y. Lee and M. Lee (2005) Variations of soil radon and thoron concentrations in a fault zone and prospective earthquakes in SW Taiwan, Radiat. Meas., 40, 496–502.

Yang T. F., Wen H.Y., Fu C.C., Lee H.F., Lan F., Chen A.T., Hong L., Lin S.J., Walia V., (2011) Soil radon flux and concentrations in hydrothermal area of the Tatun Volcano Group, Northern Taiwan. Geochem. J. 45: 483- 490.

Zhuo W., Iida T., Furukawa M., (2006) Modeling Radon flux density from the earth's surface. Journal of nuclear science and Technology. Vol. 43, 4, 479-482.

Zhou W., Guo Q., Chen B., Cheng G., (2008) Estimating the amount and distribution of radon flux density from the soil surface in china. Journal of environmental radioactivity 99, 1143-1148.

PUBLICATIONS

(Published/Accepted)

1) G. Kumar, Kumar A, Walia V, Kumar J, Gupta V, Yang TF, Singh S, Bajwa BS, (2013) Soil gas radon -thoron monitoring in Dharamshala area of North-West Himalayas, India using solid state nuclear track detectors. Journal of Earth System Science (springer) 122 (5), 1295-1301 DOI: 10.1007/s12040-013-0344-55 [in UGC list sr. no.183 in first list].

2) G. Kumar, A. Kumar, M. Kumar, V. Walia, S. Prasher, M.A. Tuccu. (2016) Indoor radon monitoring in the Mandi district of Himachal Pradesh, India, for health hazard assessment. Radioprotection, (Cambridge Journal) 51(1), 47-50. DOI: 10.1051/radiopro/2015024. [in UGC journal list sr. no. 31289 in first list].

3) G. Kumar, P. Kumari, A. Kumar, S. Prasher, M. Kumar (2017) A study of radon and thoron concentration in the soils along the active fault of NW Himalayas in India. Annals of geophysics, 60. 3. 2017, S0329. DOI: 10.4401/ag-7057 [in UGC list sr. no.2801 in first list].

4) G. Kumar, P. Kumari, M. Kumar, A. Kumar, S. Prasher, S. Dhar (2017) Radon estimation in water resources of Mandi - Dharamshala region of Himachal Pradesh, India and health risk assessments. AIP proceeding journal 1860, 020014. DOI: 10.1063/1.4990313 [in UGC list sr. no. 7446 in newly added journal list]**.**

5) G. Kumar, A. Kumar, M. Kumar, S. Prasher, P. Kumari "Radon exhalation rates in the soil samples of Dharamshala Region of Himachal Pradesh NW Himalaya, India and their comparison with developing a theoretical model" **(Communicated)**

Papers in conference Proceeding (Presented & Published)

1) G. Kumar, A. Kumar, J. Kumar, V. Walia (2013) Indoor Radon measurement in some houses of Mandi district of Himachal Pradesh, INDIA using solid state

nuclear track detectors. International Journal of Engineering research and Technology, MAM-2013 conference proceeding pp 57-59, ISSN 22780181

Papers presented in conferences during research work for PhD

1) Paper presented in IInd Annual Conference on science: Emerging scenario and future Challenges-II on 17th-18th May 2014 at Himalayan Forest Research Institute Shimla Himachal Pradesh, titled "Indoor radon concentrations in the dwellings of the Palampur-Jogindernagar region of Himachal Pradesh, India, using solid state nuclear track detectors". G. Kumar*, A. Kumar, M. Kumar, J. Kumar.

2) Paper presented in "International conference on Science Emerging scenario and future challenges" (SESFC) on 11th -12th June, 2016 at Hotel Inclover, Dharamshala Himachal Pradesh, titled "Radon concentration in water samples and its correlation with radium contents of soil Keeping in view the health of the population consuming water from various water resources of Mandi - Dharamshala region of Himachal Pradesh, India" (winner of best poster award)

G. Kumar*, A. Kumar, M. Kumar, S. Dhar.